THE ASTROPHYSICAL JOURNAL SUPPLEMENT SERIES, 93:1–46, 1994 July


# Mg II ABSORPTION IN A SAMPLE OF 56 STEEP-SPECTRUM QUASARS

THOMAS L. ALDCROFT[1]
Department of Physics, Stanford University, Stanford, CA 94305-4060
JILL BECHTOLD
Steward Observatory, University of Arizona, Tucson, AZ 85721
AND
MARTIN ELVIS
Harvard-Smithsonian Center for Astrophysics, 60 Garden Street, Cambridge, MA 02138
*Received 1993 November 1; accepted 1993 December 1*

## ABSTRACT

We present an analysis of the statistical properties of Mg II absorbers found in the spectra of 56 intrinsically faint, steep-spectrum radio quasars. We observe for the first time a significant excess of associated Mg II absorbers over the number expected from cosmologically distributed absorbers. This result is in contrast to previous Mg II surveys in which the QSOs were optically selected. This distinction is similar to the result for associated C IV absorbers, in which intrinsically faint, steep-spectrum quasars show excess associated absorption and intrinsically bright QSOs (both radio-loud and radio-quiet) do not show an excess.

From our spectra a statistically complete list of absorption lines is derived, and we find 29 Mg II absorbers, 18 of which have not been previously reported. We also determine several characteristics of the quasar emission lines in our spectra. The Mg II absorber distribution as a function of redshift and equivalent width is calculated both for our sample alone and from our sample combined with spectra from other surveys. For the redshift distribution $n(z) = n(1+z)^\gamma$, we obtain, using the combined sample, the values $\gamma = 1.11 \pm 0.46$ for $W_{\rm min} = 0.6$ Å and $\gamma = 2.47 \pm 0.68$ for $W_{\rm min} = 1.0$ Å. We find that the distribution of strong absorbers is inconsistent with no evolution at a confidence level between 2.2 and 2.9 $\sigma$, depending on the deceleration parameter $q_0$. The deviation from no evolution is similar to what had been previously reported.

*Subject headings:* quasars: absorption lines

## 1. INTRODUCTION

Recent imaging and spectroscopic studies have found that Mg II–selected objects are normal, relatively bright spiral galaxies (Steidel 1992; Bergeron, Cristiani, & Shaver 1992; Bergeron & Boissé 1991; however, see Yanny & York 1992 for an opposing viewpoint). This means that these absorption lines provide a useful tool for studying the properties of gas-rich galaxies over much of the age of the universe. In particular, the statistical analysis of absorber properties can shed light on a number of issues in galaxy structure and evolution. For the Mg II absorbers, numerous surveys have been carried out (for references see Steidel & Sargent 1992, hereafter SS). The most recent and comprehensive is the data set in SS, which is combined with spectra from Sargent, Steidel, & Boksenberg (1988b, hereafter SSB1). One very interesting finding by SS is that weak absorption systems ($W_0 \geq 0.3$ Å) are consistent with no evolution, whereas the strong systems ($W_0 \geq 1.0$ Å) require evolution at 2–3 $\sigma$ confidence.

As a complement to previous surveys, we have observed 56 steep-spectrum radio-loud quasars at the Multiple Mirror Telescope[2] (MMT) and the Palomar 5.08 m telescope[3] during a total of 13 nights between 1988 June and 1989 May. The majority of quasars in our sample are at moderate redshift ($z_{\rm em} = 0.7$–$1.5$) and have been observed at a resolution between 100–360 km s$^{-1}$. The primary purpose of this survey was to find Mg II absorption-line systems in lobe-dominated quasars (Aldcroft, Elvis, & Bechtold 1993, hereafter Paper I). In these quasars we will search for Mg II–selected H I 21 cm absorption at redshifts between 0.4 and 1.4. For positive detections, the different line of sight between the optical and the lobe-dominated radio emission means that direct limits will be placed on the overall linear size of the absorber. The detection of absorption in resolved radio emission also gives limits on the sizes of individual absorbing clouds.

Because of the restrictive radio selection criteria described in § 2, we were forced to observe objects which are generally fainter in the optical than those of previous surveys. The average absolute magnitude of objects in our sample is about 2 mag fainter than in the sample of SS. Thus the typical rest equivalent width limit in our spectra is somewhat higher than in previous surveys, about 0.6 Å. However, a beneficial consequence is that the quasars in our sample have very different intrinsic optical and radio properties from those in any previous Mg II survey. This is important for study of associated Mg II absorbers, and in fact we have detected in our sample an excess of associated absorbers, in contrast to previous results (SS; Lanzetta, Turnshek, & Wolfe 1987). Even more significant is our finding that the quasars showing associated absorp-

[1] Present address: Center for Astrophysics, 60 Garden Street, Cambridge, MA 02138.
[2] The Multiple Mirror Telescope Observatory is a joint facility of the University of Arizona and the Smithsonian Institution.
[3] Palomar Observatory is owned and operated by the California Institute of Technology.

tion have rest-frame colors very much redder than the rest of our sample, the details of which are presented in Aldcroft, Elvis, & Bechtold (1994).

In this paper we present the optical spectra, a statistically complete list of absorption lines in those spectra, plots of Mg II detection equivalent width limit versus redshift, and a statistical analysis of the Mg II absorption systems. We also combine our lines with those published in SS and SSB1 to further constrain several evolutionary parameters.

## 2. DEFINING THE SAMPLE

The starting point defining the objects in our survey is the sample of 73 quasars presented in Paper I. These were selected from the Véron-Cetty & Véron (1989) QSO catalog based on the following criteria:

$$S(2.7\ \mathrm{GHz}) \geq 1\ \mathrm{Jy}, \quad m_V \leq 19.5, \quad \alpha \geq 0.4\ ,$$

$$z_{\mathrm{em}} \geq 0.5, \quad \delta \geq -30°\ .$$

Here $S$ is the radio flux, $m_V$ is the visual magnitude, $\alpha$ is the radio spectral index ($S \sim \nu^{-\alpha}$), $z_{\mathrm{em}}$ is the quasar emission redshift, and $\delta$ is the declination.

Of these objects, we did not obtain spectra of 17, for the following reasons, with the number of objects following in parentheses: we were unable to determine the radio lobe dominance, making the object unusable for the purposes of Paper I (4); low redshift (7); various problems with the observation (e.g., bad bias) rendering the spectrum unusable (4); the object was much fainter than the published magnitude (1); and a high-quality spectrum had already been published (1). Thus our sample is defined by criteria which are uncorrelated with any absorber properties. This is important because several objects in our sample have absorption systems which were known at the time of the observations and might otherwise raise questions about bias in the sample.

## 3. OBSERVATIONS AND DATA REDUCTION

In Table 1 we show a journal of our observations. In this table is the object name, quasar emission redshift, wavelength range in angstroms, FWHM spectral resolution in angstroms, date, instrument, integration time in minutes, and spectrum identification. In the instrument column, P200 DS is the Palomar Double Spectrograph, MMT blue is the MMT blue channel, and MMT red is the MMT low-resolution echellette spectrograph. For observations with the P200 DS and MMT blue channel, the spectral resolution listed is the average FWHM of several calibration-lamp lines over the width of the spectrum. For the MMT red channel observations the resolution is given in terms of $X_\lambda$, which is defined by $X_\lambda \equiv \lambda/3000$ Å.

The spectra labeled "MMT blue" in Table 1 were obtained at the Multiple Mirror Telescope with the blue spectrograph, "Big Blue" image tube and photon-counting Reticon (Latham 1982). The 800 line mm$^{-1}$ grating was used in second order with the image stacker (Chaffee & Latham 1982), resulting in spectral resolution of about 120 km s$^{-1}$ FWHM. Each QSO was placed alternately in one of two sets of apertures, and sky spectra were recorded simultaneously in the other aperture. Pixel-to-pixel variations in detector response were divided out using a long quartz-lamp exposure obtained during the day. At the beginning and end of each object integration, a short exposure of a helium-neon-argon-cadmium-mercury lamp was obtained to calibrate the wavelength-to-pixel transformation. Individual exposures of each QSO were wavelength-calibrated with bracketing arcs, rebinned to a linear wavelength scale, and co-added. A variance array for each spectrum, derived from the total object and sky counts, was maintained throughout. Exposures of IIDS standard stars were obtained at the beginning and end of each night to look for residual instrumental features. Data were reduced using standard routines with the Ohio State IRS software package as implemented at Steward Observatory. No flux calibration was performed.

The spectra labeled "MMT red" in Table 1 were obtained at the Multiple Mirror Telescope with the red channel CCD spectrograph used in low-resolution cross-dispersed mode (Schmidt, Weymann, & Foltz 1989). This instrument consists of a cross-dispersion prism together with an 81 line mm$^{-1}$ grating used in orders 4–8. This was used with a 1200 × 800 Loral CCD and a 2″ × 20″ slit, giving a resolution of 350 km s$^{-1}$. The observations included bias frames and dome flats obtained during the day, quartz flats taken after each object exposure, and helium-neon-argon comparison lamps bracketing each exposure. The spectra were reduced using the IRAF `noao.imred.echelle` package. After wavelength calibration, the individual echelle orders were divided by the continuum fit of a standard star (observed and reduced in the same manner) and then combined. The resulting spectra are thus not flux-calibrated. The variance array for each spectrum was calculated using the known noise characteristics of the CCD.

The "PS 200" observations at the Palomar 5 m telescope used the double spectrograph instrument (Oke & Gunn 1982) with a 2″ slit. In 1988 June the TI-CCD No. 8 was used in the blue side of the spectrograph with the 600 line mm$^{-1}$ grating in first order. The resulting resolution is 180 km s$^{-1}$ (FWHM). The TI-CCD No. 2 was used in the red side with the 600 line mm$^{-1}$ grating in first order, with resulting spectral resolution of 360 km s$^{-1}$. In 1988 July the TI-CCD No. 432 was used in the blue side of the spectrograph with the 300 line mm$^{-1}$ grating in first order. The resulting resolution is 180 km s$^{-1}$. The TI-CCD No. 167 was used in the red side with the 310 line mm$^{-1}$ grating in first order, with resulting spectral resolution of 330 km s$^{-1}$. For both sets of observations, bias frames and dome flats were taken during the day, and iron-argon and helium-neon-argon comparison-lamp exposures bracketed each object integration. A standard star was observed at the beginning and end of each night. The spectra were reduced using the IRAF `noao.twodspec` package. This included flux calibration using standard stars. In the data taken in 1988 July there was a severe problem with the flat-fielding below 4100 Å. For unknown reasons the position of defects on the chip appears to have been unstable by one to two pixels in the wavelength direction. This means that in many of these spectra there are spurious features which can be mistaken for absorption lines. In addition, below about 3900 Å many of the spectra show significant continuum structure which is clearly an artifact. For this reason we do not apply our line-finding algorithm to this spectral region, nor do we include it in any statistical analyses.

TABLE 1

JOURNAL OF OBSERVATIONS

| Object | | $z_{em}$ | $m_V$ | Wavelength | FWHM | Date | Instrument | $t_{int}$ | Sp. # |
|---|---|---|---|---|---|---|---|---|---|
| Q0056-0009 | PHL 923 | 0.717 | 17.3 | 3104 - 4727 | 4.7 | 10-Jul-88 | P200 DS | 50 | 1 |
| | | | | 4832 - 7242 | 6.5 | 10-Jul-88 | P200 DS | 50 | 2 |
| Q0159-1147 | 3C 57 | 0.670 | 16.4 | 4035 - 5064 | 1.5 | 05-Mar-89 | MMT blue | 30 | 1 |
| Q0229+1309 | PKS 0229+13 | 2.065 | 17.7 | 4249 - 8145 | $3.5X_\lambda$ | 05-Dec-88 | MMT red | 60 | 1 |
| Q0229+3410 | 3C 68.1 | 1.240 | 19.0 | 4657 - 8156 | $3.7X_\lambda$ | 05-Dec-88 | MMT red | 120 | 1 |
| Q0237-2322 | PKS 0237-23 | 2.224 | 16.6 | 4291 - 8156 | $3.7X_\lambda$ | 05-Dec-88 | MMT red | 30 | 1 |
| Q0350-0719 | 3C 94 | 0.962 | 16.5 | 4277 - 8124 | $3.7X_\lambda$ | 04-Dec-88 | MMT red | 40 | 1 |
| Q0420-0127 | PKS 0420-01 | 0.915 | 17.0 | 4259 - 8167 | $3.7X_\lambda$ | 05-Dec-88 | MMT red | 30 | 1 |
| Q0538+4949 | 3C 147 | 0.545 | 17.8 | 3220 - 5064 | 1.6 | 05-Mar-89 | MMT blue | 120 | 1 |
| Q0610+2605 | 3C 154 | 0.580 | 17.5 | 3221 - 5071 | 1.6 | 08-Nov-88 | MMT blue | 100 | 1 |
| Q0642+4454 | OH 471 | 3.400 | 18.5 | 4291 - 8156 | $3.7X_\lambda$ | 05-Dec-88 | MMT red | 60 | 1 |
| Q0710+1151 | 3C 175 | 0.768 | 16.6 | 3118 - 5068 | 1.6 | 08-Nov-88 | MMT blue | 40 | 1 |
| Q0725+1443 | 3C 181 | 1.382 | 18.9 | 4291 - 8135 | $3.7X_\lambda$ | 05-Dec-88 | MMT red | 60 | 1 |
| Q0736-0620 | PKS 0736-06 | 1.898 | 18.5 | 4259 - 8156 | $3.7X_\lambda$ | 05-Dec-88 | MMT red | 30 | 1 |
| Q0809+4822 | 3C 196 | 0.871 | 17.8 | 3137 - 5119 | 1.6 | 08-Jan-89 | MMT blue | 120 | 1 |
| Q0835+5804 | 3C 205 | 1.534 | 17.6 | 4249 - 8156 | $3.7X_\lambda$ | 05-Dec-88 | MMT red | 30 | 1 |
| Q0855+1421 | 3C 212 | 1.043 | 19.1 | 4506 - 9371 | $3.5X_\lambda$ | 06-May-89 | MMT red | 90 | 1 |
| Q0859-1403 | PKS 0859-14 | 1.327 | 16.6 | 3200 - 5066 | 1.6 | 08-Nov-88 | MMT blue | 30 | 1 |
| | | | | 4452 - 10182 | $3.3X_\lambda$ | 11-Apr-89 | MMT red | 30 | 2 |
| Q0906+4305 | 3C 216 | 0.670 | 18.1 | 3114 - 5061 | 1.6 | 08-Nov-88 | MMT blue | 60 | 1 |
| Q1007+4147 | 4C 41.21 | 0.613 | 16.2 | 3158 - 5067 | 1.6 | 08-Nov-88 | MMT blue | 15 | 1 |
| Q1040+1219 | 3C 245 | 1.029 | 17.3 | 3139 - 5123 | 1.6 | 08-Jan-89 | MMT blue | 60 | 1 |
| Q1055+2007 | PKS 1055+20 | 1.110 | 17.1 | 3142 - 5122 | 1.6 | 08-Jan-89 | MMT blue | 30 | 1 |
| | | | | 5040 - 8115 | 3.5 | 12-Apr-89 | MMT red | 30 | 2 |
| Q1111+4053 | 3C 254 | 0.734 | 18.0 | 3129 - 5064 | 1.6 | 05-Mar-89 | MMT blue | 60 | 1 |
| Q1136-1334 | PKS 1136-13 | 0.554 | 16.2 | 3180 - 5061 | 1.6 | 05-Mar-89 | MMT blue | 53 | 1 |
| Q1137+6604 | 3C 263 | 0.652 | 16.3 | 3198 - 5062 | 1.6 | 05-Mar-89 | MMT blue | 20 | 1 |
| Q1148-0007 | PKS 1148-00 | 1.982 | 17.6 | 4480 - 10004 | $3.5X_\lambda$ | 07-May-89 | MMT red | 30 | 1 |
| Q1153+3144 | 4C 31.38 | 0.418 | 19.0 | 4444 - 10057 | $3.5X_\lambda$ | 12-Apr-89 | MMT red | 100 | 1 |
| Q1156+2931 | 4C 29.45 | 0.729 | 14.4 | 3175 - 5059 | 1.6 | 08-Jan-89 | MMT blue | 55 | 1 |
| Q1206+4356 | 3C 268.4 | 1.400 | 18.4 | 4506 - 10091 | $3.5X_\lambda$ | 06-May-89 | MMT blue | 45 | 1 |
| Q1213+5352 | 4C 53.24 | 1.065 | 18.0 | 4542 - 9898 | $3.2X_\lambda$ | 07-May-89 | MMT red | 45 | 1 |
| Q1218+3359 | 3C 270.1 | 1.519 | 18.6 | 3137 - 4704 | 4.9 | 09-Jul-88 | P200 DS | 30 | 1 |
| | | | | 4827 - 7243 | 6.6 | 09-Jul-88 | P200 DS | 30 | 2 |
| Q1229-0207 | PKS 1229-02 | 1.038 | 16.8 | 4486 - 10111 | $3.5X_\lambda$ | 06-May-89 | P200 DS | 20 | 1 |
| Q1318+1122 | PKS 1318+11 | 2.171 | 19.1 | 3258 - 4705 | 4.9 | 10-Jul-88 | P200 DS | 40 | 1 |
| | | | | 4820 - 7239 | 6.7 | 10-Jul-88 | P200 DS | 40 | 2 |
| Q1327-2126 | PKS 1327-21 | 0.528 | 16.7 | 3190 - 5062 | 1.6 | 05-Mar-89 | MMT blue | 60 | 1 |
| Q1328+2524 | 3C 287 | 1.055 | 17.7 | 4452 - 10165 | $3.3X_\lambda$ | 12-Apr-89 | MMT red | 50 | 1 |
| Q1328+3045 | 3C 286 | 0.846 | 17.2 | 3104 - 4742 | 4.9 | 10-Jul-88 | P200 DS | 30 | 1 |
| | | | | 4817 - 7251 | 6.7 | 10-Jul-88 | P200 DS | 30 | 2 |
| Q1335-0611 | PKS 1335-06 | 0.625 | 17.7 | 3261 - 5066 | 1.6 | 05-Mar-89 | MMT blue | 95 | 1 |
| Q1354-1512 | PKS 1354-15 | 1.890 | 18.5 | 4571 - 9838 | $3.2X_\lambda$ | 07-May-89 | MMT red | 75 | 1 |
| Q1437+6224 | OQ 663 | 1.090 | 19.0 | 4560 - 10111 | $3.3X_\lambda$ | 06-May-89 | MMT red | 90 | 1 |
| Q1442+1011 | OQ 172 | 3.530 | 17.8 | 4435 - 10135 | $3.3X_\lambda$ | 12-Apr-89 | MMT red | 74 | 1 |
| Q1453-1056 | PKS 1453-10 | 0.938 | 17.4 | 3302 - 4708 | 5.1 | 09-Jul-88 | P200 DS | 20 | 1 |
| | | | | 4827 - 7249 | 6.5 | 09-Jul-88 | P200 DS | 20 | 2 |
| Q1458+7152 | 3C 309.1 | 0.905 | 16.8 | 3740 - 4607 | 2.5 | 18-Jun-88 | P200 DS | 30 | 1 |
| | | | | 4683 - 5976 | 3.8 | 18-Jun-88 | P200 DS | 30 | 2 |
| Q1508-0531 | PKS 1508-05 | 1.191 | 18.5 | 3135 - 4729 | 4.9 | 10-Jul-88 | P200 DS | 30 | 1 |
| | | | | 4823 - 7242 | 6.7 | 10-Jul-88 | P200 DS | 30 | 2 |
| Q1618+1743 | 3C 334 | 0.555 | 16.4 | 3111 - 4727 | 4.9 | 10-Jul-88 | P200 DS | 20 | 1 |
| | | | | 4826 - 7235 | 6.7 | 10-Jul-88 | P200 DS | 20 | 2 |
| Q1622+2352 | 3C 336 | 0.927 | 17.5 | 3742 - 4613 | 2.4 | 16-Jun-88 | P200 DS | 90 | 1 |
| | | | | 4684 - 5982 | 3.5 | 16-Jun-88 | P200 DS | 90 | 2 |
| Q1629+1202 | PKS 1629+12 | 1.795 | 18.4 | 3137 - 4710 | 5.1 | 09-Jul-88 | P200 DS | 40 | 1 |
| | | | | 4821 - 7234 | 6.7 | 09-Jul-88 | P200 DS | 40 | 2 |
| | | | | 3741 - 4613 | 2.5 | 18-Jun-88 | P200 DS | 60 | 3 |
| | | | | 4718 - 5981 | 3.8 | 18-Jun-88 | P200 DS | 60 | 4 |
| Q1634+6251 | 3C 343 | 0.988 | 20.6 | 4580 - 10004 | $3.3X_\lambda$ | 07-May-89 | MMT red | 135 | 1 |
| Q1828+4842 | 3C 380 | 0.695 | 16.8 | 3104 - 4759 | 5.0 | 10-Jul-88 | P200 DS | 25 | 1 |
| | | | | 4817 - 7239 | 6.5 | 10-Jul-88 | P200 DS | 25 | 2 |
| | | | | 3740 - 4607 | 2.5 | 17-Jun-88 | P200 DS | 60 | 3 |
| | | | | 4694 - 5981 | 3.6 | 17-Jun-88 | P200 DS | 60 | 4 |
| | | | | 4527 - 10145 | $3.5X_\lambda$ | 06-May-89 | P200 DS | 30 | 5 |
| Q1901+3155 | 3C 395 | 0.635 | 17.5 | 3742 - 4613 | 2.4 | 16-Jun-88 | P200 DS | 60 | 1 |
| | | | | 4689 - 5977 | 3.6 | 16-Jun-88 | P200 DS | 60 | 2 |
| Q2003-0232 | 4C -02.79 | 1.457 | 19.0 | 3280 - 4708 | 5.0 | 09-Jul-88 | P200 DS | 50 | 1 |
| | | | | 4824 - 7154 | 6.5 | 09-Jul-88 | P200 DS | 50 | 2 |
| | | | | 3742 - 4613 | 2.5 | 16-Jun-88 | P200 DS | 60 | 3 |
| | | | | 4687 - 5979 | 3.6 | 16-Jun-88 | P200 DS | 60 | 4 |
| Q2044-0247 | 3C 422 | 0.942 | 19.5 | 3740 - 4613 | 2.5 | 18-Jun-88 | P200 DS | 67 | 1 |
| | | | | 4802 - 5975 | 3.8 | 18-Jun-88 | P200 DS | 67 | 2 |
| Q2115-3031 | PKS 2115-30 | 0.980 | 16.5 | 3211 - 4693 | 5.1 | 09-Jul-88 | P200 DS | 20 | 1 |
| | | | | 4831 - 7151 | 6.6 | 09-Jul-88 | P200 DS | 20 | 2 |
| Q2143-1541 | PKS 2143-15 | 0.700 | 0.0 | 3124 - 4729 | 4.9 | 10-Jul-88 | P200 DS | 45 | 1 |
| | | | | 4820 - 7242 | 6.7 | 10-Jul-88 | P200 DS | 45 | 2 |
| Q2223+2102 | PKS 2223+21 | 1.959 | 18.0 | 3137 - 4719 | 5.1 | 09-Jul-88 | P200 DS | 45 | 1 |
| | | | | 4827 - 7158 | 6.7 | 09-Jul-88 | P200 DS | 45 | 2 |
| Q2230+1128 | CTA 102 | 1.037 | 17.3 | 3157 - 4723 | 5.1 | 09-Jul-88 | P200 DS | 44 | 1 |
| | | | | 4827 - 7151 | 6.7 | 09-Jul-88 | P200 DS | 44 | 2 |
| Q2249+1832 | 3C 454 | 1.757 | 18.4 | 3104 - 4705 | 4.9 | 10-Jul-88 | P200 DS | 50 | 1 |
| | | | | 4823 - 7242 | 6.7 | 10-Jul-88 | P200 DS | 50 | 2 |
| Q2251+2429 | PKS 2251+24 | 2.328 | 17.8 | 3137 - 4673 | 5.0 | 09-Jul-88 | P200 DS | 45 | 1 |
| | | | | 4824 - 7158 | 6.7 | 09-Jul-88 | P200 DS | 45 | 2 |
| | | | | 4277 - 8123 | 6.5 | 04-Dec-88 | MMT red | 90 | 3 |

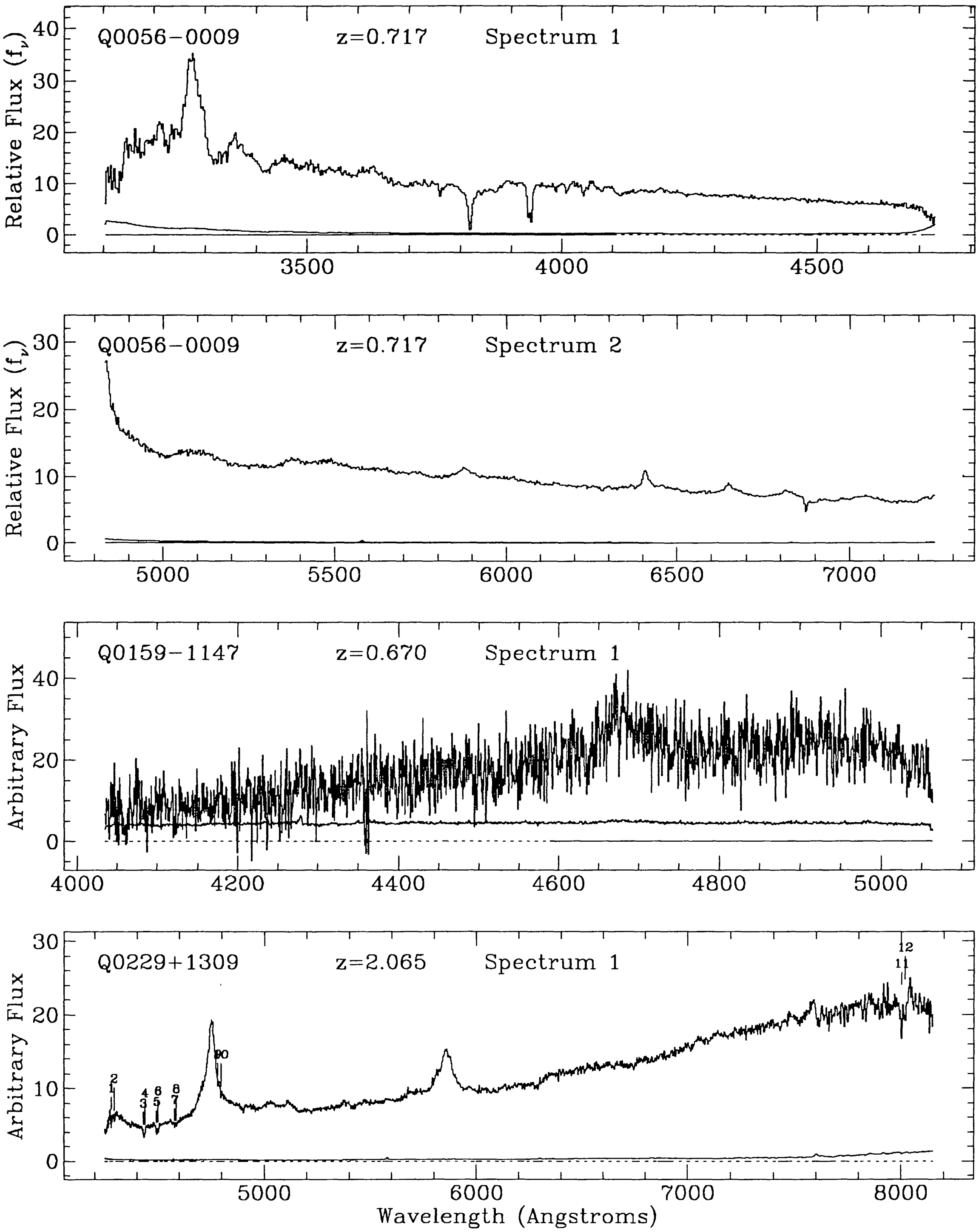


FIG. 1.—Quasar spectra

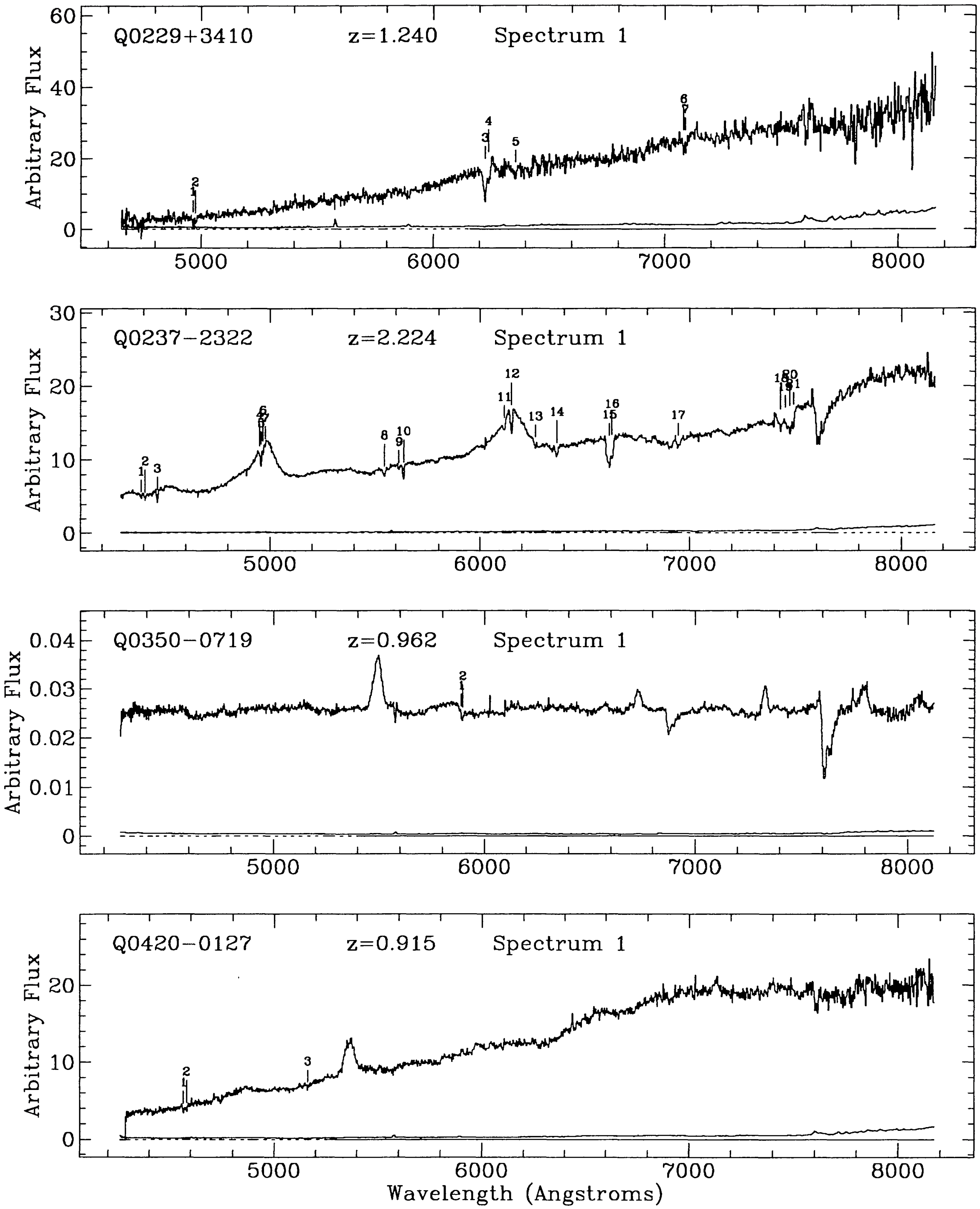


FIG. 1—*Continued*

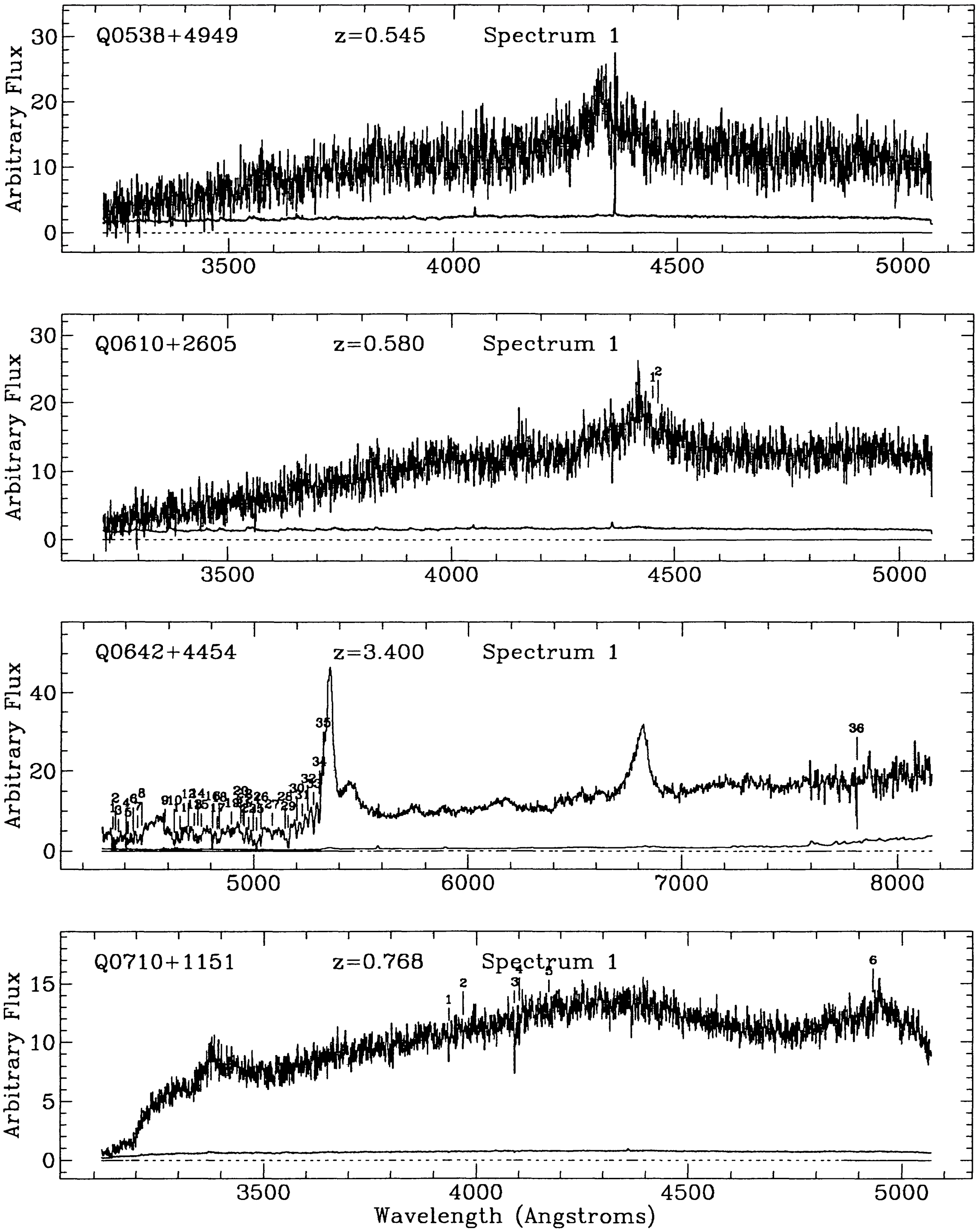


FIG. 1—*Continued*

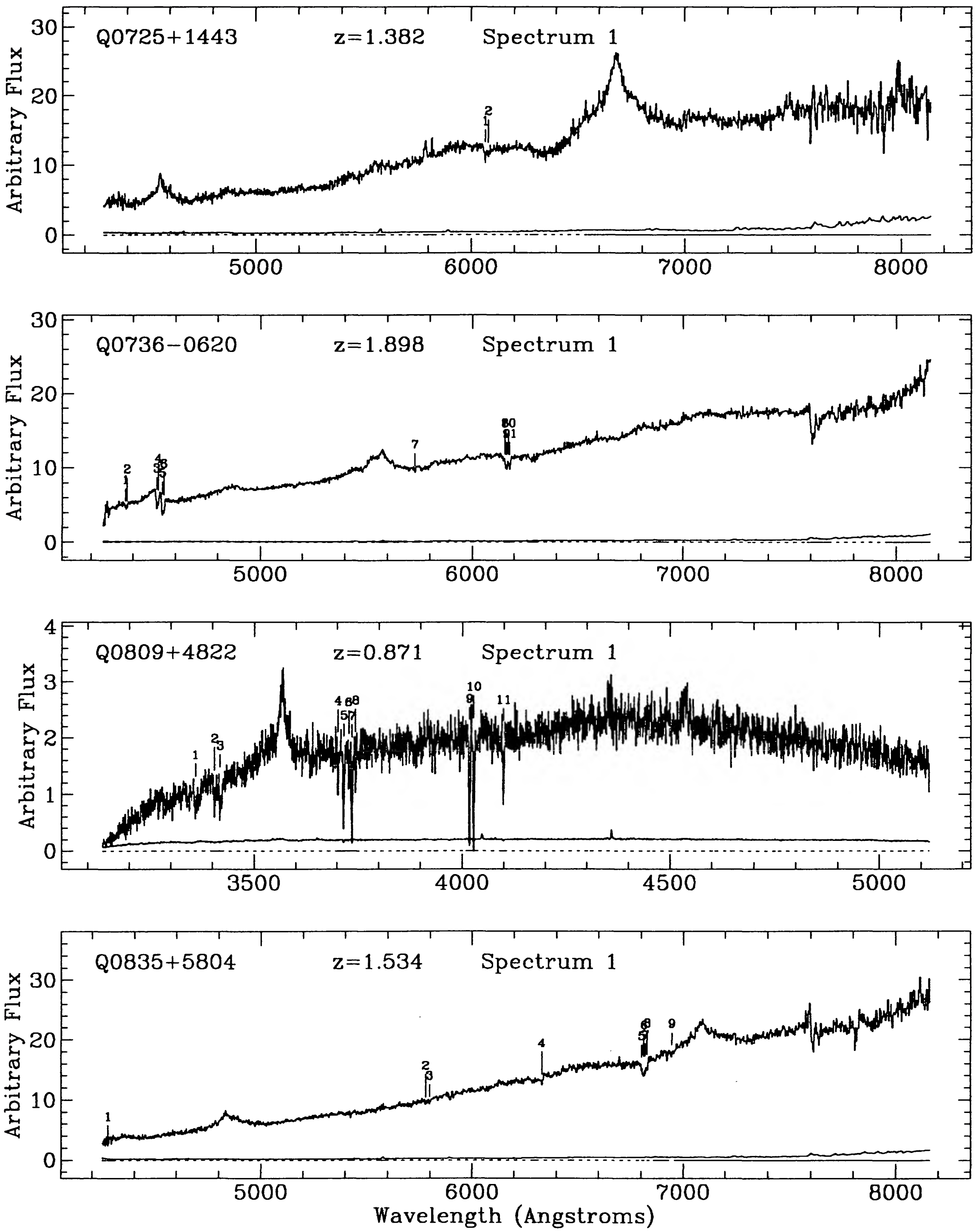


FIG. 1—*Continued*

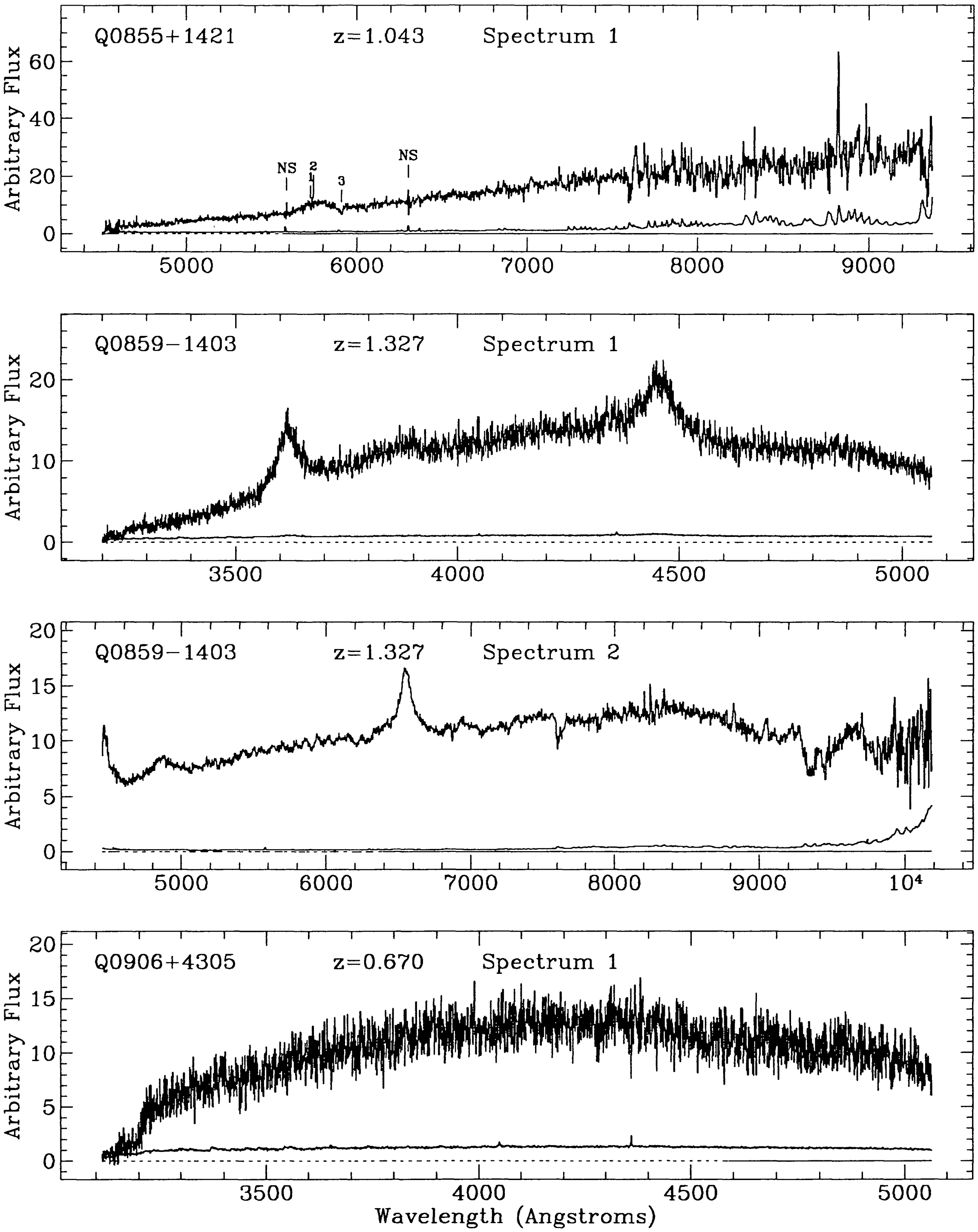


FIG. 1—*Continued*

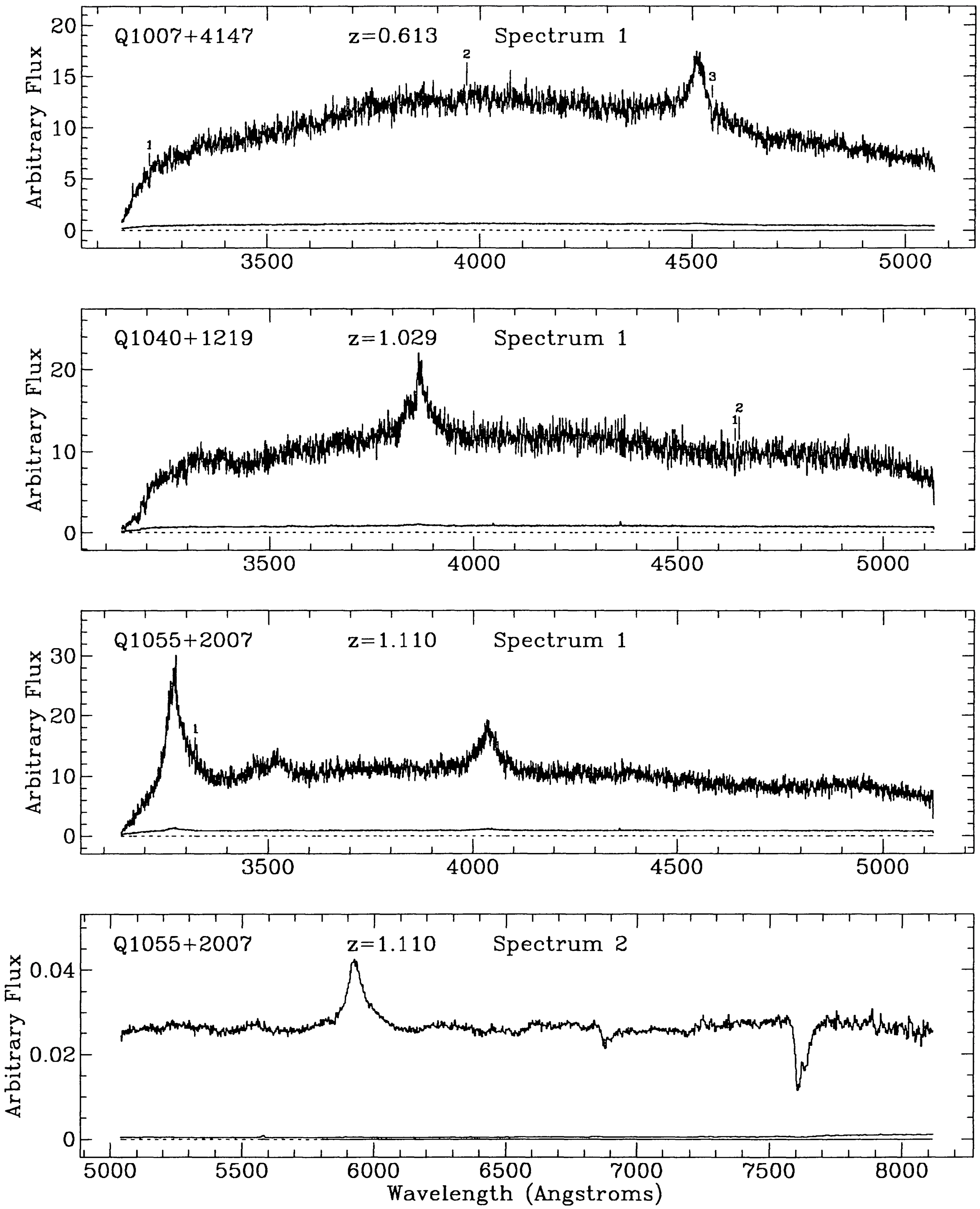


FIG. 1—*Continued*

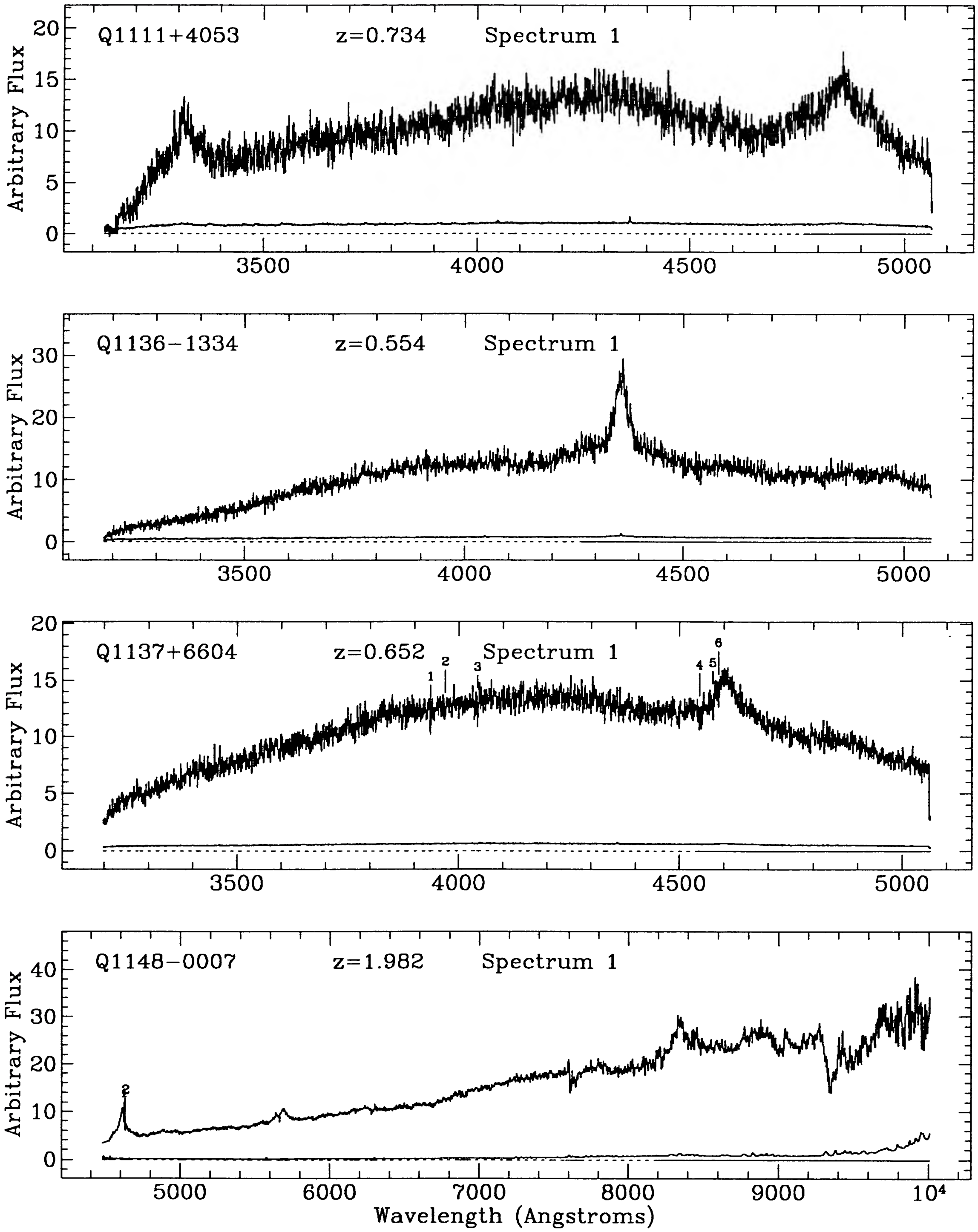


FIG. 1—*Continued*

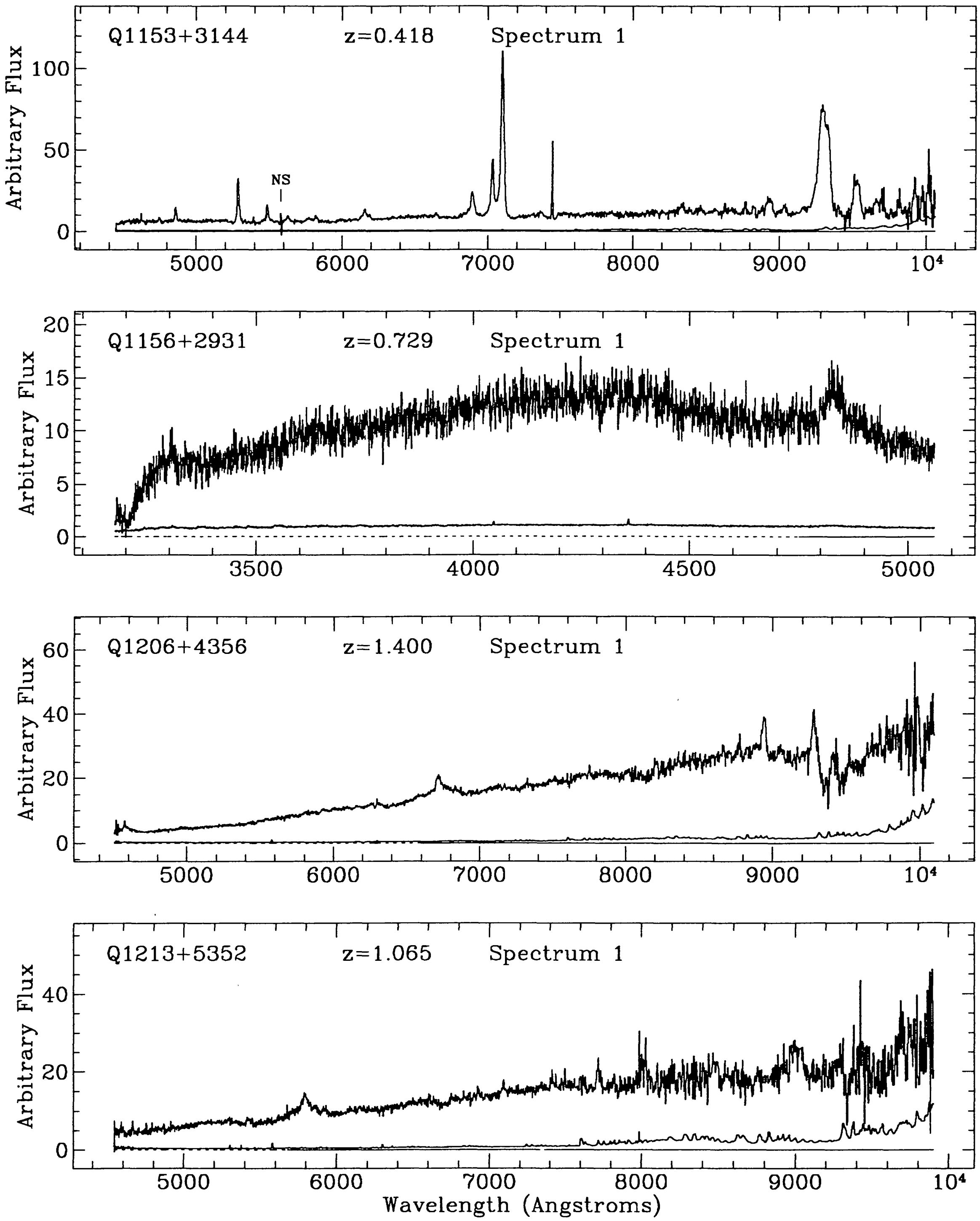


FIG. 1—*Continued*

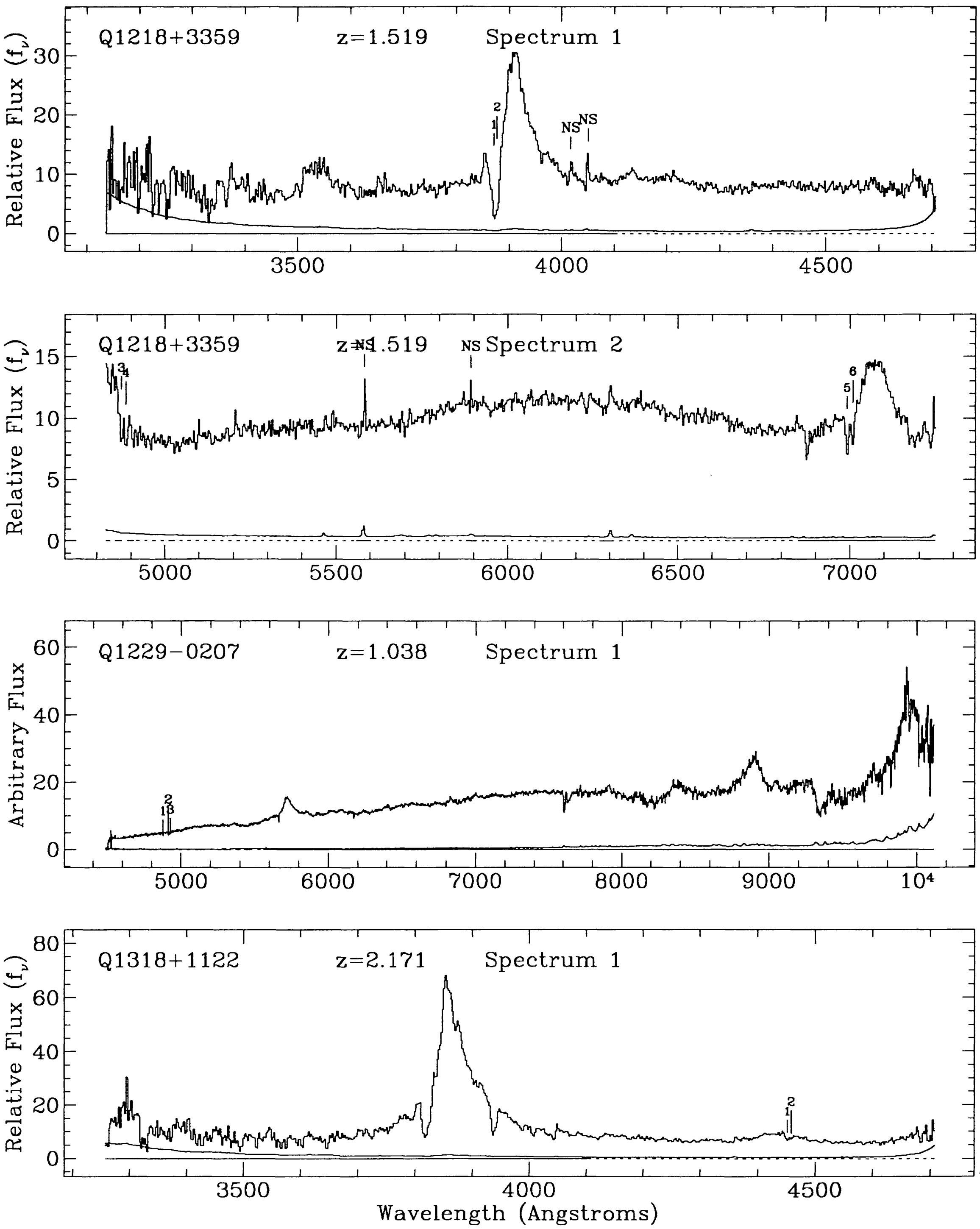


FIG. 1—*Continued*

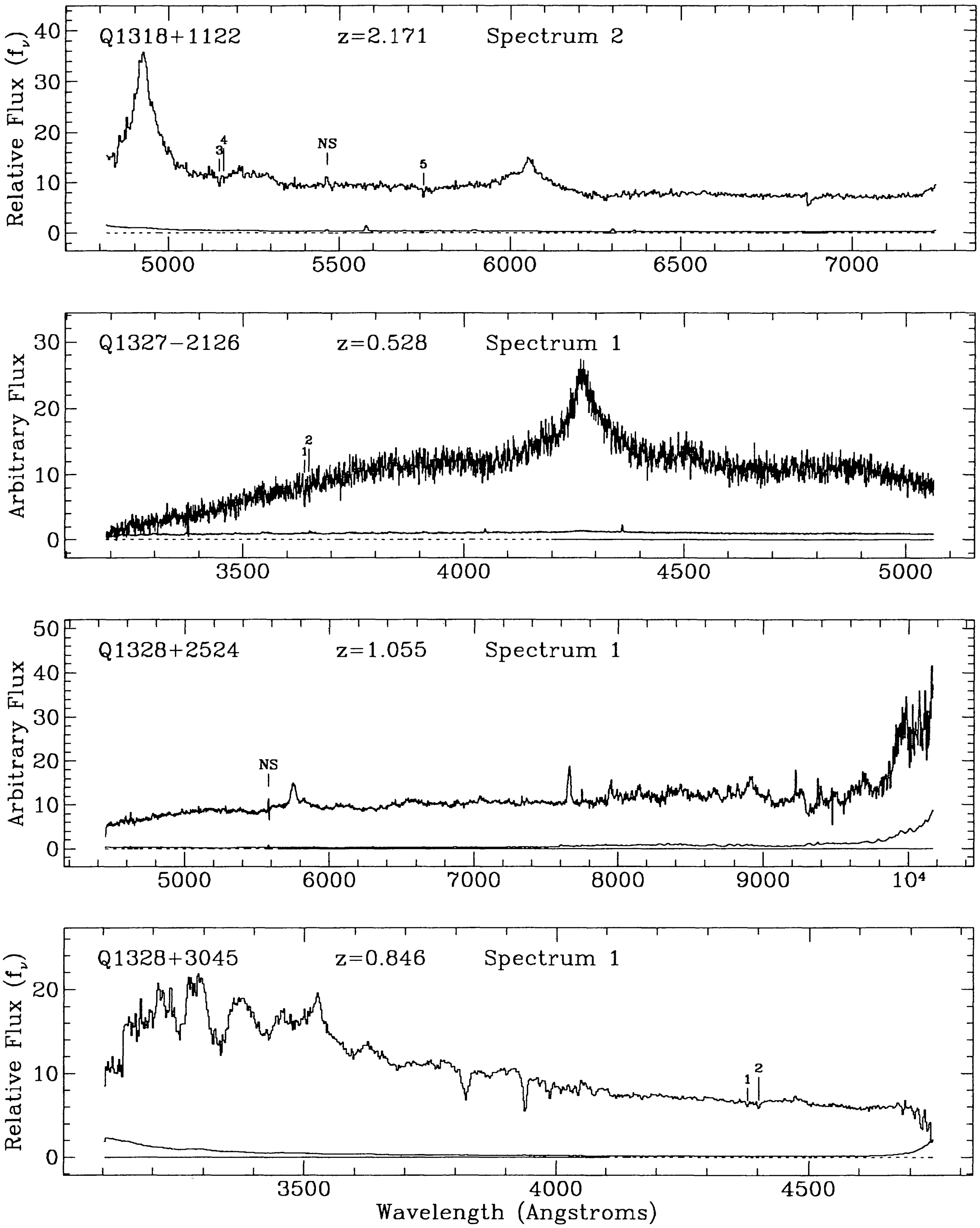


FIG. 1—*Continued*

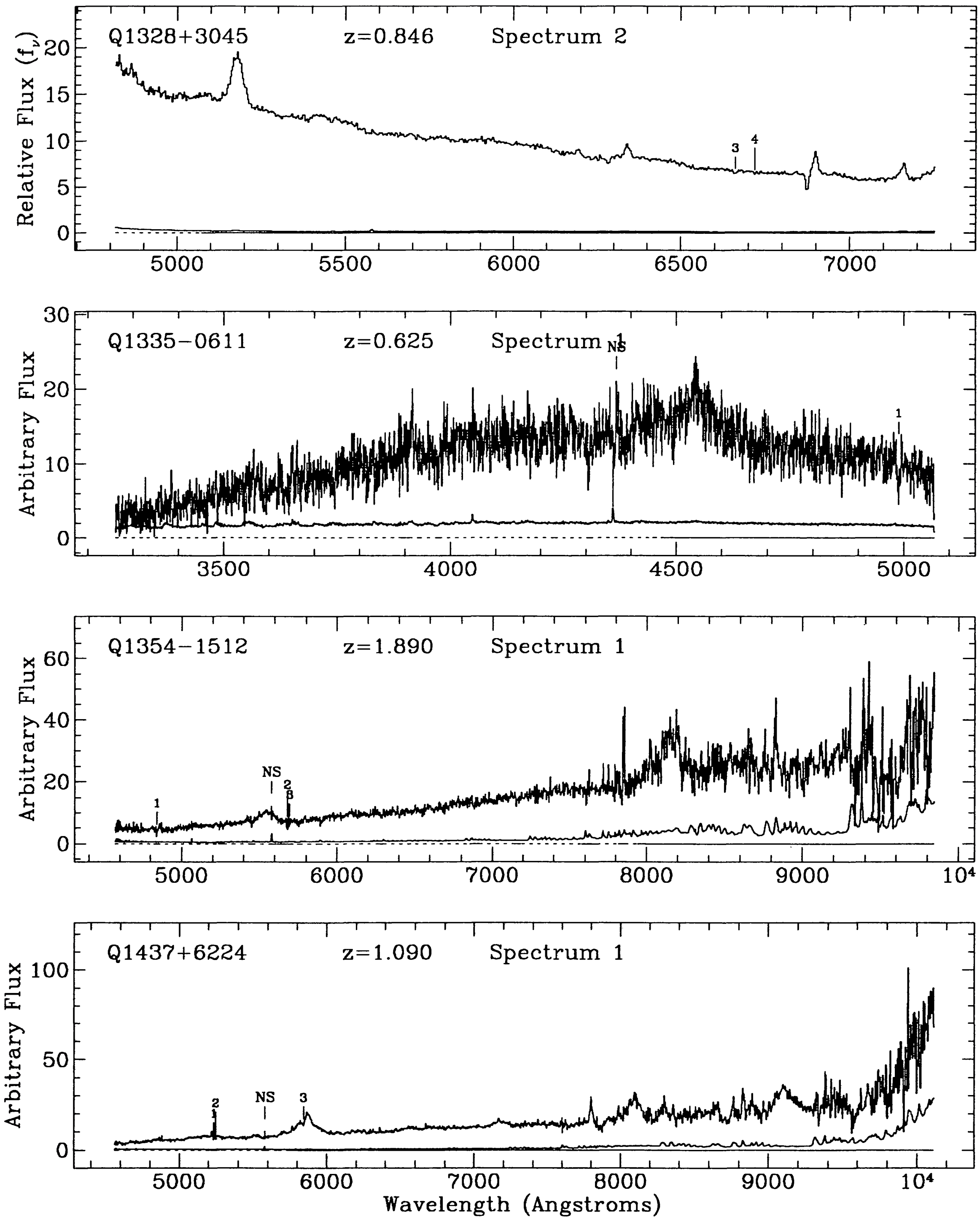


FIG. 1—*Continued*

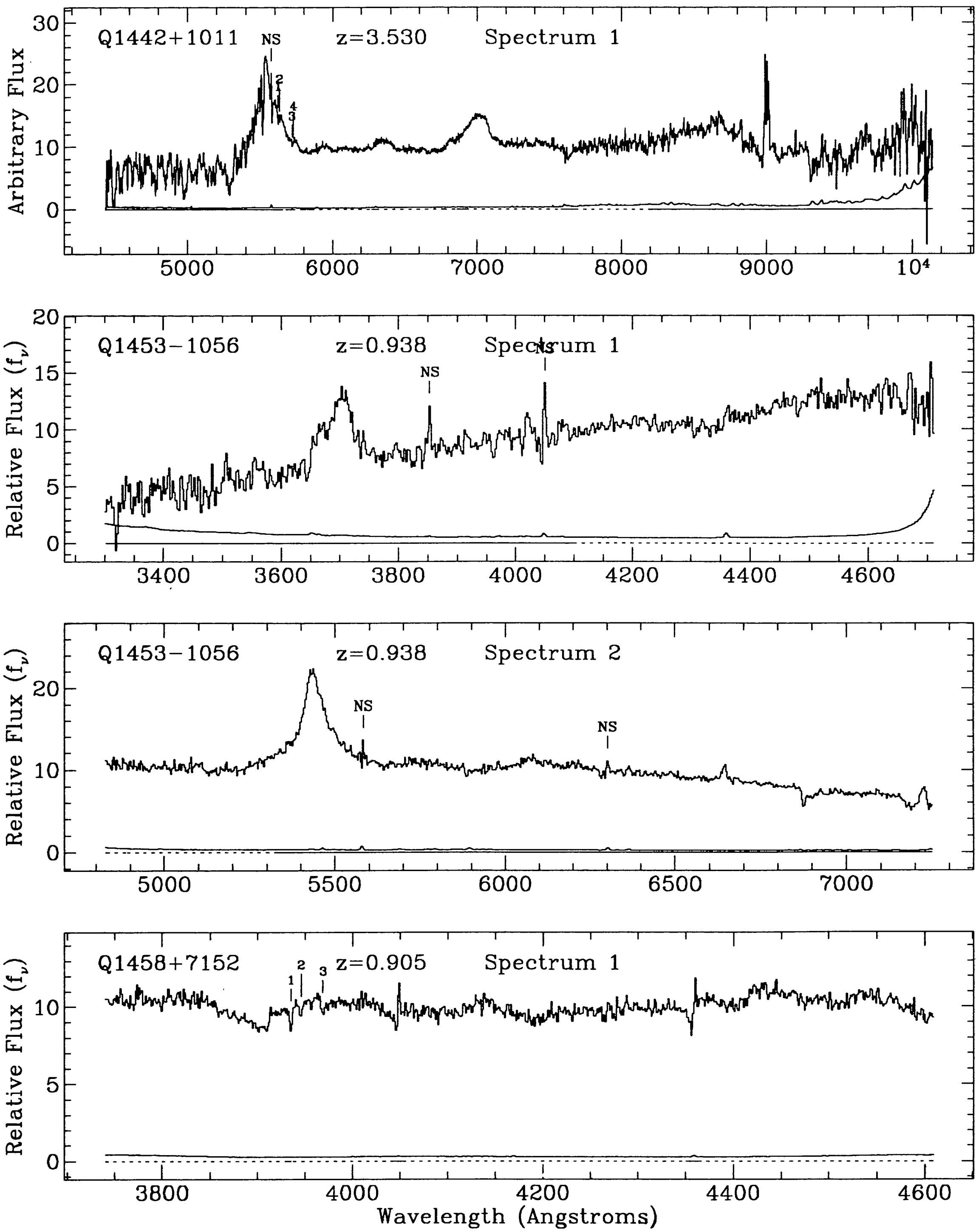


FIG. 1—*Continued*

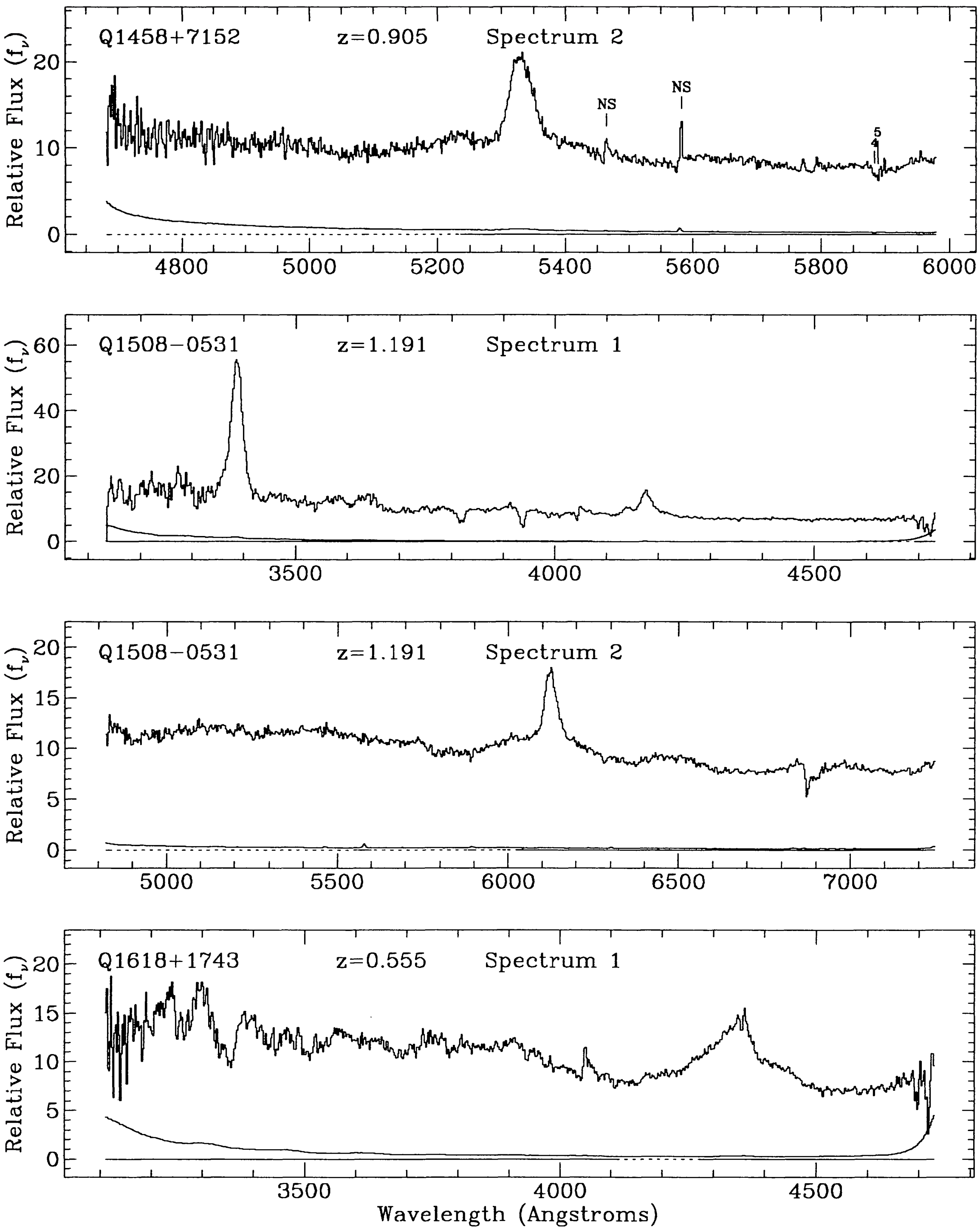


FIG. 1—*Continued*

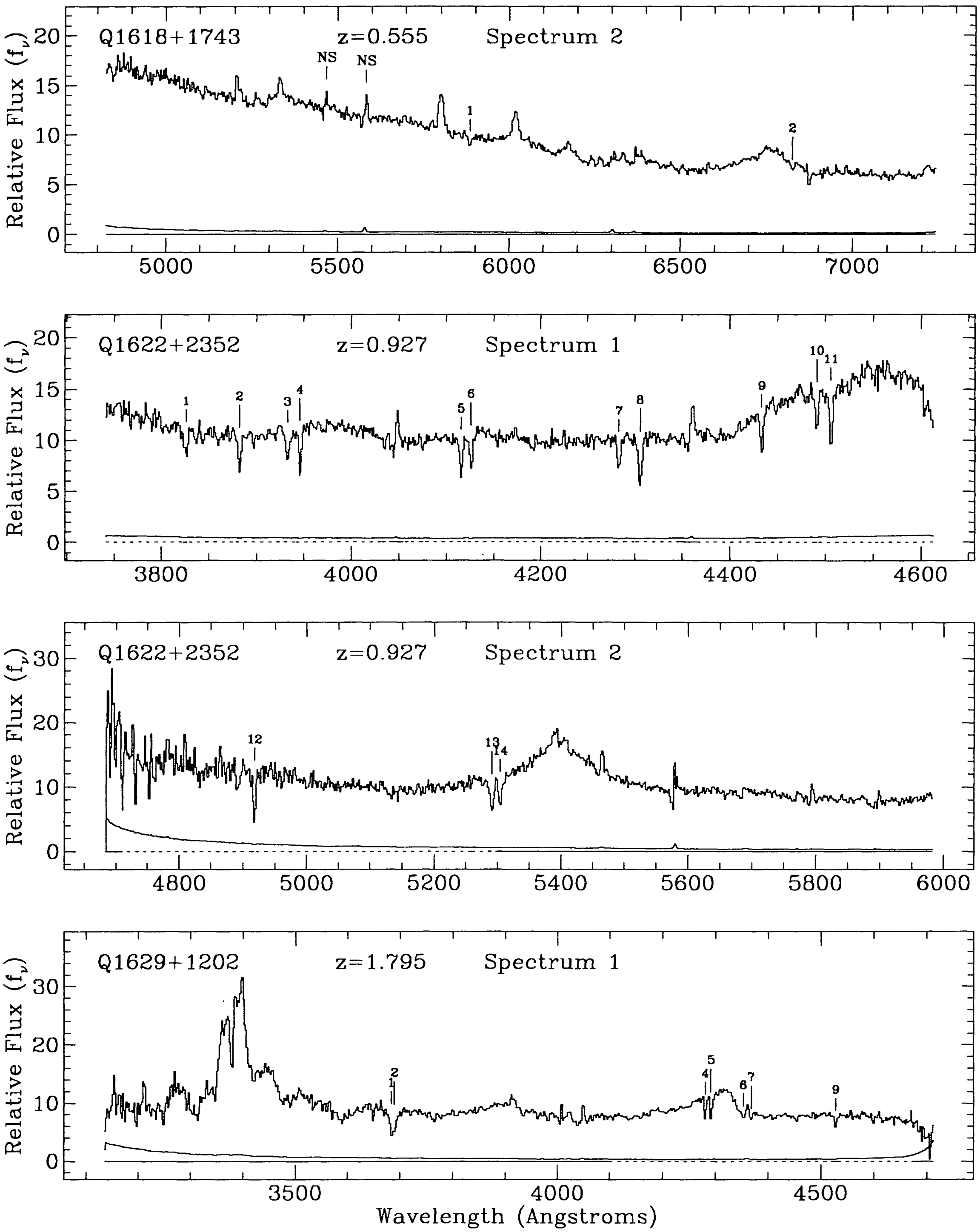


FIG. 1—*Continued*

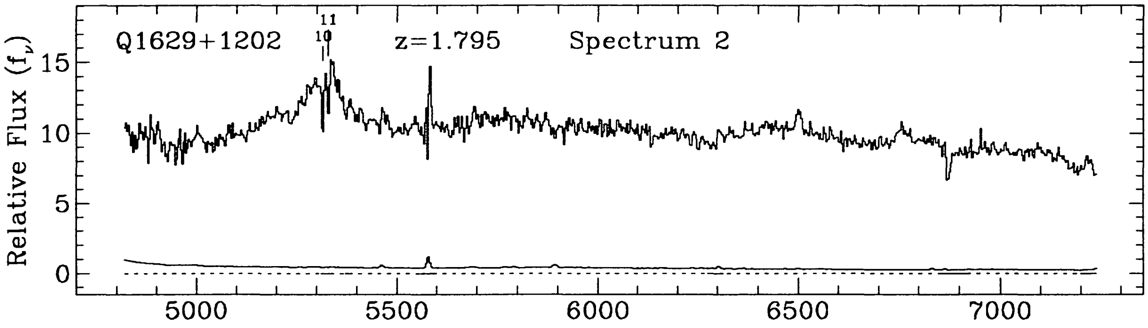


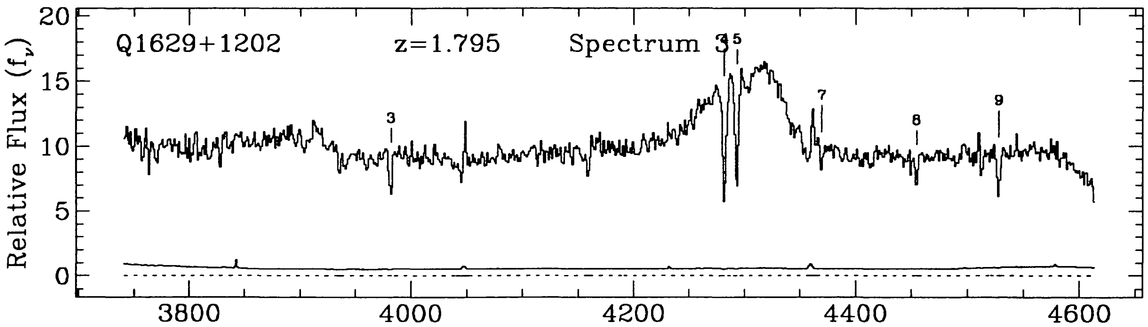


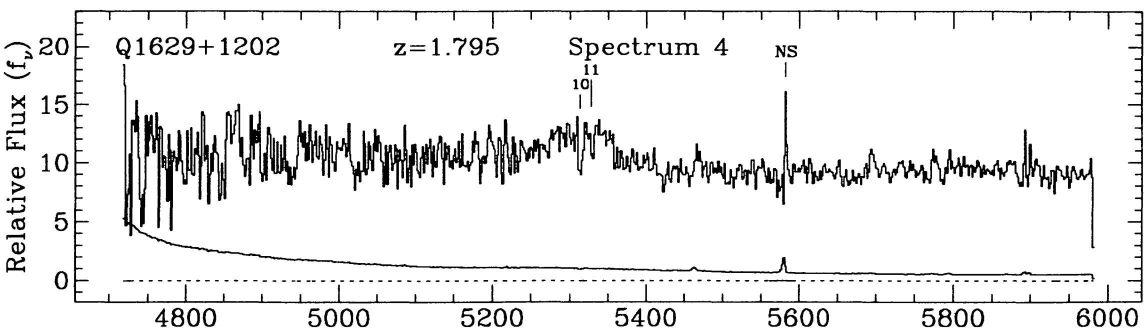


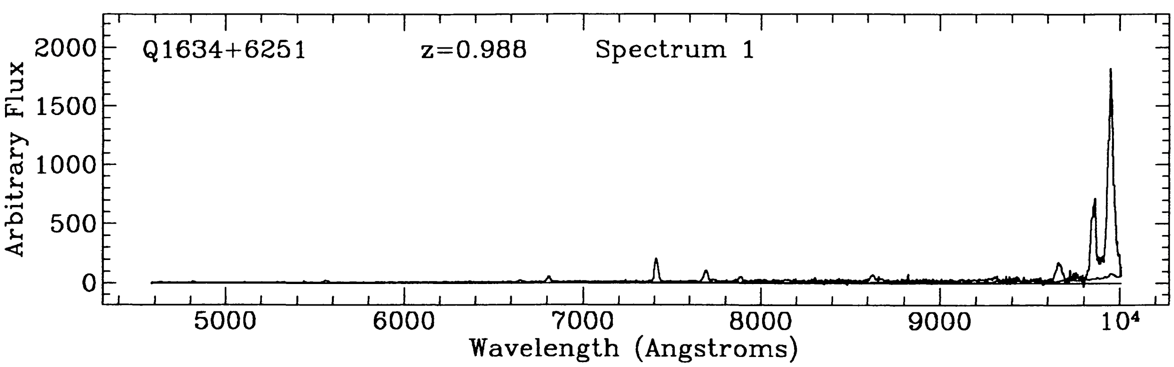


FIG. 1—*Continued*

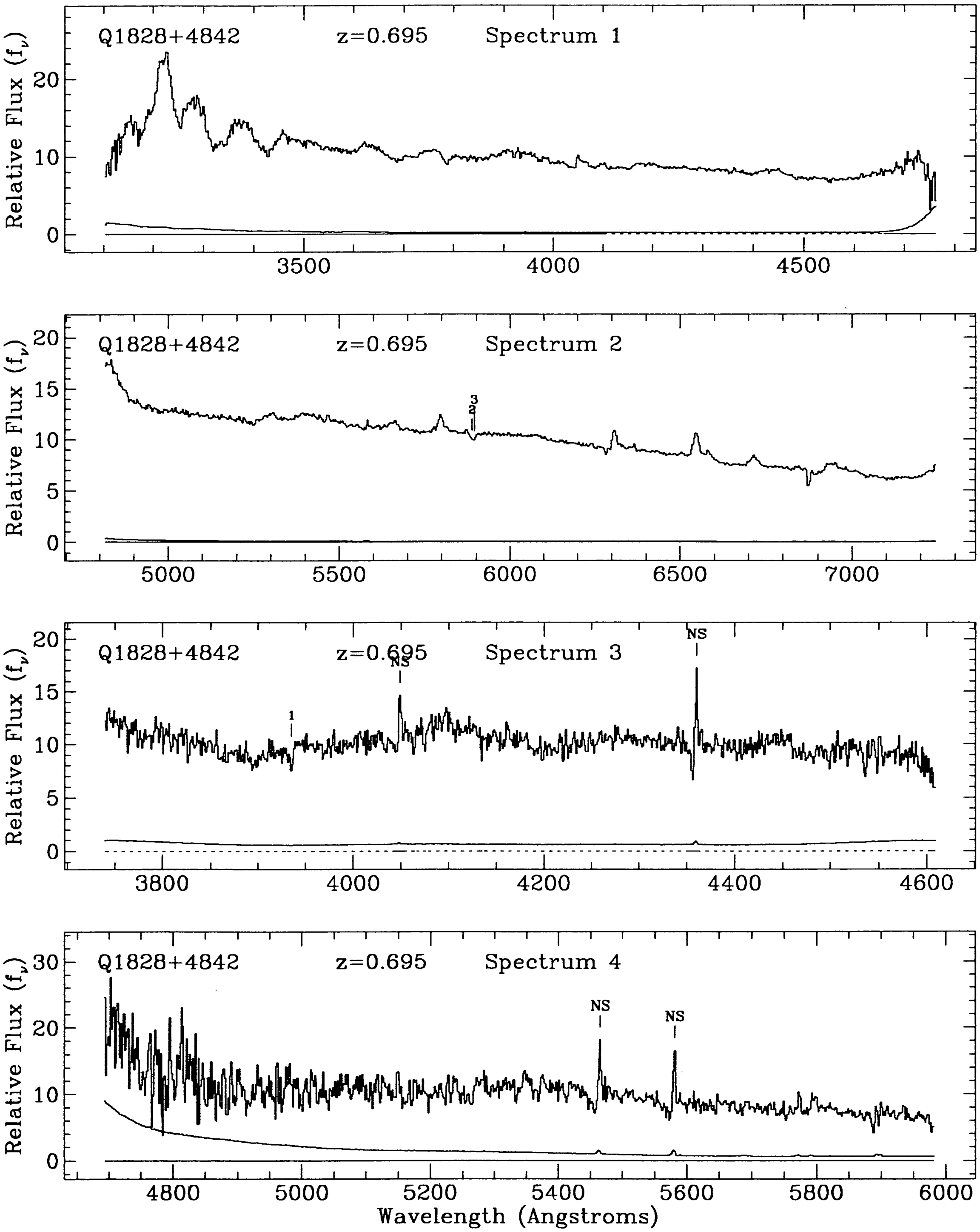


FIG. 1—*Continued*

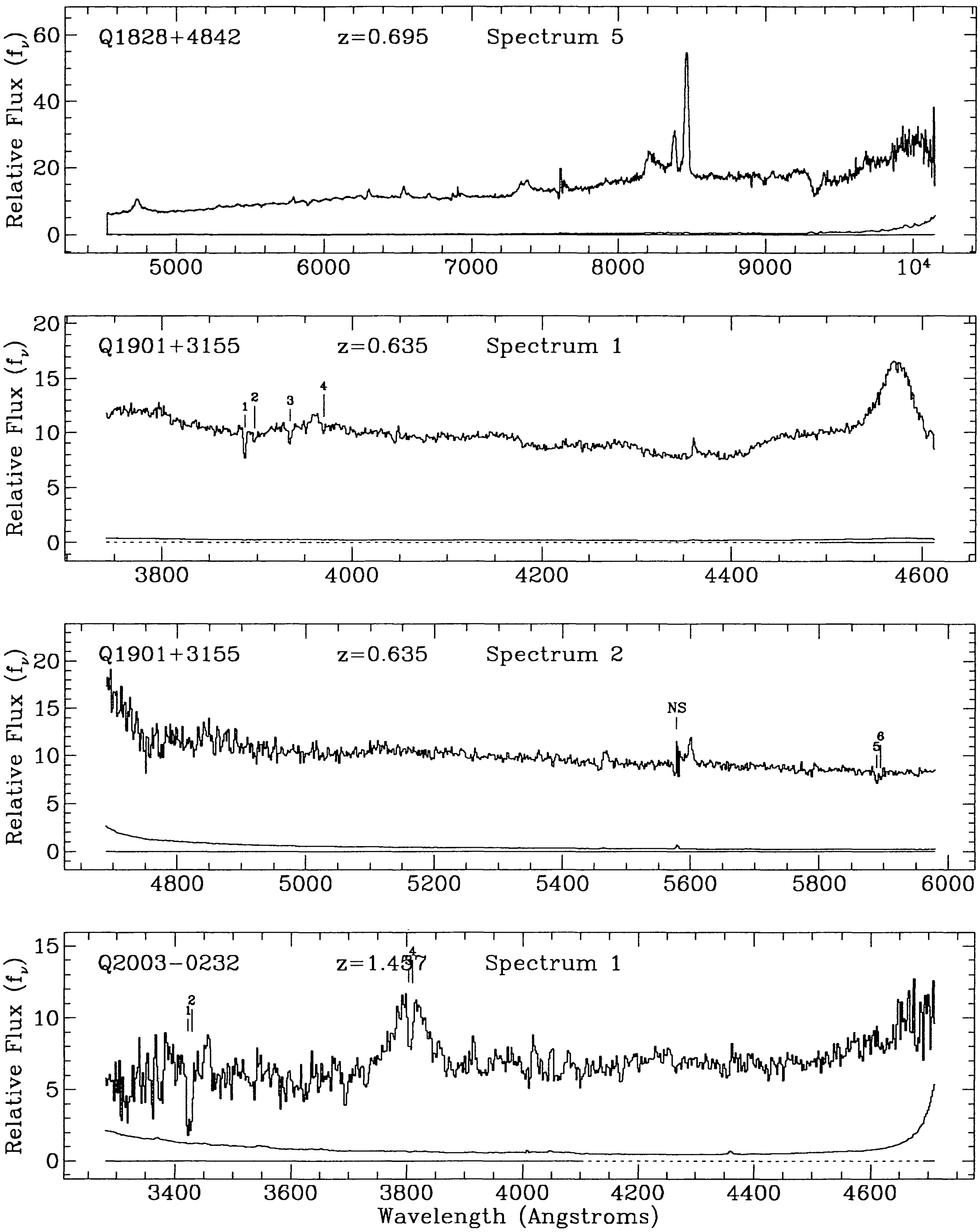


FIG. 1—*Continued*

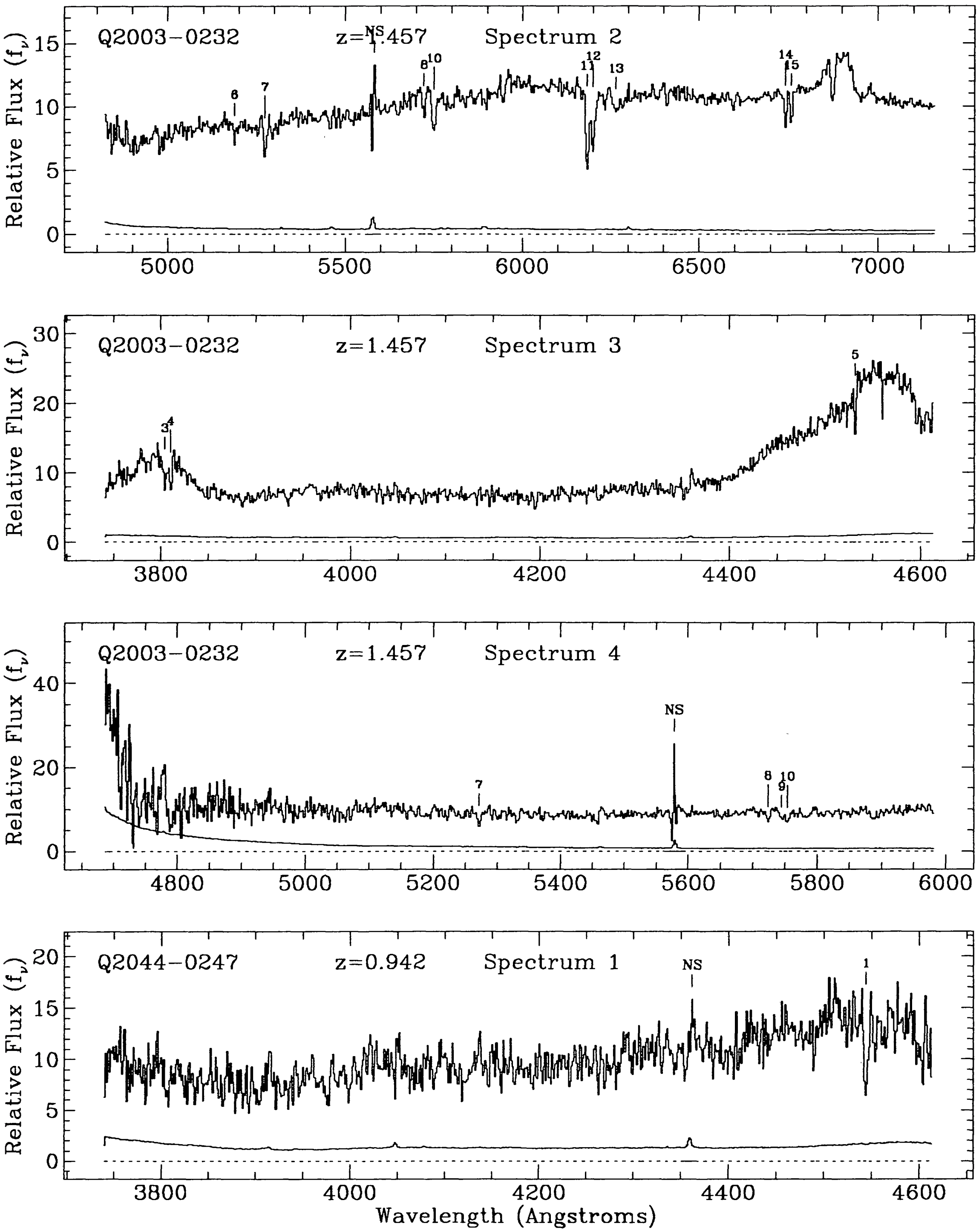


FIG. 1—*Continued*

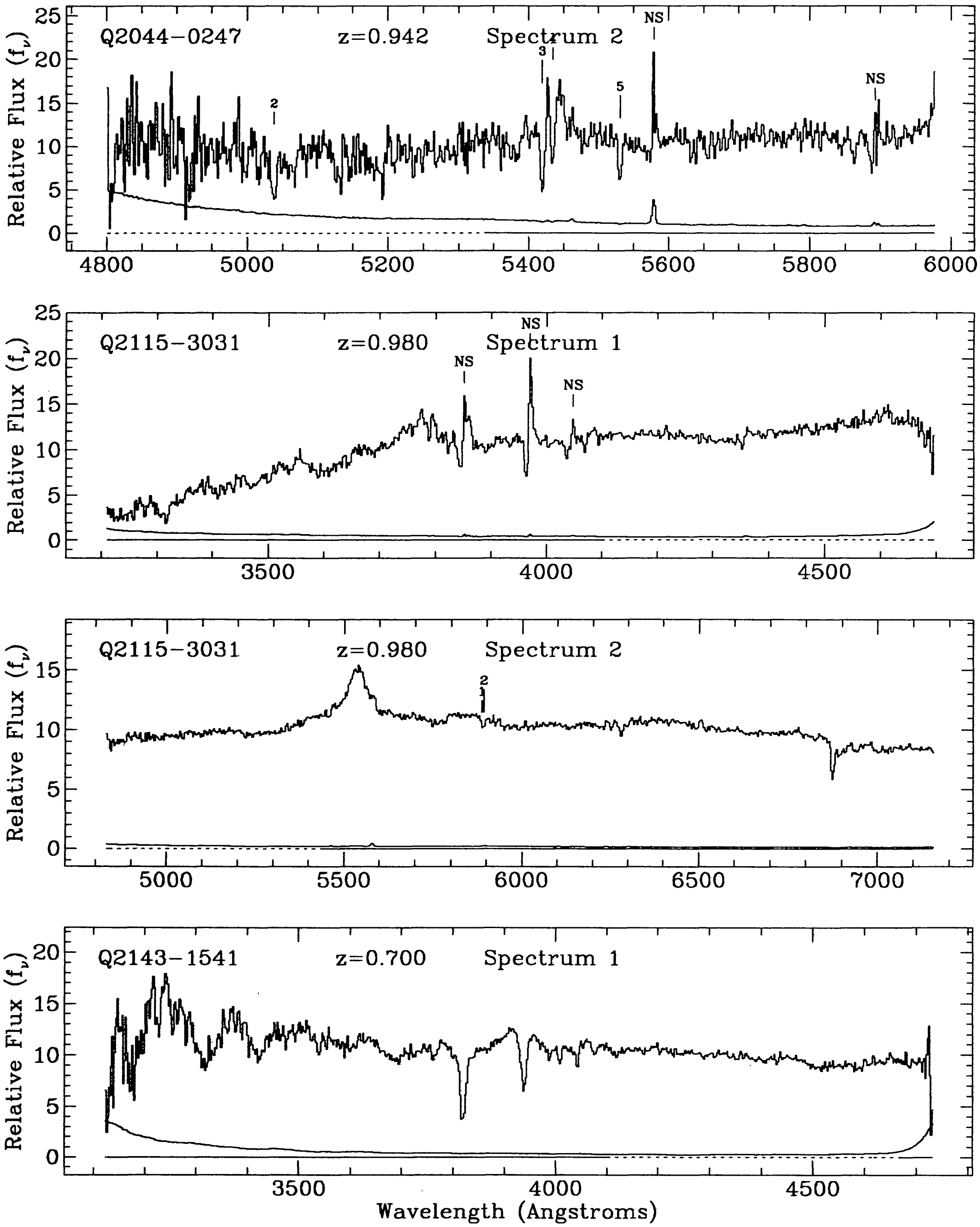


FIG. 1—*Continued*

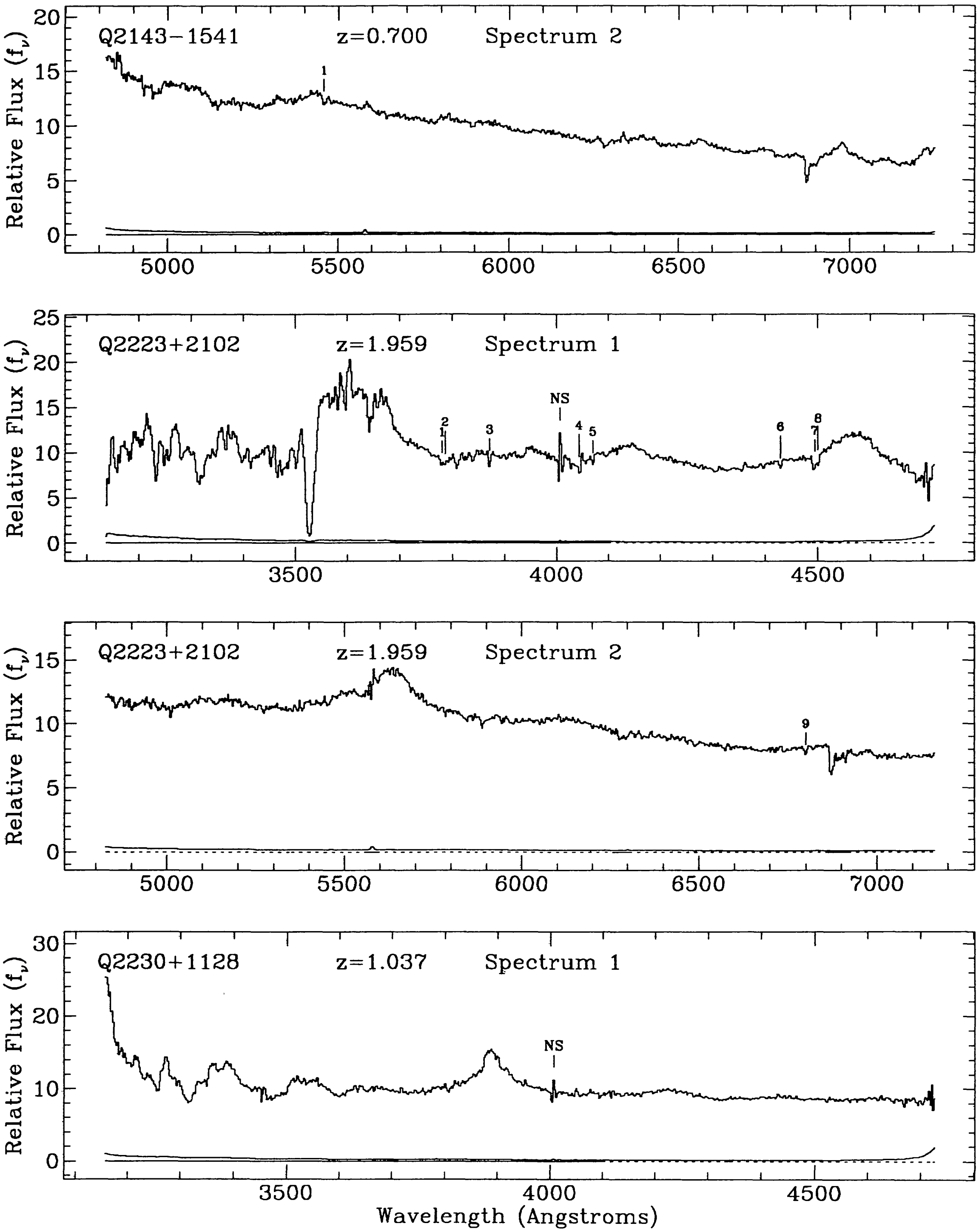


FIG. 1—*Continued*

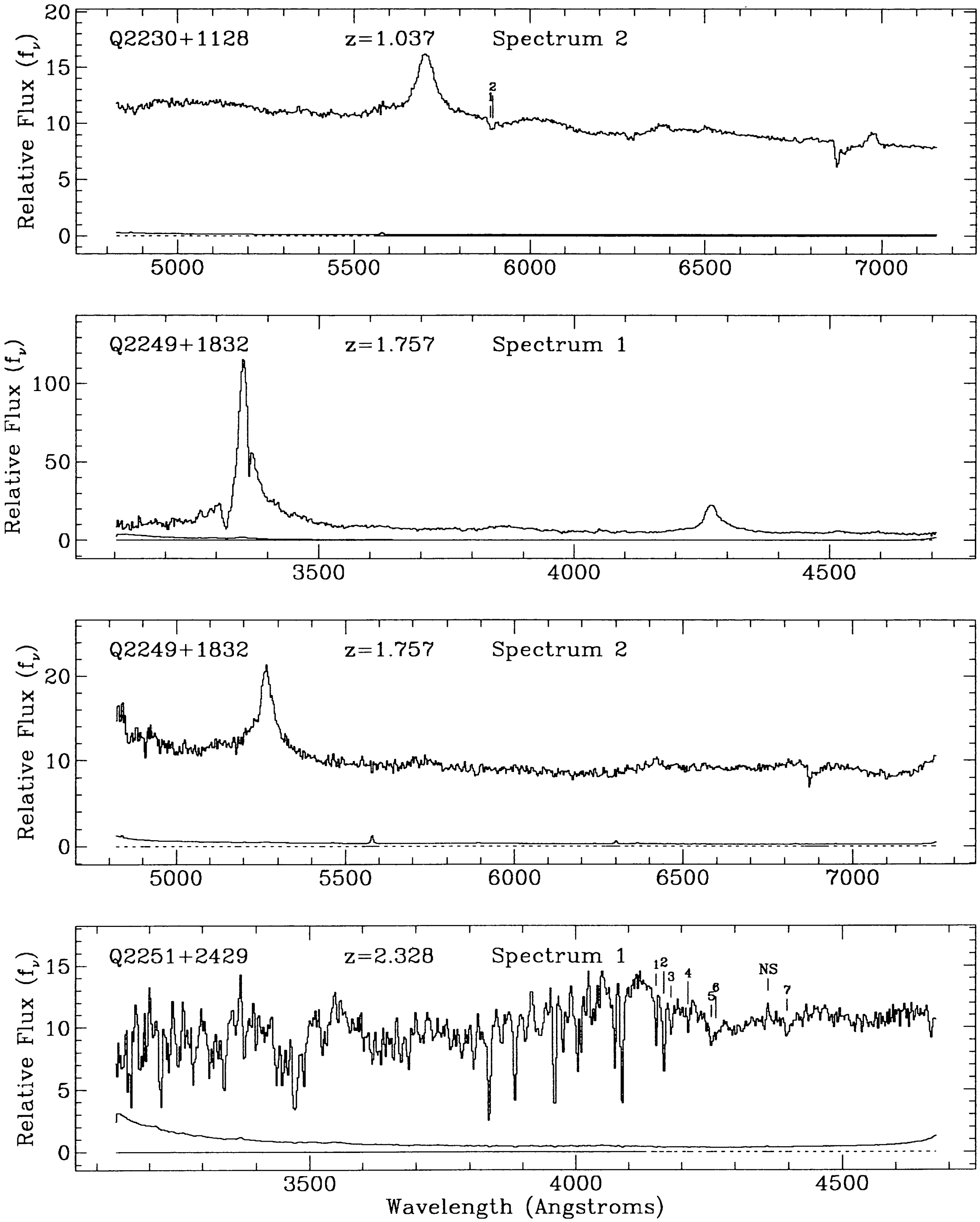


FIG. 1—*Continued*

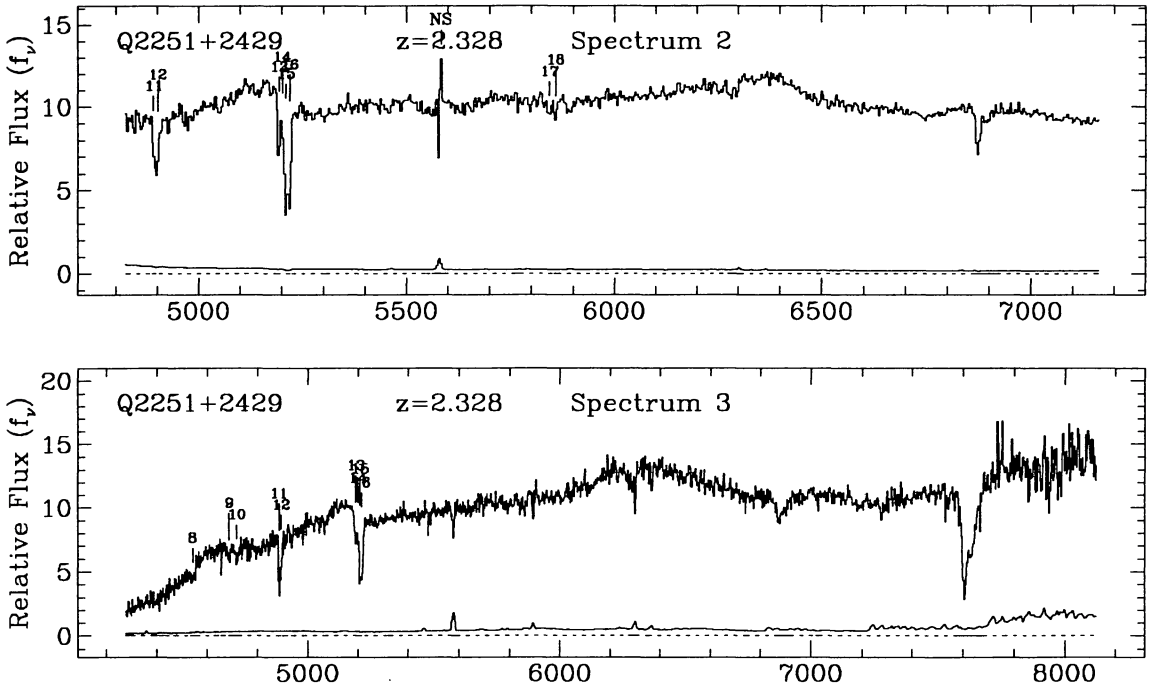


FIG. 1—*Continued*

## 4. QSO SPECTRA

In Figure 1 we show all of the spectra which we obtained in this survey. Each spectrum is labeled by the quasar name, the quasar emission redshift, and the spectrum number. This number corresponds to the number in the journal of observations given in Table 1. At the bottom of each spectrum the error array of 1 $\sigma$ uncertainty is plotted. The error array is plotted as a thick line in regions which we considered unusable for statistically complete detection of Mg II absorption lines. The spectra taken at Palomar are flux-calibrated up to an arbitrary normalization, and the $y$-axis is labeled "Relative Flux ($f_\nu$)," while the rest are not flux-calibrated. In each spectrum we also mark the statistically significant absorption lines which are listed in Table 3. Note that the telluric absorption bands 6290, 6880, and 7620 Å have not been removed and are visible in some of our spectra.

For 33 of the spectra in our sample we found no high-quality spectra previously published, or else we significantly extend the spectral coverage. A large number of the objects with published spectra had not been included in a statistical analysis, in particular those of Barthel, Tytler, & Thomson (1990, hereafter BTT). There are eight objects which overlap with the samples of SS and SSB1.

## 5. EMISSION-LINE PROPERTIES

In Table 2 we list the emission-line properties of the 56 quasars in our survey. The columns in this table are the line name, the line rest wavelength in angstroms, the observed wavelength in angstroms, the rest equivalent width in angstroms, the emission redshift, the line-width parameter (LW) in angstroms, and the line asymmetry (ASM). The line wavelength is defined to be the peak of a cubic spline fit to the smoothed spectrum. Both the LW and the ASM, as well as $\lambda_1$, $\lambda_2$, and $\lambda_m$, are taken from BTT and are defined by the following equations:

$$W = \sum_i (1 - y_i/c_i) ,$$

$$\sum_{-\infty}^{\lambda_1} (1 - y_i/c_i) \equiv 0.1587W ,$$

$$\sum_{-\infty}^{\lambda_m} (1 - y_i/c_i) \equiv 0.5W ,$$

$$\sum_{-\infty}^{\lambda_2} (1 - y_i/c_i) \equiv 0.8413W ,$$

$$\mathrm{LW} = 1.1775(\lambda_2 - \lambda_1) ,$$

$$\mathrm{ASM} = 100[0.5(\lambda_1 + \lambda_2) - \lambda_m]/\mathrm{LW} .$$

Here $y_i$ and $c_i$ are the spectrum and continuum at pixel $i$, respectively. The LW gives an estimate of the line width and equals the FWHM for a Gaussian line. The ASM indicates the degree of asymmetry in the line.

The set of emission lines listed in Table 2 is not complete in a statistical sense, since we measured only lines in which a well-defined continuum was discernible. In the cases where the Mg II emission was not clearly distinguishable from the Fe II and Balmer continuum emission, the continuum is taken to be the underlying power-law component, and we label the line Mg II + Fe II. When the Mg II emission can be clearly separated from the Fe II, we measure both Mg II and Mg II + Fe II.

## 6. ABSORPTION-LINE PROPERTIES

The extraction of absorption lines was carried out in the following manner. The continuum was determined by iteratively fitting a cubic spline to the spectrum and excluding pix-

TABLE 2

EMISSION LINES IN SAMPLE

| Line | $\lambda_0$ | $\lambda_{obs}$ | $W_0$ | $z_{em}$ | LW | ASM |
|---|---|---|---|---|---|---|
| Q0056-0009 (PHL 923) | | | | | | |
| [NV] | 3426 | 5875.9 | 4.6 | 0.7151 | 58 | 5.3 |
| [OII] | 3727 | 6406.7 | 3.7 | 0.7190 | 18 | 25.5 |
| [NeIII] | 3869 | 6649.0 | 5.4 | 0.7185 | 50 | 12.1 |
| Q0159-1147 (3C 57) | | | | | | |
| MgII+FeII | 2799 | 4672.7 | 13.2 | 0.6696 | 53 | 8.5 |
| Q0229+1309 (PKS 0229+13) | | | | | | |
| CIV | 1549 | 4750.1 | 40.0 | 2.0664 | 84 | 1.1 |
| HeII | 1641 | 5029.0 | 3.2 | 2.0655 | 63 | 2.8 |
| OIII] | 1664 | 5109.7 | 3.0 | 2.0708 | 48 | 3.6 |
| CIII] | 1909 | 5856.0 | 13.7 | 2.0680 | 76 | -3.7 |
| Q0229+3410 (3C 68.1) | | | | | | |
| — *No emission lines measured* — | | | | | | |
| Q0237-2322 (PKS 0237-23) | | | | | | |
| SiIV+OIV] | 1400 | 4522.7 | 5.2 | 2.2314 | 96 | -1.4 |
| CIV | 1549 | 4976.5 | 35.2 | 2.2126 | 167 | -9.6 |
| CIII] | 1909 | 6146.0 | 25.2 | 2.2199 | 171 | -6.3 |
| Q0350-0719 (3C 94) | | | | | | |
| MgII+FeII | 2799 | 5494.7 | 11.2 | 0.9633 | 50 | 1.9 |
| [NV] | 3426 | 6729.0 | 3.2 | 0.9641 | 42 | 0.1 |
| [OII] | 3727 | 7326.4 | 2.4 | 0.9658 | 20 | 6.1 |
| Q0420-0127 (PKS 0420-01) | | | | | | |
| MgII+FeII | 2799 | 5362.8 | 15.8 | 0.9162 | 55 | 3.4 |
| Q0538+4949 (3C 147) | | | | | | |
| MgII+FeII | 2799 | 4327.5 | 33.7 | 0.5462 | 113 | 5.3 |
| Q0610+2605 (3C 154) | | | | | | |
| MgII+FeII | 2799 | 4419.7 | 35.9 | 0.5792 | 143 | -4.7 |
| Q0642+4454 (OH 471) | | | | | | |
| HI | 1216 | 5352.7 | 57.4 | 3.4031 | 48 | -1.8 |
| NV | 1240 | 5443.8 | 25.5 | 3.3897 | 101 | 10.1 |
| OI | 1304 | 5749.1 | 3.3 | 3.4105 | 50 | 3.9 |
| CII | 1336 | 5887.8 | 1.7 | 3.4080 | 49 | 10.2 |
| SiIV+OIV] | 1400 | 6159.6 | 6.4 | 3.4009 | 97 | -4.1 |
| CIV | 1549 | 6818.2 | 26.7 | 3.4015 | 99 | -7.9 |
| HeII | 1641 | 7205.0 | 3.9 | 3.3919 | 107 | -4.3 |
| OIII] | 1664 | 7315.6 | 3.2 | 3.3964 | 92 | 13.4 |
| Q0710+1151 (3C 175) | | | | | | |
| CIII] | 1909 | 3375.4 | 13.9 | 0.7684 | 78 | 12.2 |
| Q0725+1443 (3C 181) | | | | | | |
| CIII] | 1909 | 4551.7 | 20.9 | 1.3847 | 88 | 6.2 |
| CII | 2326 | 5548.1 | 2.0 | 1.3852 | 46 | 18.3 |
| MgII+FeII | 2799 | 6678.6 | 56.2 | 1.3863 | 228 | -1.2 |
| Q0736-0620 (PKS 0736-06) | | | | | | |
| CIII] | 1909 | 5573.0 | 10.5 | 1.9198 | 105 | 0.2 |
| CII | 2326 | 6793.2 | 1.8 | 1.9205 | 80 | 0.1 |
| Q0809+4822 (3C 196) | | | | | | |
| CIII] | 1909 | 3569.1 | 19.6 | 0.8699 | 64 | -13.6 |
| CII | 2326 | 4351.1 | 1.4 | 0.8706 | 13 | 19.3 |
| Q0835+5804 (3C 205) | | | | | | |
| CIII] | 1909 | 4832.1 | 19.6 | 1.5316 | 124 | 3.5 |
| MgII+FeII | 2799 | 7085.6 | 13.7 | 1.5317 | 170 | 3.7 |
| Q0855+1421 (3C212) | | | | | | |
| MgII+FeII | 2799 | 5766.1 | 34.3 | 1.0603 | 170 | 4.2 |
| Q0859-1403 (PKS 0859-14) | | | | | | |
| CIV | 1549 | 3614.8 | 27.8 | 1.3335 | 69 | 6.2 |
| CIII] | 1909 | 4453.4 | 16.5 | 1.3332 | 86 | 2.3 |
| MgII+FeII | 2799 | 6543.7 | 31.8 | 1.3381 | 164 | -5.1 |
| Q0906+4305 (3C 216) | | | | | | |
| — *No emission lines measured* — | | | | | | |
| Q1007+4147 (4C 41.21) | | | | | | |
| MgII | 2799 | 4513.0 | 11.6 | 0.6125 | 43 | -4.1 |
| MgII+FeII | 2799 | 4413.0 | 21.9 | 0.6125 | 94 | -16.3 |
| Q1040+1219 (3C 245) | | | | | | |
| CIII] | 1909 | 3867.8 | 18.2 | 1.0267 | 72 | -2.8 |
| Q1055+2007 (PKS 1055+20) | | | | | | |
| CIV | 1549 | 3272.3 | 52.7 | 1.1125 | 61 | 8.7 |
| HeII | 1641 | 3464.6 | 3.1 | 1.1119 | 31 | 0.8 |
| OIII] | 1664 | 3521.9 | 6.2 | 1.1165 | 43 | 1.7 |
| CIII] | 1909 | 4034.5 | 16.8 | 1.1137 | 62 | 1.6 |
| MgII+FeII | 2799 | 5923.7 | 29.7 | 1.1165 | 121 | 6.7 |
| Q1111+4053 (3C 254) | | | | | | |
| — *No emission lines measured* — | | | | | | |
| Q1136-1334 (PKS 1136-13) | | | | | | |
| MgII | 2799 | 4356.9 | 17.6 | 0.5567 | 36 | 2.1 |
| MgII+FeII | 2799 | 4356.9 | 54.2 | 0.5567 | 127 | -6.9 |
| Q1137+6604 (3C 263) | | | | | | |
| MgII+FeII | 2799 | 4603.3 | 11.5 | 0.6448 | 74 | 9.2 |
| Q1148-0007 (PKS 1148-00) | | | | | | |
| CIV | 1549 | 4614.7 | 32.5 | 1.9790 | 89 | 1.0 |
| CIII] | 1909 | 5688.3 | 8.4 | 1.9801 | 89 | -6.2 |
| MgII+FeII | 2799 | 8337.6 | 17.7 | 1.9790 | 178 | 11.2 |
| Q1153+3144 (4C 31.38) | | | | | | |
| [OII] | 3727 | 5283.9 | 55.9 | 0.4177 | 17 | 0.0 |
| [NeIII] | 3869 | 5483.8 | 29.0 | 0.4174 | 28 | 3.3 |
| HI | 4861 | 6889.3 | 30.3 | 0.4173 | 30 | 3.9 |
| [OIII] | 4959 | 7027.5 | 84.2 | 0.4171 | 30 | 3.9 |
| [OIII] | 5007 | 7095.1 | 215.9 | 0.4170 | 25 | -4.7 |
| HI | 6562 | 9296.0 | 347.2 | 0.4166 | 73 | 0.1 |
| Q1156+2931 (4C 29.45) | | | | | | |
| MgII+FeII | 2799 | 4831.1 | 11.9 | 0.7262 | 60 | 7.5 |
| Q1206+4356 (3C 268.4) | | | | | | |
| MgII | 2799 | 6706.2 | 4.7 | 1.3961 | 37 | 6.1 |
| MgII+FeII | 2799 | 6706.2 | 21.6 | 1.3961 | 151 | 6.9 |
| Q1213+5352 (4C 53.24) | | | | | | |
| MgII+FeII | 2799 | 5786.0 | 37.0 | 1.0674 | 161 | -0.3 |
| [NV] | 3426 | 7091.4 | 3.4 | 1.0690 | 50 | 18.9 |
| [OII] | 3727 | 7713.5 | 4.4 | 1.0696 | 24 | 10.6 |
| [NeIII] | 3869 | 8012.3 | 10.8 | 1.0709 | 53 | -2.4 |

TABLE 2—*Continued*

| Line | $\lambda_0$ | $\lambda_{obs}$ | $W_0$ | $z_{em}$ | LW | ASM |
|---|---|---|---|---|---|---|
| **Q1218+3359 (3C 270.1)** | | | | | | |
| SiIV+OIV] | 1400 | 3533.1 | 13.9 | 1.5243 | 43 | 2.5 |
| CIV | 1549 | 3914.1 | 64.2 | 1.5267 | 71 | 6.1 |
| HeII | 1641 | 4135.4 | 3.0 | 1.5207 | 31 | 7.1 |
| OIII] | 1664 | 4208.3 | 4.7 | 1.5291 | 56 | 0.0 |
| MgII+FeII | 2799 | 7073.9 | 27.7 | 1.5219 | 112 | 1.4 |
| **Q1229-0207 (PKS 1229-02)** | | | | | | |
| MgII+FeII | 2799 | 5720.2 | 29.4 | 1.0439 | 108 | 7.2 |
| [NV] | 3426 | 6999.9 | 1.9 | 1.0432 | 38 | 0.0 |
| [NeIII] | 3869 | 7910.1 | 4.5 | 1.0444 | 59 | 2.3 |
| **Q1318+1122 (PKS 1318+11)** | | | | | | |
| HI | 1216 | 3855.7 | 171.9 | 2.1716 | 110 | 6.9 |
| CIV | 1549 | 4923.6 | ... | 2.1785 | ... | ... |
| CIII] | 1909 | 6054.4 | 34.1 | 2.1720 | 176 | -4.3 |
| **Q1327-2126 (PKS 1327-21)** | | | | | | |
| MgII+FeII | 2799 | 4267.4 | 71.1 | 0.5248 | 138 | -3.4 |
| **Q1328+2524 (3C 287)** | | | | | | |
| MgII | 2799 | 5747.6 | 8.5 | 1.0536 | 34 | 2.9 |
| MgII+FeII | 2799 | 5747.6 | 24.7 | 1.0536 | 134 | 8.1 |
| [NV] | 3426 | 7039.3 | 2.1 | 1.0547 | 42 | 14.2 |
| [OII] | 3727 | 7657.4 | 9.4 | 1.0546 | 18 | 14.2 |
| [NeIII] | 3869 | 7953.5 | 6.1 | 1.0557 | 56 | 23.6 |
| **Q1328+3045 (3C 286)** | | | | | | |
| MgII+FeII | 2799 | 5180.0 | 9.3 | 0.8508 | 40 | 3.9 |
| [NV] | 3426 | 6339.2 | 1.7 | 0.8503 | 11 | 14.2 |
| [NeIII] | 3869 | 7158.1 | 3.6 | 0.8501 | 25 | -6.1 |
| **Q1335-0611 (PKS 1335-06)** | | | | | | |
| MgII+FeII | 2799 | 4542.8 | 27.9 | 0.6232 | 112 | -8.0 |
| **Q1354-1512 (PKS 1354-15)** | | | | | | |
| CIII] | 1909 | 5541.3 | 23.1 | 1.9032 | 122 | -2.8 |
| MgII+FeII | 2799 | 8164.8 | 33.0 | 1.9173 | 198 | -12.1 |
| **Q1437+6224 (OQ663)** | | | | | | |
| MgII+FeII | 2799 | 5871.5 | 81.9 | 1.0979 | 154 | -4.2 |
| [NV] | 3426 | 7167.1 | 12.2 | 1.0920 | 93 | 6.5 |
| [OII] | 3727 | 7796.7 | 15.7 | 1.0919 | 46 | -19.8 |
| [NeIII] | 3869 | 8096.9 | 43.0 | 1.0928 | 124 | -5.3 |
| **Q1442+1011 (OQ 172)** | | | | | | |
| HI+NV | 1216 | 5543.8 | 54.3 | 3.5603 | 179 | 7.5 |
| OI | 1304 | 5933.9 | 1.9 | 3.5523 | 86 | -5.6 |
| SiIV+OIV] | 1400 | 6340.6 | 4.2 | 3.5302 | 102 | 3.3 |
| CIV | 1549 | 7004.4 | 23.9 | 3.5217 | 200 | -6.1 |
| **Q1453-1056 (PKS 1453-10)** | | | | | | |
| CIII] | 1909 | 3704.2 | 25.0 | 0.9406 | 56 | -3.9 |
| MgII+FeII | 2799 | 5432.4 | 64.2 | 0.9410 | 133 | 1.1 |
| [NV] | 3426 | 6642.2 | 1.9 | 0.9388 | 18 | -8.5 |
| **Q1458+7152 (3C 309.1)** | | | | | | |
| MgII+FeII | 2799 | 5328.8 | 22.7 | 0.9040 | 40 | 6.1 |
| **Q1508-0531 (PKS 1508-05)** | | | | | | |
| CIII] | 1909 | 4173.9 | 7.3 | 1.1867 | 23 | 14.2 |
| MgII+FeII | 2799 | 6123.2 | 12.4 | 1.1879 | 40 | 3.9 |
| **Q1618+1743 (3C 334)** | | | | | | |
| MgII+FeII | 2799 | 4354.8 | 20.6 | 0.5560 | 79 | -6.8 |
| [NV] | 3426 | 5330.3 | 1.3 | 0.5558 | 11 | 14.2 |
| [OII] | 3727 | 5800.0 | 4.1 | 0.5562 | 11 | 14.2 |
| [NeIII] | 3869 | 6018.5 | 4.1 | 0.5556 | 18 | 8.5 |
| **Q1622+2352 (3C 336)** | | | | | | |
| MgII+FeII | 2799 | 5393.9 | 34.7 | 0.9273 | 110 | 5.2 |
| **Q1629+1202 (PKS 1629+12)** | | | | | | |
| CIV | 1549 | 4317.1 | 17.9 | 1.7869 | 72 | -4.6 |
| CIII] | 1909 | 5329.2 | 10.8 | 1.7920 | 90 | -1.7 |
| CII | 2326 | 6499.2 | 0.9 | 1.7942 | 11 | 14.2 |
| **Q1634+6251 (3C 343)** | | | | | | |
| MgII+FeII | 2799 | 5563.1 | 38.8 | 0.9877 | 24 | 3.9 |
| [NV] | 3426 | 6809.2 | 50.0 | 0.9875 | 19 | 6.1 |
| [OII] | 3727 | 7410.2 | 197.1 | 0.9882 | 23 | 10.6 |
| [NeIII] | 3869 | 7694.8 | 120.9 | 0.9888 | 30 | 17.0 |
| HI | 4861 | 9660.6 | ... | 0.9874 | 30 | 10.6 |
| [OIII] | 4959 | 9856.6 | ... | 0.9876 | 31 | 10.6 |
| [OIII] | 5007 | 9951.1 | ... | 0.9874 | 35 | 4.8 |
| **Q1828+4842 (3C 380)** | | | | | | |
| [NV] | 3426 | 5795.4 | 1.9 | 0.6916 | 18 | 8.5 |
| [OII] | 3727 | 6306.9 | 1.7 | 0.6922 | 14 | 21.2 |
| [NeIII] | 3869 | 6546.7 | 3.0 | 0.6921 | 14 | 0.0 |
| HI | 4861 | 8204.8 | 20.6 | 0.6879 | 81 | 12.0 |
| [OIII] | 4959 | 8382.4 | 11.3 | 0.6904 | 26 | 0.0 |
| [OIII] | 5007 | 8464.1 | 34.5 | 0.6905 | 23 | 6.1 |
| **Q1901+3155 (3C 395)** | | | | | | |
| — *No emission lines measured* — | | | | | | |
| **Q2003-0232 (4C -02.79)** | | | | | | |
| MgII+FeII | 2799 | 6879.2.1 | 8.5 | 1.4579 | 68 | -2.2 |
| **Q2044-0247 (3C 422)** | | | | | | |
| — *No emission lines measured* — | | | | | | |
| **Q2115-3031 (PKS 2115-30)** | | | | | | |
| CIII] | 1909 | 3775.3 | 9.9 | 0.9779 | 64 | -1.7 |
| MgII+FeII | 2799 | 5538.8 | 10.5 | 0.9790 | 61 | 2.5 |
| **Q2143-1541 (PKS 2143-15)** | | | | | | |
| [NV] | 3426 | 5812.6 | 1.2 | 0.6966 | 40 | -3.9 |
| [NeIII] | 3869 | 6556.8 | 3.7 | 0.6947 | 65 | 4.7 |
| **Q2223+2102 (PKS 2223+21)** | | | | | | |
| CIII] | 1909 | 5637.3 | 18.3 | 1.9535 | 202 | -7.6 |
| **Q2230+1128 (CTA 102)** | | | | | | |
| CIII] | 1909 | 3885.7 | 23.9 | 1.0357 | 94 | 1.1 |
| MgII+FeII | 2799 | 5703.5 | 13.2 | 1.0379 | 58 | 5.3 |
| [NV] | 3426 | 6976.4 | 2.5 | 1.0363 | 25 | -6.1 |
| **Q2249+1832 (3C 454)** | | | | | | |
| HI | 1216 | 3350.5 | 170.7 | 1.7561 | 76 | 11.3 |
| CIV | 1549 | 4269.0 | 44.6 | 1.7559 | 51 | 12.7 |
| CIII] | 1909 | 5264.9 | 15.7 | 1.7583 | 61 | -2.5 |
| CII | 2326 | 6416.8 | 4.9 | 1.7587 | 104 | -1.5 |
| **Q2251+2429 (PKS 2251+24)** | | | | | | |
| — *No emission lines measured* — | | | | | | |

els which deviate negatively by more than 3 $\sigma$. Next the distribution of deviations was compared with the expected Gaussian distribution, based on the known error array. This occasionally revealed non-Gaussian noise due to instrumental problems, but more typically shows that the error array required some adjustment to accurately represent the observed noise in the spectrum. We found that in general the Palomar spectra required no scaling and the MMT blue channel error arrays required adjustment by 5%–20%. In the MMT red channel data the discrepancy between observed and calculated noise was more serious, from 20% to 50%. The exact cause of this is unknown. However, after scaling the error array by a constant so that the $\chi^2$ per degree of freedom was unity, we found that in all cases the error array gave a locally accurate estimate of noise throughout the spectrum. This gives us complete confidence in the error arrays which were ultimately used.

Absorption lines were detected using the optimal extraction algorithm described by Schneider et al. (1992). In this method the normalized instrumental point-spread function (PSF) is used as a profile for optimal extraction of an unresolved line centered at pixel $i$. The equivalent width $\mathrm{EW}_i$ and uncertainty $\sigma_{\mathrm{EW}_i}$ at each pixel define a detection significance level $\mathrm{SL}_i \equiv \mathrm{EW}_i / \sigma_{\mathrm{EW}_i}$. In regions of the detection array with $\mathrm{SL}_i > 3.5$ the peaks were flagged as possible lines. After scanning the entire spectrum, each flagged line was fitted with a Gaussian to determine the equivalent width, velocity width, central wavelength, and associated uncertainties. In the case where lines were blended, simultaneous fitting of multiple Gaussians was performed. As mentioned in Schneider et al. (1992), it is important to make the distinction between the optimal extraction parameters, which define the detection significance level (SL), and the Gaussian determination of line parameters. The SL is used strictly as the criterion for statistically complete line detection, whereas the Gaussian parameters are used for all subsequent quantitative analysis.

The significant lines were then identified using interactive software which graphically displays the positions of strong absorption lines (Morton & Smith 1973) at a selected redshift. All absorption systems were identified on the basis of a confirmed absorption doublet. We define this as a system which could be well fitted with two Gaussians whose wavelengths and velocity widths were constrained, and whose absorber strengths were physically allowed.

In Table 3 we list the absorption lines found in our sample of quasars. The columns are absorption-line wavelength and uncertainty in angstroms, observed equivalent width and uncertainty in angstroms, detection significance level, identification (if any), corresponding redshift with uncertainty on the last digit in parentheses, and spectrum number. The uncertainty in wavelength and redshift takes into account the noise in the spectrum and rms deviations in the wavelength calibration. In this list we include all lines which have detection significance level SL $\geq$ 5.0, as well as lines for which there is corroborating evidence and SL $\geq$ 3.5. Lines which are considered tentative are identified with a question mark.

In Table 4 we list the Mg II absorption systems which form the basis of our statistical analysis. The columns are the object name, the QSO emission redshift, the absorber redshift, and the rest equivalent widths for Mg II λ2796, Mg II λ2803, and Mg I λ2852, respectively. The uncertainties follow each value in parentheses. For the Mg I line, upper limits are given where no line was detected, and the field is blank in cases where the line could not have been observed. In the Mg II lines in this table the stronger member is detected at better than 5 $\sigma$ confidence, and the weaker member is detected at better than 3.5 $\sigma$ confidence. The doublet ratio is required to be consistent with the physically allowed range of 1–2. Our line list is complete at these limits. The redshift and equivalent widths of each doublet were determined by simultaneously fitting two Gaussians constrained to have equal velocity width and the wavelength ratio of the Mg II doublet. The lines which are identified in Table 3 with a question mark are not included in our analysis.

In our sample we find a total of 29 Mg II absorbers, of which 18 are new systems. All but three of the 29 absorbers have rest equivalent width greater than 0.5 Å, as one might expect, given that our survey was designed to detect strong absorbers. A surprisingly large number of systems, six out of 29, have an apparent ejection velocity with respect to the quasar of less than 6000 km s$^{-1}$. This is discussed in § 9.3. We also find in our spectra four new C IV absorbers, four new Galactic Ca II systems, and six new Galactic Na I systems.

## 7. NOTES ON INDIVIDUAL OBJECTS

The literature references in this section are based in large part on the extensive compilations of Junkkarinen, Hewitt, & Burbidge (1991) and York et al. (1991), as well as on NED.[4]

The apparent ejection velocities of associated absorbers which we quote are based on the Mg II emission redshifts listed in Table 2. The emission redshift listed along with the object name is the value given by VCV.

### 7.1. *Q0056−0009* (*PHL 923*, $z_{\mathrm{em}} = 0.717$)

We find no published spectra for this object, and no lines were detected in our spectrum. Spectrum 1 for this object suffers from the flattening problem in the 1988 July spectra.

### 7.2. *Q0159−1147* (*3C 57*, $z_{\mathrm{em}} = 0.670$)

This object was observed previously by Tytler et al. (1987), who found no absorption lines in the range 4021–4929 Å. We also find no lines.

### 7.3. *Q0229+1309* (*PKS 0229+13*, $z_{\mathrm{em}} = 2.065$)

This object has previously been studied by Sargent, Boksenberg, & Steidel (1988a, hereafter SBS) in the range 3950–4975 Å. They identified Mg II systems at $z_{\mathrm{abs}} = 0.3723$ and 0.4177, and C IV at $z_{\mathrm{abs}} = 1.8622$, 1.9024, and 1.9584. Mg II at the latter two C IV redshifts is not in our spectral coverage. Of the unidentified lines in our spectra, one was also seen and not identified by SBS, and another is possibly present in their published spectrum. Bergeron & Boissé (1991) have imaged this field, and they find a nearby emission-line galaxy at $z = 0.417$, but were unable to find a candidate for the $z_{\mathrm{abs}} = 0.3723$ system. In our spectra we confirm the C IV lines and find an Mg II systems:

[4] The NASA/IPAC Extragalactic Database (NED) is operated by the Jet Propulsion Laboratory, California Institute of Technology, under contract with the National Aeronautics and Space Administration.

TABLE 3

Absorption Lines in Sample

| No. | $\lambda_{abs}$ | $\sigma(\lambda)$ | EW | $\sigma$(EW) | SL | ID | $z_{abs}$ | Sp.# |
|---|---|---|---|---|---|---|---|---|
| | Q0056-0009 | | PHL 923 | | | $z_{em} = 0.717$ | | |
| | | | — No lines detected — | | | | | |
| | Q0159-1147 | | 3C 57 | | | $z_{em} = 0.670$ | | |
| | | | — No lines detected — | | | | | |
| | Q0229+1309 | | PKS 0229+13 | | | $z_{em} = 2.065$ | | |
| 1 | 4278.6 | 0.8 | 1.54 | 0.18 | 10.8 | | | 1 |
| 2 | 4292.4 | 0.8 | 0.67 | 0.12 | 6.6 | | | 1 |
| 3 | 4431.0 | 0.8 | 1.98 | 0.19 | 13.3 | CIV(1548) | 1.8620(5) | 1 |
| 4 | 4438.4 | 0.8 | 1.15 | 0.15 | 10.4 | CIV(1550) | 1.8620(5) | 1 |
| 5 | 4494.5 | 0.8 | 1.84 | 0.13 | 17.3 | CIV(1548) | 1.9030(5) | 1 |
| 6 | 4501.3 | 0.8 | 1.15 | 0.12 | 11.4 | CIV(1550) | 1.9026(5) | 1 |
| 7 | 4580.1 | 1.0 | 0.52 | 0.10 | 10.3 | CIV(1548) | 1.9583(7) | 1 |
| 8 | 4587.1 | 1.1 | 0.44 | 0.10 | 9.9 | CIV(1550) | 1.9579(7) | 1 |
| 9 | 4781.1 | 0.8 | 0.37 | 0.07 | 6.8 | AlII(1670) | 1.8616(5) | 1 |
| 10 | 4795.8 | 0.8 | 0.45 | 0.08 | 6.9 | | | 1 |
| 11 | 8001.3 | 1.2 | 2.93 | 0.39 | 7.9 | MgII(2796) | 1.8613(4) | 1 |
| 12 | 8017.4 | 0.8 | 2.00 | 0.39 | 5.5 | MgII(2803) | 1.8598(3) | 1 |
| | Q0229+3410 | | 3C 68.1 | | | $z_{em} = 1.240$ | | |
| 1 | 4965.5 | 0.9 | 3.40 | 0.72 | 5.0 | MgII(2796) | 0.7757(3) | 1 |
| 2 | 4976.4 | 0.8 | 3.58 | 0.64 | 5.6 | MgII(2803) | 0.7750(3) | 1 |
| 3 | 6221.8 | 0.9 | 7.72 | 0.36 | 19.1 | MgII(2796) | 1.2250(3) | 1 |
| 4 | 6236.6 | 0.8 | 4.77 | 0.36 | 14.3 | MgII(2803) | 1.2245(3) | 1 |
| 5 | 6353.4 | 1.2 | 1.25 | 0.36 | 4.3 | MgI(2853) | 1.2269(4) | 1 |
| 6 | 7081.7 | 1.5 | 1.25 | 0.28 | 5.5 | NaI(5891) | 0.2020(3) | 1 |
| 7 | 7089.2 | 1.7 | 1.01 | 0.28 | 5.0 | NaI(5897) | 0.2021(3) | 1 |
| | Q0237-2322 | | PKS 0237-23 | | | $z_{em} = 2.224$ | | |
| 1 | 4386.4 | 0.9 | 0.58 | 0.11 | 6.2 | AlIII(1854) | 1.3650(5) | 1 |
| 2 | 4406.1 | 0.9 | 0.87 | 0.12 | 8.6 | AlIII(1862) | 1.3653(5) | 1 |
| 3 | 4464.4 | 0.8 | 1.55 | 0.09 | 20.7 | AlII(1670) | 1.6721(5) | 1 |
| 4 | 4951.6 | 1.0 | 0.43 | 0.06 | 13.8 | AlII(1862) | 1.6582(5) | 1 |
| 5 | 4957.7 | 0.8 | 1.49 | 0.06 | 32.8 | CIV(1548) | 2.2023(5) | 1 |
| 6 | 4966.5 | 0.8 | 0.76 | 0.05 | 17.9 | CIV(1550) | 2.2026(5) | 1 |
| 7 | 4978.1 | 0.9 | 0.36 | 0.05 | 6.2 | AlII(1862) | 1.6724(5) | 1 |
| 8 | 5544.2 | 0.9 | 1.33 | 0.13 | 12.5 | FeII(2344) | 1.3651(4) | 1 |
| 9 | 5614.1 | 1.3 | 0.46 | 0.11 | 4.8 | FeII(2374) | 1.3644(5) | 1 |
| 10 | 5634.9 | 0.8 | 2.13 | 0.11 | 23.7 | FeII(2382) | 1.3648(3) | 1 |
| 11 | 6114.6 | 1.0 | 1.02 | 0.11 | 10.9 | FeII(2586) | 1.3639(4) | 1 |
| 12 | 6148.1 | 0.8 | 1.99 | 0.09 | 27.2 | FeII(2600) | 1.3645(3) | 1 |
| 13 | 6262.7 | 1.2 | 0.66 | 0.15 | 6.6 | FeII(2344) | 1.6716(5) | 1 |
| 14 | 6366.2 | 1.0 | 1.19 | 0.16 | 8.7 | FeII(2382) | 1.6718(4) | 1 |
| 15 | 6616.5 | 0.9 | 4.52 | 0.18 | 30.6 | MgII(2796) | 1.3661(3) | 1 |
| 16 | 6630.1 | 0.8 | 3.37 | 0.18 | 23.0 | MgII(2803) | 1.3649(3) | 1 |
| 17 | 6944.8 | 1.3 | 1.08 | 0.19 | 6.5 | FeII(2600) | 1.6709(5) | 1 |
| 18 | 7431.7 | 0.9 | 1.46 | 0.13 | 11.2 | MgII(2796) | 1.6576(3) | 1 |
| 19 | 7451.3 | 0.8 | 1.12 | 0.13 | 8.0 | MgII(2803) | 1.6578(3) | 1 |
| 20 | 7473.3 | 0.8 | 2.15 | 0.13 | 16.2 | MgII(2796) | 1.6725(3) | 1 |
| 21 | 7491.1 | 0.8 | 1.62 | 0.13 | 12.0 | MgII(2803) | 1.6720(3) | 1 |
| | Q0350-0719 | | 3C 94 | | | $z_{em} = 0.962$ | | |
| 1 | 5891.7 | 1.7 | 0.45 | 0.17 | 5.9 | NaI(5891) | 0.0000(3) | 1 |
| 2 | 5897.6 | 0.8 | 0.38 | 0.17 | 6.4 | NaI(5897) | 0.0000(1) | 1 |
| | Q0420-0127 | | PKS 0420-01 | | | $z_{em} = 0.915$ | | |
| 1 | 4565.8 | 0.9 | 1.67 | 0.17 | 10.1 | MgII(2796) | 0.6328(3) | 1 |
| 2 | 4579.3 | 0.8 | 1.40 | 0.17 | 8.2 | MgII(2803) | 0.6334(3) | 1 |
| 3 | 5160.9 | 1.0 | 0.56 | 0.09 | 6.1 | | | 1 |
| | Q0538+4949 | | 3C 147 | | | $z_{em} = 0.545$ | | |
| | | | — No lines detected — | | | | | |
| | Q0610+2605 | | 3C 154 | | | $z_{em} = 0.580$ | | |
| 1 | 4450.8 | 0.6 | 1.05 | 0.24 | 4.2 | MgII(2796) ? | 0.5917(2) | 1 |
| 2 | 4463.2 | 0.2 | 0.55 | 0.21 | 1.4 | MgII(2803) ? | 0.5920(1) | 1 |

TABLE 3—*Continued*

| No. | $\lambda_{abs}$ | $\sigma(\lambda)$ | EW | $\sigma$(EW) | SL | ID | $z_{abs}$ | Sp.# |
|---|---|---|---|---|---|---|---|---|
| | Q0642+4454 | | OH 471 | | | $z_{em}$ = 3.400 | | |
| 1 | 4339.9 | 0.8 | 6.64 | 0.70 | 16.7 | | | 1 |
| 2 | 4352.0 | 1.0 | 7.42 | 1.04 | 12.4 | | | 1 |
| 3 | 4366.3 | 1.2 | 3.63 | 0.86 | 6.3 | | | 1 |
| 4 | 4404.4 | 0.8 | 2.46 | 0.58 | 7.6 | | | 1 |
| 5 | 4412.7 | 1.1 | 4.78 | 0.91 | 7.6 | | | 1 |
| 6 | 4436.4 | 0.9 | 3.76 | 0.51 | 8.7 | | | 1 |
| 7 | 4457.3 | 0.9 | 7.82 | 0.71 | 15.7 | | | 1 |
| 8 | 4475.3 | 0.9 | 8.54 | 0.67 | 20.2 | | | 1 |
| 9 | 4584.3 | 1.0 | 4.48 | 0.46 | 10.7 | | | 1 |
| 10 | 4628.9 | 0.9 | 8.49 | 0.74 | 10.8 | | | 1 |
| 11 | 4655.4 | 0.9 | 5.54 | 0.61 | 9.4 | | | 1 |
| 12 | 4694.8 | 0.8 | 3.65 | 0.36 | 12.4 | | | 1 |
| 13 | 4722.3 | 0.9 | 4.99 | 0.53 | 16.8 | | | 1 |
| 14 | 4738.5 | 1.0 | 8.68 | 1.05 | 15.5 | | | 1 |
| 15 | 4753.6 | 1.1 | 4.61 | 0.87 | 10.8 | | | 1 |
| 16 | 4806.5 | 0.8 | 5.69 | 0.49 | 15.3 | | | 1 |
| 17 | 4828.5 | 0.9 | 3.19 | 0.94 | 11.7 | | | 1 |
| 18 | 4838.9 | 1.2 | 6.61 | 1.11 | 10.5 | | | 1 |
| 19 | 4896.6 | 0.9 | 2.17 | 0.34 | 7.5 | | | 1 |
| 20 | 4938.4 | 1.5 | 3.63 | 0.84 | 8.3 | | | 1 |
| 21 | 4950.0 | 0.8 | 1.85 | 0.85 | 15.4 | | | 1 |
| 22 | 4954.9 | 0.8 | 4.84 | 0.55 | 17.1 | | | 1 |
| 23 | 4975.4 | 0.9 | 5.52 | 0.52 | 12.6 | | | 1 |
| 24 | 4995.5 | 0.9 | 5.24 | 0.65 | 13.7 | | | 1 |
| 25 | 5011.7 | 0.9 | 13.45 | 0.86 | 15.7 | | | 1 |
| 26 | 5032.8 | 0.8 | 5.45 | 0.43 | 17.1 | | | 1 |
| 27 | 5084.1 | 0.9 | 7.31 | 0.51 | 15.7 | | | 1 |
| 28 | 5145.3 | 1.0 | 5.23 | 0.66 | 13.6 | | | 1 |
| 29 | 5159.4 | 0.8 | 9.21 | 0.59 | 31.7 | | | 1 |
| 30 | 5199.8 | 0.8 | 4.92 | 0.32 | 19.2 | | | 1 |
| 31 | 5225.7 | 0.9 | 4.72 | 0.33 | 19.3 | | | 1 |
| 32 | 5252.2 | 0.8 | 2.94 | 0.25 | 14.8 | | | 1 |
| 33 | 5279.2 | 0.8 | 6.17 | 0.22 | 36.4 | | | 1 |
| 34 | 5305.5 | 0.8 | 5.19 | 0.20 | 51.7 | | | 1 |
| 35 | 5323.3 | 0.8 | 0.52 | 0.09 | 9.4 | | | 1 |
| 36 | 7811.4 | 0.9 | 4.23 | 0.70 | 6.7 | | | 1 |
| | Q0710+1151 | | 3C 175 | | | $z_{em}$ = 0.768 | | |
| 1 | 3934.8 | 0.4 | 0.55 | 0.11 | 6.2 | CaII(3934) | 0.0000(1) | 1 |
| 2 | 3969.6 | 0.3 | 0.25 | 0.08 | 4.0 | CaII(3969) | 0.0000(1) | 1 |
| 3 | 4090.9 | 0.3 | 0.91 | 0.09 | 12.0 | MgII(2796) | 0.4629(1) | 1 |
| 4 | 4101.3 | 0.2 | 0.43 | 0.08 | 5.8 | MgII(2803) | 0.4629(1) | 1 |
| 5 | 4171.9 | 0.6 | 0.35 | 0.12 | 3.4 | MgI(2853) | 0.4623(2) | 1 |
| 6 | 4932.3 | 0.3 | 0.35 | 0.08 | 5.1 | | | 1 |
| | Q0725+1443 | | 3C 181 | | | $z_{em}$ = 1.382 | | |
| 1 | 6066.7 | 1.0 | 1.34 | 0.19 | 7.9 | MgII(2796) | 1.1695(4) | 1 |
| 2 | 6080.4 | 0.8 | 0.78 | 0.18 | 4.5 | MgII(2803) | 1.1688(3) | 1 |
| | Q0736-0620 | | PKS 0736-06 | | | $z_{em}$ = 1.898 | | |
| 1 | 4362.1 | 0.9 | 0.74 | 0.10 | 8.2 | CIV(1548) | 1.8175(6) | 1 |
| 2 | 4369.3 | 0.9 | 0.71 | 0.09 | 8.8 | CIV(1550) | 1.8175(6) | 1 |
| 3 | 4510.0 | 0.8 | 2.46 | 0.14 | 41.5 | CIV(1548) | 1.9131(5) | 1 |
| 4 | 4517.6 | 0.8 | 1.45 | 0.13 | 31.4 | CIV(1550) | 1.9131(5) | 1 |
| 5 | 4538.6 | 0.8 | 3.56 | 0.23 | 55.3 | CIV(1548) | 1.9316(5) | 1 |
| 6 | 4544.8 | 0.8 | 2.12 | 0.22 | 42.4 | CIV(1550) | 1.9306(5) | 1 |
| 7 | 5729.7 | 1.5 | 0.25 | 0.10 | 4.2 | FeII(2600) | 1.2036(6) | 1 |
| 8 | 6154.8 | 1.4 | 0.41 | 0.10 | 9.4 | MgII(2796) | 1.2010(5) | 1 |
| 9 | 6161.5 | 0.9 | 1.07 | 0.09 | 16.3 | MgII(2796) | 1.2034(3) | 1 |
| 10 | 6171.2 | 0.8 | 0.36 | 0.09 | 10.0 | MgII(2803) | 1.2012(3) | 1 |
| 11 | 6176.3 | 0.8 | 0.90 | 0.10 | 12.6 | MgII(2803) | 1.2030(3) | 1 |
| | Q0809+4822 | | 3C 196 | | | $z_{em}$ = 0.871 | | |
| 1 | 3359.7 | 0.7 | 1.92 | 0.45 | 5.3 | FeII(2344) | 0.4332(3) | 1 |
| 2 | 3406.0 | 0.4 | 1.15 | 0.23 | 6.0 | FeII(2374) | 0.4344(2) | 1 |
| 3 | 3418.9 | 0.4 | 1.76 | 0.31 | 6.7 | FeII(2382) | 0.4348(2) | 1 |
| 4 | 3702.6 | 0.3 | 0.93 | 0.15 | 7.6 | MnII(2577) | 0.4369(1) | 1 |
| 5 | 3716.1 | 0.3 | 2.05 | 0.16 | 16.9 | FeII(2586) | 0.4367(1) | 1 |
| 6 | 3727.1 | 0.3 | 0.62 | 0.14 | 5.5 | MnII(2594) | 0.4365(1) | 1 |
| 7 | 3735.4 | 0.3 | 2.73 | 0.18 | 20.8 | FeII(2600) | 0.4366(1) | 1 |
| 8 | 3744.1 | 0.3 | 0.85 | 0.17 | 6.1 | MnII(2606) | 0.4365(1) | 1 |
| 9 | 4017.7 | 0.2 | 3.04 | 0.16 | 25.9 | MgII(2796) | 0.4368(1) | 1 |
| 10 | 4028.0 | 0.2 | 2.91 | 0.15 | 24.3 | MgII(2803) | 0.4367(1) | 1 |
| 11 | 4099.4 | 0.3 | 1.48 | 0.15 | 11.9 | MgI(2853) | 0.4369(1) | 1 |

TABLE 3—*Continued*

| No. | $\lambda_{abs}$ | $\sigma(\lambda)$ | EW | $\sigma$(EW) | SL | ID | $z_{abs}$ | Sp.# |
|---|---|---|---|---|---|---|---|---|
| | Q0835+5804 | | 3C 205 | | | $z_{em}$ = 1.534 | | |
| 1 | 4274.2 | 0.8 | 1.09 | 0.23 | 5.4 | | | 1 |
| 2 | 5780.1 | 1.1 | 0.56 | 0.13 | 5.1 | FeII(2374) | 1.4343(5) | 1 |
| 3 | 5798.6 | 1.2 | 0.54 | 0.14 | 4.6 | FeII(2382) | 1.4336(5) | 1 |
| 4 | 6330.1 | 1.2 | 0.75 | 0.17 | 5.4 | FeII(2600) | 1.4345(5) | 1 |
| 5 | 6802.6 | 1.5 | 0.60 | 0.16 | 4.9 | MgII(2796) | 1.4327(6) | 1 |
| 6 | 6814.0 | 1.2 | 1.25 | 0.16 | 11.5 | MgII(2796) | 1.4367(4) | 1 |
| 7 | 6820.8 | 0.8 | 0.75 | 0.18 | 8.4 | MgII(2803) | 1.4329(3) | 1 |
| 8 | 6829.9 | 0.8 | 0.82 | 0.17 | 6.1 | MgII(2803) | 1.4362(3) | 1 |
| 9 | 6944.8 | 1.6 | 0.50 | 0.14 | 3.6 | MgI(2853) | 1.4342(6) | 1 |
| | Q0855+1421 | | 3C 212 | | | $z_{em}$ = 1.043 | | |
| 1 | 5728.8 | 0.9 | 1.56 | 0.32 | 5.4 | MgII(2796) | 1.0487(3) | 1 |
| 2 | 5744.1 | 0.8 | 1.02 | 0.29 | 3.7 | MgII(2803) | 1.0489(3) | 1 |
| 3 | 5909.5 | 1.7 | 5.51 | 0.89 | 7.5 | | | 1 |
| | Q0859-1403 | | PKS 0859-14 | | | $z_{em}$ = 1.327 | | |
| | | | — No lines detected — | | | | | |
| | Q0906+4305 | | 3C 216 | | | $z_{em}$ = 0.670 | | |
| | | | — No lines detected — | | | | | |
| | Q1007+4147 | | 4C 41.21 | | | $z_{em}$ = 0.613 | | |
| 1 | 3222.1 | 0.3 | 0.73 | 0.13 | 6.5 | | | 1 |
| 2 | 3968.0 | 0.4 | 0.40 | 0.09 | 5.0 | | | 1 |
| 3 | 4547.8 | 0.4 | 0.57 | 0.10 | 6.4 | | | 1 |
| | Q1040+1219 | | 3C 245 | | | $z_{em}$ = 1.029 | | |
| 1 | 4640.3 | 0.4 | 0.97 | 0.17 | 6.6 | MgII(2796) | 0.6594(1) | 1 |
| 2 | 4650.5 | 0.4 | 0.69 | 0.16 | 5.0 | MgII(2803) | 0.6588(2) | 1 |
| | Q1055+2007 | | PKS 1055+20 | | | $z_{em}$ = 1.110 | | |
| 1 | 3323.6 | 0.4 | 0.62 | 0.13 | 5.8 | | | 1 |

| No. | $\lambda_{abs}$ | $\sigma(\lambda)$ | EW | $\sigma$(EW) | SL | ID | $z_{abs}$ | Sp.# |
|---|---|---|---|---|---|---|---|---|
| | Q1111+4053 | | 3C 254 | | | $z_{em}$ = 0.734 | | |
| | | | — No lines detected — | | | | | |
| | Q1136-1334 | | PKS 1136-13 | | | $z_{em}$ = 0.554 | | |
| | | | — No lines detected — | | | | | |
| | Q1137+6604 | | 3C 263 | | | $z_{em}$ = 0.652 | | |
| 1 | 3935.2 | 0.3 | 0.28 | 0.05 | 5.4 | CaII(3934) | 0.0001(1) | 1 |
| 2 | 3968.6 | 0.4 | 0.18 | 0.05 | 3.3 | CaII(3969) | -.0002(1) | 1 |
| 3 | 4041.8 | 0.3 | 0.27 | 0.06 | 5.1 | | | 1 |
| 4 | 4544.4 | 0.3 | 0.27 | 0.07 | 5.2 | | | 1 |
| 5 | 4574.8 | 0.4 | 0.25 | 0.07 | 3.9 | MgII(2796) ? | 0.6360(1) | 1 |
| 6 | 4587.4 | 0.2 | 0.26 | 0.07 | 4.5 | MgII(2803) ? | 0.6363(1) | 1 |
| | Q1148-0007 | | PKS 1148-00 | | | $z_{em}$ = 1.982 | | |
| 1 | 4624.0 | 0.8 | 0.59 | 0.07 | 9.5 | CIV(1548) | 1.9867(5) | 1 |
| 2 | 4633.3 | 0.8 | 0.87 | 0.08 | 11.9 | CIV(1550) | 1.9878(5) | 1 |
| | Q1153+3144 | | 4C 31.38 | | | $z_{em}$ = 0.418 | | |
| | | | — No lines detected — | | | | | |
| | Q1156+2931 | | 4C 29.45 | | | $z_{em}$ = 0.729 | | |
| | | | — No lines detected — | | | | | |
| | Q1206+4356 | | 3C 268.4 | | | $z_{em}$ = 1.400 | | |
| | | | — No lines detected — | | | | | |
| | Q1213+5352 | | 4C 53.24 | | | $z_{em}$ = 1.065 | | |
| | | | — No lines detected — | | | | | |

TABLE 3—*Continued*

| No. | $\lambda_{abs}$ | $\sigma(\lambda)$ | EW | $\sigma$(EW) | SL | ID | $z_{abs}$ | Sp.# |
|---|---|---|---|---|---|---|---|---|
| | Q1218+3359 | | 3C 270.1 | | | $z_{em}$ = 1.519 | | |
| 1 | 3870.7 | 1.4 | 5.76 | 2.56 | 36.3 | CIV(1548) | 1.5001(9) | 1 |
| 2 | 3877.2 | 0.3 | 8.09 | 2.66 | 38.3 | CIV(1550) | 1.5002(2) | 1 |
| 3 | 4871.8 | 0.9 | 2.34 | 0.51 | 5.8 | MgII(2796) | 0.7422(3) | 2 |
| 4 | 4884.7 | 1.0 | 1.88 | 0.50 | 4.8 | MgII(2803) | 0.7423(3) | 2 |
| 5 | 6991.4 | 0.4 | 3.13 | 0.22 | 18.5 | MgII(2796) | 1.5002(1) | 2 |
| 6 | 7008.1 | 0.5 | 2.91 | 0.23 | 15.3 | MgII(2803) | 1.4997(2) | 2 |
| | Q1229-0207 | | PKS 1229-02 | | | $z_{em}$ = 1.038 | | |
| 1 | 4875.6 | 0.8 | 0.84 | 0.14 | 7.2 | | | 1 |
| 2 | 4913.5 | 0.8 | 0.92 | 0.13 | 7.1 | MgII(2796) | 0.7571(3) | 1 |
| 3 | 4926.0 | 0.8 | 0.85 | 0.12 | 6.7 | MgII(2803) | 0.7571(3) | 1 |
| | Q1318+1122 | | PKS 1318+11 | | | $z_{em}$ = 2.171 | | |
| 1 | 4452.2 | 0.6 | 1.28 | 0.21 | 6.7 | CIV(1548) | 1.8757(4) | 1 |
| 2 | 4458.7 | 1.1 | 0.70 | 0.22 | 3.7 | CIV(1550) | 1.8751(7) | 1 |
| 3 | 5148.9 | 0.9 | 1.18 | 0.25 | 4.7 | MgII(2796) | 0.8413(3) | 2 |
| 4 | 5161.7 | 1.5 | 0.69 | 0.25 | 2.7 | MgII(2803) | 0.8411(5) | 2 |
| 5 | 5745.6 | 0.9 | 1.11 | 0.23 | 4.7 | MgII(2796) ? | 1.0547(3) | 2 |
| | Q1327-2126 | | PKS 1327-21 | | | $z_{em}$ = 0.528 | | |
| 1 | 3638.6 | 0.3 | 0.84 | 0.19 | 4.9 | MgII(2796) ? | 0.3012(1) | 1 |
| 2 | 3649.0 | 0.5 | 0.57 | 0.21 | 3.0 | MgII(2803) ? | 0.3016(2) | 1 |
| | Q1328+2524 | | 3C 287 | | | $z_{em}$ = 1.055 | | |
| | | | | — No lines detected — | | | | |
| | Q1328+3045 | | 3C 286 | | | $z_{em}$ = 0.846 | | |
| 1 | 4378.6 | 0.6 | 0.30 | 0.08 | 4.4 | FeII(2586) | 0.6928(2) | 1 |
| 2 | 4401.0 | 0.5 | 0.73 | 0.10 | 9.2 | FeII(2600) | 0.6926(2) | 1 |
| 3 | 6661.3 | 1.1 | 0.46 | 0.11 | 4.7 | CaII(3934) | 0.6929(3) | 2 |
| 4 | 6719.3 | 1.5 | 0.23 | 0.08 | 2.8 | CaII(3969) | 0.6927(4) | 2 |
| | Q1335-0611 | | PKS 1335-06 | | | $z_{em}$ = 0.625 | | |
| 1 | 4988.4 | 0.7 | 2.29 | 0.47 | 5.1 | | | 1 |
| | Q1354-1512 | | PKS 1354-15 | | | $z_{em}$ = 1.890 | | |
| 1 | 4838.8 | 0.9 | 2.35 | 0.43 | 5.4 | | | 1 |
| 2 | 5679.1 | 0.9 | 2.60 | 0.43 | 7.4 | MgII(2796) | 1.0309(3) | 1 |
| 3 | 5694.5 | 0.8 | 1.49 | 0.45 | 3.5 | MgII(2803) | 1.0312(3) | 1 |
| | Q1437+6224 | | OQ 663 | | | $z_{em}$ = 1.090 | | |
| 1 | 5236.0 | 0.8 | 1.32 | 0.16 | 7.8 | MgII(2796) | 0.8724(3) | 1 |
| 2 | 5248.5 | 0.8 | 1.19 | 0.16 | 7.2 | MgII(2803) | 0.8721(3) | 1 |
| 3 | 5843.7 | 1.0 | 1.87 | 0.22 | 10.0 | | | 1 |
| | Q1442+1011 | | OQ 172 | | | $z_{em}$ = 3.530 | | |
| 1 | 5624.6 | 0.8 | 0.88 | 0.09 | 11.8 | CIV(1548) | 2.6330(5) | 1 |
| 2 | 5634.0 | 0.8 | 0.45 | 0.08 | 6.2 | CIV(1550) | 2.6330(5) | 1 |
| 3 | 5719.2 | 0.9 | 0.45 | 0.11 | 4.4 | CIV(1548) ? | 2.6941(6) | 1 |
| 4 | 5728.8 | 0.8 | 0.17 | 0.09 | 1.0 | CIV(1550) ? | 2.6941(5) | 1 |
| | Q1453-1056 | | PKS 1453-10 | | | $z_{em}$ = 0.938 | | |
| | | | | — No lines detected — | | | | |
| | Q1458+7152 | | 3C 309.1 | | | $z_{em}$ = 0.905 | | |
| 1 | 3934.8 | 0.2 | 0.41 | 0.07 | 7.1 | CaII(3934) | 0.0000(1) | 1 |
| 2 | 3945.6 | 0.4 | 0.20 | 0.06 | 3.5 | AlI(3945) | 0.0001(1) | 1 |
| 3 | 3968.8 | 0.5 | 0.38 | 0.09 | 5.1 | CaII(3969) | -.0002(1) | 1 |
| 4 | 5883.2 | 0.5 | 0.55 | 0.12 | 5.3 | NaI(5891) ? | -.0014(1) | 2 |
| 5 | 5888.0 | 0.3 | 0.89 | 0.13 | 7.6 | NaI(5897) ? | -.0016(1) | 2 |
| | Q1508-0531 | | PKS 1508-05 | | | $z_{em}$ = 1.191 | | |
| | | | | — No lines detected — | | | | |
| | Q1618+1743 | | 3C 334 | | | $z_{em}$ = 0.555 | | |
| 1 | 5884.1 | 1.0 | 0.94 | 0.21 | 5.3 | | | 2 |
| 2 | 6825.3 | 1.0 | 1.00 | 0.21 | 5.6 | | | 2 |

TABLE 3—*Continued*

| No. | $\lambda_{abs}$ | $\sigma(\lambda)$ | EW | $\sigma$(EW) | SL | ID | $z_{abs}$ | Sp.# |
|---|---|---|---|---|---|---|---|---|
| | Q1622+2352 | | 3C 336 | | | $z_{em}$ = 0.927 | | |
| 1 | 3826.4 | 0.3 | 0.92 | 0.14 | 7.3 | FeII(2600) | 0.4716(1) | 1 |
| 2 | 3882.2 | 0.2 | 1.16 | 0.11 | 12.2 | FeII(2344) | 0.6561(1) | 1 |
| 3 | 3932.9 | 0.3 | 1.28 | 0.13 | 10.7 | FeII(2374) | 0.6564(1) | 1 |
| 4 | 3946.1 | 0.1 | 1.39 | 0.10 | 16.0 | FeII(2382) | 0.6561(1) | 1 |
| 5 | 4115.8 | 0.2 | 1.40 | 0.11 | 15.7 | MgII(2796) | 0.4718(1) | 1 |
| 6 | 4126.4 | 0.2 | 1.50 | 0.12 | 14.9 | MgII(2803) | 0.4719(1) | 1 |
| 7 | 4282.9 | 0.2 | 1.03 | 0.11 | 11.3 | FeII(2586) | 0.6558(1) | 1 |
| 8 | 4305.4 | 0.1 | 2.09 | 0.12 | 20.8 | FeII(2600) | 0.6558(1) | 1 |
| 9 | 4433.2 | 0.2 | 0.97 | 0.09 | 12.5 | FeII(2344) | 0.8911(1) | 1 |
| 10 | 4490.6 | 0.2 | 0.91 | 0.10 | 10.1 | FeII(2374) | 0.8912(1) | 1 |
| 11 | 4505.8 | 0.2 | 1.43 | 0.11 | 15.2 | FeII(2382) | 0.8910(1) | 1 |
| 12 | 4917.8 | 0.4 | 2.52 | 0.35 | 8.9 | FeII(2600) | 0.8913(2) | 2 |
| 13 | 5290.9 | 0.4 | 3.10 | 0.25 | 13.9 | MgII(2796) | 0.8921(2) | 2 |
| 14 | 5304.1 | 0.5 | 2.29 | 0.23 | 11.3 | MgII(2803) | 0.8919(2) | 2 |
| | Q1629+1202 | | PKS 1629+12 | | | $z_{em}$ = 1.795 | | |
| 1 | 3682.5 | 0.4 | 3.16 | 0.22 | 14.2 | CIV(1548) | 1.3785(3) | 1 |
| 2 | 3688.9 | 0.3 | 2.51 | 0.23 | 14.3 | CIV(1550) | 1.3788(2) | 1 |
| 3 | 3981.8 | 0.2 | 1.08 | 0.15 | 9.1 | FeII(2600) | 0.5313(1) | 3 |
| 4 | 4281.8 | 0.1 | 2.15 | 0.10 | 24.0 | MgII(2796) | 0.5312(0) | 3 |
| | 4282.0 | 0.3 | 1.73 | 0.12 | 14.9 | " | 0.5313(1) | 1 |
| 5 | 4292.7 | 0.3 | 1.86 | 0.11 | 16.7 | MgII(2803) | 0.5312(1) | 1 |
| | 4293.1 | 0.1 | 2.06 | 0.10 | 23.5 | " | 0.5313(0) | 3 |
| 6 | 4353.6 | 0.8 | 1.10 | 0.24 | 6.0 | | | 1 |
| 7 | 4368.6 | 0.6 | 0.86 | 0.19 | 5.6 | MgI(2853) | 0.5312(2) | 1 |
| | 4369.3 | 0.3 | 0.48 | 0.13 | 4.4 | " | 0.5315(1) | 3 |
| 8 | 4454.4 | 0.3 | 0.69 | 0.15 | 5.5 | FeII(2344) | 0.9002(1) | 3 |
| 9 | 4527.5 | 0.3 | 1.02 | 0.19 | 6.9 | FeII(2382) | 0.9001(1) | 3 |
| | 4528.5 | 0.6 | 1.42 | 0.26 | 6.9 | " | 0.9005(2) | 1 |
| 10 | 5314.0 | 0.6 | 1.86 | 0.34 | 5.8 | MgII(2796) | 0.9003(2) | 4 |
| | 5315.3 | 0.4 | 2.29 | 0.17 | 11.5 | " | 0.9008(1) | 2 |
| 11 | 5327.8 | 0.3 | 1.04 | 0.31 | 3.1 | MgII(2803) | 0.9004(1) | 4 |
| | 5328.5 | 0.6 | 1.32 | 0.17 | 6.2 | " | 0.9006(2) | 2 |
| | Q1634+6251 | | 3C 343 | | | $z_{em}$ = 0.988 | | |
| | | | — No lines detected — | | | | | |
| | Q1828+4842 | | 3C 380 | | | $z_{em}$ = 0.695 | | |
| 1 | 3935.0 | 0.5 | 0.78 | 0.19 | 5.0 | CaII(3934) ? | 0.0001(1) | 3 |
| 2 | 5888.1 | 0.9 | 0.37 | 0.09 | 6.7 | NaI(5891) | -.0006(2) | 2 |
| | 5889.6 | 0.9 | 0.77 | 0.07 | 17.4 | " | -.0003(1) | 5 |
| 3 | 5894.7 | 0.3 | 0.41 | 0.09 | 8.3 | NaI(5897) | -.0005(0) | 2 |
| | 5895.5 | 0.8 | 0.46 | 0.08 | 13.7 | " | -.0003(1) | 5 |
| | Q1901+3155 | | 3C 395 | | | $z_{em}$ = 0.635 | | |
| 1 | 3887.2 | 0.1 | 0.63 | 0.06 | 11.7 | MgII(2796) | 0.3901(0) | 1 |
| 2 | 3897.4 | 0.1 | 0.21 | 0.06 | 3.9 | MgII(2803) | 0.3902(0) | 1 |
| 3 | 3934.5 | 0.3 | 0.63 | 0.08 | 9.5 | CaII(3934) | -.0001(1) | 1 |
| 4 | 3969.8 | 0.3 | 0.27 | 0.07 | 5.1 | CaII(3969) | 0.0001(1) | 1 |
| 5 | 5889.0 | 0.5 | 0.64 | 0.09 | 7.8 | NaI(5891) | -.0004(1) | 2 |
| 6 | 5895.1 | 0.3 | 0.33 | 0.09 | 4.1 | NaI(5897) | -.0004(1) | 2 |
| | Q2003-0232 | | 4C -02.79 | | | $z_{em}$ = 1.457 | | |
| 1 | 3422.8 | 0.8 | 4.07 | 0.88 | 6.5 | CIV(1548) | 1.2108(5) | 1 |
| 2 | 3429.3 | 0.3 | 3.76 | 0.86 | 5.3 | CIV(1550) | 1.2114(2) | 1 |
| 3 | 3803.6 | 0.5 | 1.71 | 0.23 | 7.5 | CIV(1548) | 1.4568(3) | 1 |
| | 3804.4 | 0.2 | 0.99 | 0.18 | 6.2 | " | 1.4573(1) | 3 |
| 4 | 3810.1 | 0.3 | 1.32 | 0.24 | 7.0 | CIV(1550) | 1.4569(2) | 1 |
| | 3810.4 | 0.1 | 0.97 | 0.18 | 6.1 | " | 1.4571(1) | 3 |
| 5 | 4531.4 | 0.3 | 0.61 | 0.10 | 6.1 | | | 3 |
| 6 | 5188.3 | 0.9 | 0.84 | 0.27 | 3.9 | FeII(2344) | 1.2132(4) | 2 |
| 7 | 5271.8 | 0.6 | 1.74 | 0.43 | 4.8 | FeII(2382) | 1.2125(3) | 4 |
| | 5274.7 | 0.6 | 2.07 | 0.33 | 7.8 | " | 1.2137(3) | 2 |
| 8 | 5722.0 | 0.9 | 1.11 | 0.26 | 4.9 | FeII(2586) | 1.2121(4) | 2 |
| | 5723.8 | 0.6 | 1.10 | 0.26 | 5.1 | " | 1.2128(2) | 4 |
| 9 | 5745.1 | 0.9 | 1.03 | 0.33 | 3.5 | FeII(2382) | 1.4111(4) | 4 |
| 10 | 5749.8 | 0.6 | 2.82 | 0.31 | 10.4 | FeII(2600) | 1.2113(2) | 2 |
| | 5753.5 | 0.7 | 1.41 | 0.32 | 5.6 | " | 1.2127(3) | 4 |
| 11 | 6184.7 | 0.4 | 5.87 | 0.31 | 28.3 | MgII(2796) | 1.2117(1) | 2 |
| 12 | 6200.0 | 0.5 | 4.80 | 0.33 | 20.1 | MgII(2803) | 1.2115(2) | 2 |
| 13 | 6264.6 | 0.9 | 0.82 | 0.19 | 4.3 | FeII(2600) | 1.4093(4) | 2 |
| 14 | 6741.4 | 0.4 | 1.78 | 0.17 | 13.3 | MgII(2796) | 1.4108(1) | 2 |
| 15 | 6757.5 | 0.4 | 1.50 | 0.16 | 11.6 | MgII(2803) | 1.4104(1) | 2 |

TABLE 3—*Continued*

| No. | $\lambda_{abs}$ | $\sigma(\lambda)$ | EW | $\sigma$(EW) | SL | ID | $z_{abs}$ | Sp.# |
|---|---|---|---|---|---|---|---|---|
| | Q2044-0247 | | 3C 422 | | | $z_{em}$ = 0.942 | | |
| 1 | 4544.0 | 0.3 | 2.35 | 0.38 | 7.4 | FeII(2344) | 0.9384(1) | 1 |
| 2 | 5038.6 | 1.1 | 4.24 | 1.32 | 3.6 | FeII(2600) | 0.9378(4) | 2 |
| 3 | 5420.0 | 0.4 | 5.51 | 0.41 | 13.2 | MgII(2796) | 0.9382(1) | 2 |
| 4 | 5434.7 | 0.3 | 4.20 | 0.35 | 11.8 | MgII(2803) | 0.9385(1) | 2 |
| 5 | 5531.0 | 0.6 | 2.74 | 0.45 | 7.3 | MgI(2853) | 0.9387(2) | 2 |
| | Q2115-3031 | | PKS 2115-30 | | | $z_{em}$ = 0.980 | | |
| 1 | 5885.5 | 1.5 | 0.41 | 0.16 | 4.9 | NaI(5891) | -.0010(3) | 2 |
| 2 | 5891.6 | 1.5 | 0.47 | 0.16 | 5.9 | NaI(5897) | -.0010(2) | 2 |
| | Q2143-1541 | | PKS 2143-15 | | | $z_{em}$ = 0.700 | | |
| 1 | 5457.4 | 1.0 | 0.76 | 0.13 | 6.6 | | | 2 |
| | Q2223+2102 | | PKS 2223+21 | | | $z_{em}$ = 1.959 | | |
| 1 | 3779.8 | 0.6 | 0.60 | 0.09 | 7.1 | CIV(1548) ? | 1.4414(4) | 1 |
| 2 | 3786.3 | 0.7 | 0.50 | 0.09 | 5.7 | CIV(1550) ? | 1.4416(4) | 1 |
| | | | | | | +SiII(1304) ? | 1.9028(5) | 1 |
| 3 | 3871.1 | 0.4 | 0.57 | 0.09 | 7.8 | CII(1334) | 1.9007(3) | 1 |
| 4 | 4043.6 | 0.4 | 0.75 | 0.20 | 11.8 | SiIV(1393) | 1.9012(3) | 1 |
| 5 | 4069.9 | 0.5 | 0.53 | 0.09 | 6.9 | SiIV(1402) | 1.9014(3) | 1 |
| 6 | 4429.0 | 0.6 | 0.38 | 0.09 | 5.2 | SiII(1526) | 1.9010(4) | 1 |
| 7 | 4493.4 | 0.4 | 1.01 | 0.08 | 12.8 | CIV(1548) | 1.9023(3) | 1 |
| 8 | 4500.3 | 0.3 | 0.79 | 0.08 | 10.1 | CIV(1550) | 1.9019(2) | 1 |
| 9 | 6800.5 | 0.7 | 0.51 | 0.10 | 6.4 | FeII(2344) | 1.9010(3) | 2 |
| | Q2230+1128 | | CTA 102 | | | $z_{em}$ = 1.037 | | |
| 1 | 5888.5 | 0.9 | 0.53 | 0.11 | 8.4 | NaI(5891) | -.0005(2) | 2 |
| 2 | 5894.7 | 0.3 | 0.44 | 0.12 | 7.6 | NaI(5897) | -.0005(0) | 2 |
| | Q2249+1832 | | 3C 454 | | | $z_{em}$ = 1.757 | | |
| | | | — No lines detected — | | | | | |

| No. | $\lambda_{abs}$ | $\sigma(\lambda)$ | EW | $\sigma$(EW) | SL | ID | $z_{abs}$ | Sp.# |
|---|---|---|---|---|---|---|---|---|
| | Q2251+2429 | | PKS 2251+24 | | | $z_{em}$ = 2.328 | | |
| 1 | 4151.9 | 0.4 | 1.61 | 0.14 | 14.3 | NV(1238) | 2.3515(3) | 1 |
| 2 | 4166.7 | 0.4 | 2.87 | 0.16 | 22.1 | NV(1242) | 2.3526(3) | 1 |
| 3 | 4180.4 | 0.5 | 1.07 | 0.16 | 8.4 | NV(1242) | 2.3637(4) | 1 |
| 4 | 4212.6 | 2.5 | 0.31 | 0.24 | 4.2 | CII(1334) | 2.1566(*) | 1 |
| 5 | 4256.5 | 0.7 | 0.94 | 0.17 | 6.6 | CIV(1548) | 1.7493(4) | 1 |
| 6 | 4264.4 | 0.3 | 0.49 | 0.16 | 3.7 | CIV(1550) | 1.7499(2) | 1 |
| 7 | 4397.5 | 0.9 | 1.12 | 0.23 | 5.4 | SiIV(1393) | 2.1551(7) | 1 |
| 8 | 4542.3 | 1.4 | 2.26 | 0.43 | 6.3 | | | 3 |
| 9 | 4689.3 | 1.2 | 1.11 | 0.27 | 5.0 | SiIV(1393) | 2.3645(9) | 3 |
| 10 | 4719.1 | 1.1 | 1.57 | 0.29 | 6.4 | SiIV(1402) | 2.3641(8) | 3 |
| 11 | 4885.9 | 0.8 | 3.61 | 0.22 | 18.0 | CIV(1548) | 2.1559(5) | 3 |
| | 4891.7 | 0.5 | 1.52 | 0.26 | 8.6 | " | 2.1596(3) | 2 |
| 12 | 4894.1 | 0.8 | 2.02 | 0.21 | 12.3 | CIV(1550) | 2.1559(5) | 3 |
| | 4900.9 | 0.3 | 2.58 | 0.24 | 9.6 | " | 2.1603(2) | 2 |
| 13 | 5190.3 | 0.9 | 2.09 | 0.19 | 14.5 | CIV(1548) | 2.3525(6) | 3 |
| | 5193.3 | 0.3 | 2.17 | 0.14 | 16.7 | " | 2.3544(2) | 2 |
| 14 | 5198.7 | 0.8 | 1.55 | 0.22 | 13.6 | CIV(1550) | 2.3523(5) | 3 |
| | 5200.5 | 0.3 | 1.24 | 0.14 | 13.7 | " | 2.3535(2) | 2 |
| 15 | 5207.3 | 0.8 | 5.10 | 0.22 | 34.4 | CIV(1548) | 2.3635(5) | 3 |
| | 5209.7 | 0.3 | 5.01 | 0.14 | 43.5 | " | 2.3650(2) | 2 |
| 16 | 5214.3 | 0.8 | 4.58 | 0.23 | 33.0 | CIV(1550) | 2.3624(5) | 3 |
| | 5218.9 | 0.3 | 4.71 | 0.14 | 38.9 | " | 2.3653(2) | 2 |
| 17 | 5843.2 | 0.7 | 0.53 | 0.13 | 4.0 | MgII(2796) | 1.0896(3) | 2 |
| 18 | 5857.7 | 0.3 | 0.59 | 0.13 | 4.5 | MgII(2803) | 1.0894(1) | 2 |

TABLE 4

Mg II λλ2796, 2803 ABSORPTION LINES

| Object | $z_{em}$ | $z_{abs}$ | New | $W_0(\lambda 2796)$ | $W_0(\lambda 2803)$ | $W_0$(MgI λ2852) |
|---|---|---|---|---|---|---|
| Q0229+1309 | 2.065 | 1.8609(4) | * | 1.02(14) | 0.70(14) | <0.57 |
| Q0229+3410 | 1.240 | 0.7754(3) | * | 1.92(41) | 2.02(36) | <1.13 |
| | | 1.2248(3) | * | 3.47(16) | 2.14(16) | 0.56(16) |
| Q0237-2322 | 2.224 | 1.3647(3) | | 1.91( 8) | 1.43( 8) | <0.16 |
| | | 1.6582(3) | | 0.55( 5) | 0.42( 5) | ... |
| | | 1.6719(3) | | 0.80( 5) | 0.61( 5) | ... |
| Q0420-0127 | 0.915 | 0.6330(3) | | 1.02(10) | 0.86(10) | <0.36 |
| Q0710+1151 | 0.768 | 0.4630(1) | * | 0.62( 6) | 0.29( 5) | 0.24( 8) |
| Q0725+1443 | 1.382 | 1.1694(4) | * | 0.62( 9) | 0.36( 8) | <0.28 |
| Q0736-0620 | 1.898 | 1.2009(5) | * | 0.19( 5) | 0.16( 4) | ... |
| | | 1.2035(3) | * | 0.49( 4) | 0.41( 5) | ... |
| Q0809+4822 | 0.871 | 0.4367(1) | | 2.12(11) | 2.03(10) | 1.03(10) |
| Q0835+5804 | 1.534 | 1.4330(6) | | 0.25( 7) | 0.31( 7) | 0.21( 6) |
| | | 1.4365(4) | | 0.51( 7) | 0.34( 7) | <0.20 |
| Q0855+1421 | 1.043 | 1.0491(3) | * | 0.76(16) | 0.50(14) | ... |
| Q1040+1219 | 1.029 | 0.6591(1) | * | 0.58(10) | 0.42(10) | <0.19 |
| Q1218+3359 | 1.519 | 0.7423(3) | * | 1.34(29) | 1.08(29) | <0.74 |
| | | 1.5000(1) | * | 1.25( 9) | 1.16( 9) | ... |
| Q1229-0207 | 1.038 | 0.7571(3) | * | 0.52( 7) | 0.48( 7) | <0.22 |
| Q1354-1512 | 1.890 | 1.0309(3) | * | 1.28(21) | 0.73(22) | <0.88 |
| Q1437+6224 | 1.090 | 0.8723(3) | * | 0.71( 9) | 0.64( 9) | <0.42 |
| Q1622+2352 | 0.927 | 0.4718(1) | | 0.95( 7) | 1.02( 8) | <0.20 |
| | | 0.8920(2) | | 1.64(13) | 1.21(12) | ... |
| Q1629+1202 | 1.795 | 0.5313(0) | | 1.40( 7) | 1.35( 7) | 0.31( 8) |
| | | 0.9008(1) | | 1.20( 9) | 0.69( 9) | <0.39 |
| Q1901+3155 | 0.635 | 0.3901(0) | * | 0.45( 4) | 0.15( 4) | <0.13 |
| Q2003-0232 | 1.457 | 1.2116(1) | * | 2.65(14) | 2.17(15) | <0.31 |
| | | 1.4106(1) | * | 0.74( 7) | 0.62( 7) | ... |
| Q2044-0247 | 0.942 | 0.9384(1) | * | 2.84(21) | 2.17(18) | 1.41(23) |

$z_{abs}$ = 1.8609.—This strong system is most likely associated with the $z_{abs}$ = 1.8622 C IV system of SBS. Although the line wavelength ratio is rather poor, the system is fitted adequately ($\chi^2_\nu$ = 0.7) by an Mg II doublet. The redshift discrepancy is probably due to wavelength calibration error at this high wavelength.

### 7.4. *Q0229+3410 (3C 68.1,* $z_{em}$ = 1.240)

We find no published spectra for this object. We find the following absorption systems:

$z_{abs}$ = 0.2022.—We observe a Na I doublet at this redshift.

$z_{abs}$ = 0.7754.—This strong system is fitted well by a single Mg II doublet at spectral resolution. The two lines have equal equivalent widths to within the measurement uncertainties.

$z_{abs}$ = 1.2248.—This very strong Mg II doublet has an apparent ejection velocity of 2000 km s$^{-1}$ with respect to the quasar.

### 7.5. *Q0237−2322 (PKS 0237−23,* $z_{em}$ = 2.224)

This object has an unusually large number of strong absorption systems, and has been studied by SS, SBS, Lanzetta et al. (1987), and Boissé & Bergeron (1985). See SS for a comprehensive discussion of the known absorption systems. In our spectrum we confirm the systems at $z_{abs}$ = 1.3651, 1.6577, 1.6723, and 2.2028, but find no new absorption systems.

### 7.6. *Q0350−0719 (3C 94,* $z_{em}$ = 0.962)

This quasar was previously studied by Tytler et al. (1987), who found no absorption lines in the range 4021–4931 Å. We find a Galactic Na I absorption system in our spectrum.

### 7.7. *Q0420−0127 (PKS 0420−01,* $z_{em}$ = 0.915)

Wills et al. (1980) observed this object in the approximate range 3650–6700 Å and found an Mg II system at $z_{abs}$ = 0.633, but they give no quantitative treatment of the spectrum. Yanny (1992) presents narrow-band [O II] λ3727 photometry of this field and finds at least seven nearby candidate emission-line objects. Yanny & York (1992) take this and similar objects as evidence favoring the disappearing starburst or merging dwarf scenario at $z \gtrsim 0.5$. We confirm the $z_{abs}$ = 0.633 system and find no new absorbers in our spectrum.

### 7.8. *Q0538+4949 (3C 147,* $z_{em}$ = 0.545)

We find no published spectra and no absorption lines in our spectrum.

### 7.9. *Q0610+2605 (3C 154,* $z_{em}$ = 0.580)

No spectra are previously reported. We find a tentative associated Mg II absorber:

$z_{abs}$ = 0.5920.—This tentative Mg II system has an apparent infall velocity of 2400 km s$^{-1}$ relative to the quasar.

### 7.10. *Q0642+4454 (OH 471,* $z_{em}$ = 3.400)

Sargent, Steidel, & Boksenberg (1989, hereafter SSB2) obtained a spectrum of this object in the range 3150–7000 Å and found Mg II absorption at $z_{abs}$ = 1.2464 and C IV absorption at 2.9724, 3.1338, and 3.2483. Khare, York, & Green (1989) reported several tentative absorber systems, but none are confirmed by SSB2 even though they could have been observed. In our spectrum, which has lower signal-to-noise ratio than SSB2, we find no identified lines redward of the Ly$\alpha$ forest.

### 7.11. *Q0710+1151* (*3C 175*, $z_{em}$ = 0.768)

Boissé et al. (1992) obtained a spectrum in the range 3190–3946 Å and found Galactic Ca II λ3934 absorption. We confirm both members of the Ca II doublet and find an Mg II absorber:

$z_{abs}$ = 0.4630.—This moderate-strength Mg II system has tentative Mg I absorption, with a detection significance 3.4 $\sigma$.

### 7.12. *Q0725+1443* (*3C 181*, $z_{em}$ = 1.382)

Anderson et al. (1987, hereafter AWFC) obtained a high-resolution spectrum of this object covering the range 3150–4025 Å and found an associated C IV absorber at $z_{abs}$ = 1.3878. We see no evidence for the corresponding Mg II in our spectrum, but we find one new Mg II system:

$z_{abs}$ = 1.1694.—This is a definite Mg II absorber. The corresponding C IV is apparent in the spectrum of AWFC, although they do not identify it.

### 7.13. *Q0736−0620* (*PKS 0736−06*, $z_{em}$ = 1.898)

This quasar was previously observed by Young, Sargent, & Boksenberg (1982, hereafter YSB), in the range 3500–5150 Å. They found associated C IV absorption at $z_{abs}$ = 1.9132 and 1.9310. We confirm these systems and find another C IV system (not associated) and an Mg II complex:

$z_{abs}$ = 1.2009, 1.2035.—This definite Mg II complex is clearly asymmetric but is fitted well with two Mg II doublets at the spectral resolution. There is evidence for Mg I at both these redshifts, but they cannot be confirmed because they fall in an $O_2$ band which was visible in a number of our spectra at high air mass. Notice the prominent $O_2$ band near 7600 Å. We also see evidence for Fe II with 3 $\sigma$ and 4 $\sigma$ detections of λλ2382 and 2600, respectively. The corresponding C IV is out of the range of YSB.

$z_{abs}$ = 1.8175.—This weak but definite system would appear in the spectrum of YSB at about a 3.7 $\sigma$ significance.

### 7.14. *Q0809+4822* (*3C 196*, $z_{em}$ = 0.871)

This object has a famous and well-studied absorption system at $z_{abs}$ = 0.43685 which gives rise to a host of metal-line species (see Foltz, Chaffee, & Wolfe 1988, who present excellent high-resolution spectra covering 3300–4200 Å and 5150–5950 Å) and H I 21 cm absorption (Brown et al. 1988; Brown & Mitchell 1983). The 21 cm absorption is especially significant because it occurs in a resolved background source, which allows useful limits to be placed on the absorber size (Foltz et al. 1988; Brown et al. 1988). There is also an associated absorber in this object at $z$ = 0.8714 (Foltz et al. 1988), with apparent infall velocity 100 km s$^{-1}$. We find no additional absorption systems in our spectrum.

### 7.15. *Q0835+5804* (*3C 205*, $z_{em}$ = 1.534)

BTT obtained a high signal-to-noise spectrum of this object covering the range 3980–7750 Å and found Mg II systems at $z_{abs}$ = 1.4353, 1.4382, and 1.5427. AWFC found an associated C IV complex centered at $z_{abs}$ = 1.5373. We confirm the complex at $z_{abs}$ = 1.436 (although our absolute redshifts disagree by about 0.0010) and add a detection of Fe II λ2374 for the lower redshift member. We see the associated Mg II system at low confidence, about 2.5 $\sigma$, with equivalent width about half what BTT found. If present, the apparent infall velocity would be 1000 km s$^{-1}$. We find no additional absorption systems.

### 7.16. *Q0855+1421* (*3C 212*, $z_{em}$ = 1.043)

We find no published spectra for this object. The night-sky subtraction in our spectrum is worse than normal. We see an unidentified but strong, broad absorption complex just redward of the Mg II emission. This feature is consistent with either Galactic Na I absorption at −600, 150, and 750 km s$^{-1}$ or an associated Mg II complex with an apparent infall velocity of 6900 km s$^{-1}$, or a combination of the two. The associated absorber in this quasar is particularly interesting because Elvis et al. (1994) found that the X-ray spectrum shows excess soft absorption which is consistent with an absorber intrinsic to the quasar having hydrogen column density $N_H = 0.9^{+0.8}_{-0.6} \times 10^{22}$ cm$^{-2}$. This is discussed in more detail in Aldcroft et al. (1994). We find in addition the following associated Mg II system:

$z_{abs}$ = 1.0490: This is a moderate-strength associated system, with an apparent ejection velocity of 1600 km s$^{-1}$.

### 7.17. *Q0859−1403* (*PKS 0859−14*, $z_{em}$ = 1.327)

SS previously studied this object in the range 3900–6995 Å and found no absorption lines. Boissé et al. (1992) obtained a spectrum covering 3185–3946 Å and found a very tentative Mg II absorber at $z_{abs}$ = 0.2095. Our spectrum is not sensitive enough to have detected this system.

### 7.18. *Q0906+4305* (*3C 216*, $z_{em}$ = 0.670)

For this object we find no published spectra and no absorption lines in our spectrum. This object has a peculiar continuum/emission-line shape, in that the Mg II emission is almost nonexistent. Smith & Spinrad (1980) first reported the redshift based primarily on an emission line presumed to be [O II] λ3727.

### 7.19. *Q1007+4147* (*4C 41.21*, $z_{em}$ = 0.613)

We find no published spectra for this object. We find three significant lines, all unidentified. One of them is near the wavelength of Galactic Ca II, but since the other doublet member is not observed, we make no identification.

### 7.20. *Q1040+1219* (*3C 245*, $z_{em}$ = 1.029)

We find no published spectra for this object. In our spectrum we detect a new Mg II system:

$z_{abs}$ = 0.6591.—We have some reservations about this system because the calculated redshifts of the doublet members disagree by 0.0006. A fit with an Mg II doublet (with wavelength ratio constrained) clearly shows the wavelength-ratio problem, but the fit has $\chi^2_\nu \approx 1$ and so we make the identification.

### 7.21. *Q1055+2007* (*PKS 1055+20*, $z_{em}$ = 1.110)

We find no published spectra for this object. In our spectra we detect a single unidentified line on the red wing of the C IV emission.

### 7.22. *Q1111+4053* (*3C 254*, $z_{em}$ = 0.734)

We find no published spectra for this object, and we detect no absorption lines in our spectrum.

### 7.23. *Q1136−1334* (*PKS 1136−13*, $z_{em}$ = 0.554)

Boissé et al. (1992) obtained a spectrum for this object and found Galactic Ca II λ3934 absorption. We find no significant absorption lines in our spectrum.

### 7.24. *Q1137+6604* (*3C 263*, $z_{em}$ = 0.652)

We find no published spectra for this object. In our spectrum we find a Galactic Ca II absorber and a tentative associated Mg II system:

$z_{abs}$ = 0.6360.—Optimal extraction of the Mg II doublet members gives significance levels of 3.9 and 4.5 $\sigma$, respectively, with adequate agreement of the redshifts to within the uncertainties. The apparent ejection velocity is 1600 km $s^{-1}$.

### 7.25. *Q1148−0007* (*PKS 1148−00*, $z_{em}$ = 1.982)

This object has been studied by SBS and YSB, who found C IV absorption at $z_{abs}$ = 1.4669 and 1.9861. SS studied this object in the range 5148–8947 Å and found no identified absorption lines. The unidentified line they report at 6280.0 Å is most likely a weak atmospheric $O_2$ band. At the position of their line at 8854.8 Å, we observe the equivalent width $W_{obs}$ = 0.24 ± 0.23, in contrast to their value $W_{obs}$ = 1.37 ± 0.17. We find no new absorption systems in our spectrum.

### 7.26. *Q1153+3144* (*4C 31.38*, $z_{em}$ = 0.418)

This object was included in our sample based on the redshift $z_{em}$ = 1.557 given by Burbidge & Kinman (1966), although they did note that their spectrum might also be consistent with a redshift of 0.413. Our spectrum clearly shows that this object has a redshift of $z_{em}$ = 0.418 and shows emission lines typical of a Seyfert galaxy. Because of the low redshift it makes no contribution to our statistical sample. We find no absorption lines in this spectrum.

### 7.27. *Q1156+2931* (*4C 29.45*, $z_{em}$ = 0.729)

We find no published spectra for this object, and our spectrum reveals no absorption lines.

### 7.28. *Q1206+4356* (*3C 268.4*, $z_{em}$ = 1.400)

AWFC studied this object in the range 3150–4025 Å, and they found Mg II absorption at $z_{abs}$ = 0.4124 and associated C IV absorption at $z_{abs}$ = 1.3767 and 1.3963. We find no absorption lines in our spectrum. At the position of Mg II at $z_{abs}$ = 1.38 the 1 $\sigma$ rest equivalent width limit in our spectrum is 0.05 Å.

### 7.29. *Q1213+5352* (*4C 53.24*, $z_{em}$ = 1.065)

We find no published spectra for this object, and our spectrum reveals no absorption lines.

### 7.30. *Q1218+3359* (*3C 270.1*, $z_{em}$ = 1.519)

AWFC studied this object in the range 3320–4200 Å, and they found associated C IV absorption at $z_{abs}$ = 1.5004. We confirm this doublet in our spectra, find the corresponding Mg II, and find a new Mg II absorption system. Note that spectrum 1 for this object suffers from the flattening problem in the 1988 July spectra:

$z_{abs}$ = 0.7423.—This Mg II system lies at the edge of the steep red wing of the C III] λ1909 emission, and so the continuum placement is uncertain.

$z_{abs}$ = 1.5000.—This strong associated Mg II system has an apparent ejection velocity of 2600 km $s^{-1}$.

### 7.31. *Q1229−0207* (*PKS 1229−02*, $z_{em}$ = 1.038)

This object was studied by Briggs et al. (1985) over the ranges 3410–4050 Å and 5000–5910 Å. They observed the Mg II system at $z_{abs}$ = 0.395, along with the corresponding Mg I and Fe II. This system is also a 21 cm absorber (BW). In our spectrum we find one unidentified line and a new Mg II absorber:

$z_{abs}$ = 0.7571.—This moderate-strength system falls between the two spectra of Briggs et al. (1985).

### 7.32. *Q1318+1122* (*PKS 1318+11*, $z_{em}$ = 2.171)

BTT observed this object over the range 3880–7750 Å, and they found Mg II absorption at $z_{abs}$ = 0.8388 and 1.0541 and C IV at $z_{abs}$ = 1.8755. Our spectrum 1 for this object suffers from the flattening problem in the 1988 July spectra. In our spectra we confirm the Mg II at $z_{abs}$ = 0.8388, and the C IV system. The Mg II line is detected at a significance level below our 5 $\sigma$ threshold and hence is not included in the statistical analysis. For the $z_{abs}$ = 1.0541 system, we see the Mg II λ2796 line at 4.7 $\sigma$ but find no evidence for the Mg II λ2803 line at a 4.5 $\sigma$ level.

### 7.33. *Q1327−2126* (*PKS 1327−21*, $z_{em}$ = 0.528)

We find no published spectra for this object. Our spectrum shows a single tentative Mg II absorber:

$z_{abs}$ = 0.3015.—This system is regarded as tentative because it falls below our 5 $\sigma$ significance cutoff.

### 7.34. *Q1328+2524* (*3C 287*, $z_{em}$ = 1.055)

We find no published spectra for this object, and our spectrum shows no absorption lines.

### 7.35. *Q1328+3045* (*3C 286*, $z_{em}$ = 0.846)

This object contains the well-studied absorption system at $z_{abs}$ = 0.6927. At this redshift absorption has been observed in metal lines (Meyer & York 1992 and references therein), H I 21 cm (Briggs 1988), and damped Ly$\alpha$ (Cohen et al. 1992). Spectrum 1 for this object suffers from the flattening problem in the 1988 July spectra. In our spectrum we find Fe II at $z_{abs}$ = 0.6927 and no other lines. The Mg II doublet falls in the dichroic gap of the double spectrograph.

7.36. *Q1335−0611* (*PKS 1335−06*, $z_{em}$ = 0.625)

We find no published spectra for this object. Our spectrum shows one unidentified line.

7.37. *Q1354−1512* (*PKS 1354−15*, $z_{em}$ = 1.890)

We find no published spectra for this object. In our spectrum we find one new Mg II absorber:

$z_{abs}$ = 1.0309.—This is a definite Mg II system. The unidentified line at 4838 Å is at the correct wavelength for Fe II λ2382, but we see no Fe II λ2600 and so we reject this identification.

7.38. *Q1437+6224* (*OQ 663*, $z_{em}$ = 1.090)

No absorption lines have been previously reported for this object. We find a broad unidentified line which occurs in the quasar Mg II emission and a new Mg II absorber:

$z_{abs}$ = 0.8723.—This is a moderate-strength Mg II system.

7.39. *Q1442+1011* (*OQ 172*, $z_{em}$ = 3.530)

This object was observed by SBS in the range 5500–7150 Å. They found definite C IV absorption at $z_{abs}$ = 2.6336 and possible absorption at $z_{abs}$ = 2.6705, 2.6939, 3.0473, and 3.1101. BTT observed this object in the range 3875–7750 Å and did not identify any of these systems. In our spectrum we confirm the $z_{abs}$ = 2.6336 system and possibly the 2.6939 system, but not any of the others in SBS. Our 1 $\sigma$ limit on $W_{obs}$ is about 0.7–1.0 Å in this region, compared with 0.5–0.8 Å in SBS. We find no other significant lines redward of Ly$\alpha$. We have not determined wavelengths for the Ly$\alpha$ forest lines in our spectrum because the spectrum of BTT is at higher resolution.

7.40. *Q1453−1056* (*PKS 1453−10*, $z_{em}$ = 0.938)

We find no published spectra for this object, and our spectra show no absorption lines. Spectrum 1 for this object suffers from the flattening problem in the 1988 July spectra.

7.41. *Q1458+7152* (*3C 309.1*, $z_{em}$ = 0.905)

This object was previously studied by SS in the wavelength range 3100–6995 Å, and they found two unidentified lines near 5900 Å. We see only the lower wavelength line, which in our spectrum is consistent with Galactic Na I at a velocity of −450 km s$^{-1}$. We find in addition Galactic Ca II and possible Al I. These are apparent in the spectrum of SS but are not identified.

7.42. *Q1508−0531* (*PKS 1508−05*, $z_{em}$ = 1.191)

We find no published spectra for this object, and our spectra show no absorption lines. Spectrum 1 for this object suffers from the flattening problem in the 1988 July spectra.

7.43. *Q1618+1743* (*3C 334*, $z_{em}$ = 0.555)

We find no published spectra for this object. In our spectra we see two unidentified lines. Spectrum 1 for this object suffers from the flattening problem in the 1988 July spectra.

7.44. *Q1622+2352* (*3C 336*, $z_{em}$ = 0.927)

SS studied this object in the range 3100–6995 Å and found Mg II absorption at $z_{abs}$ = 0.4721, 0.6562, 0.6601, and 0.8915. We confirm these systems in our spectra and find no other absorption lines. The associated Mg II system has an apparent ejection velocity of 5500 km s$^{-1}$.

7.45. *Q1629+1202* (*PKS 1629+12*, $z_{em}$ = 1.795)

BTT obtained a spectrum of this object covering the range 3870–7750 Å and found a strong Mg II system with Mg I at $z_{abs}$ = 0.5316, and found Mg II, Mg I, and Fe II at $z_{abs}$ = 0.9004. Our spectrum 1 for this object suffers from the flattening problem in the 1988 July spectra. In our spectra we confirm the lines in BTT and find in addition Fe II λ2600 at $z_{abs}$ = 0.5313 and a new C IV absorber:

$z_{abs}$ = 1.3790.—This likely C IV absorption system is out of the range of BTT. We find no evidence for the corresponding Mg II. This system would be certain except that it falls in the badly flattened portion of the spectrum. However, there are no prominent defects near this position on the CCD and so this system is unlikely to be an artifact. There may also be Si IV absorption at this redshift, but these lines fall in the Ly$\alpha$ forest, and so we cannot make a positive identification.

7.46. *Q1634+6251* (*3C 343*, $z_{em}$ = 0.988)

We find no published spectra for this object, and our spectra show no absorption lines. This object is a Seyfert 2 galaxy with very little continuum emission.

7.47. *Q1828+4842* (*3C 380*, $z_{em}$ = 0.695)

Boissé et al. (1992) studied this object in the range 3139–3946 Å and found no lines. Spectrum 1 for this object suffers from the flattening problem in the 1988 July spectra. In our spectra we find Galactic Na I and tentative Ca II.

7.48. *Q1901+3155* (*3C 395*, $z_{em}$ = 0.635)

We find no published spectra for this object. We find in our spectra a new Mg II absorber and Galactic Ca II and Na I:

$z_{abs}$ = 0.3901.—This system is included in our statistical analysis, although the doublet ratio for this system is on the border of acceptability at 2.7 ± 0.7.

7.49. *Q2003−0232* (*4C −02.79*, $z_{em}$ = 1.457)

We find no published spectra for this object. Spectrum 1 for this object suffers from the flattening problem in the 1988 July spectra, but the lines we find are far away from known defects on the CCD or are corroborated otherwise. We find in our spectra a rich collection of lines from three absorption systems:

$z_{abs}$ = 1.212.—This very strong system is seen in C IV, Mg II, and four Fe II lines. It is apparent from the poor redshift match among different lines in these spectra that the uncertainty in the wavelength calibration is around 2–3 Å, rather more than the formal value.

$z_{abs}$ = 1.411.—This certain Mg II system shows absorption in the two strongest Fe II lines, but not in C IV. There is also what would appear to be a very strong Mg I line at this redshift, but it unfortunately falls right in a telluric band. The spectrum was taken at an air mass of 1.25, so the band is most likely contributing to the Mg I line strength at some level. However, the shape of the spectrum in this region would be unusual for pure telluric absorption. To complicate matters further, if there were Mg II at $z_{abs} = 1.457$, the line Mg II λ2796 would also be coincident with the possible $z_{abs} = 1.411$ Mg I line. If associated with the quasar, this system would have an apparent ejection velocity of 5800 km $s^{-1}$.

$z_{abs} = 1.457$.—This is a definite associated C IV absorber with an apparent ejection velocity of 100 km $s^{-1}$.

### 7.50. *Q2044−0247* (*3C 422*, $z_{em} = 0.942$)

We find no published spectra for this object. In our spectra we find one strong associated Mg II absorption system:

$z_{abs} = 0.9384$.—This definite associated system shows absorption in Mg II, Mg I, and two Fe II lines. Note that our spectra did not cover Fe II λ2382 at this redshift. The apparent ejection velocity of this system is 600 km $s^{-1}$.

### 7.51. *Q2115−3031* (*PKS 2115−30*, $z_{em} = 0.980$)

We find no published spectra for this object. In our spectra we see a likely Galactic Na I absorber. The components are not resolved, but the line was well fitted with a Na I doublet. Spectrum 1 for this object suffers from the flattening problem in the 1988 July spectra.

### 7.52. *Q2143−1541* (*PKS 2143−15*, $z_{em} = 0.700$)

We find no published spectra for this object. In our spectra we see one unidentified line. Spectrum 1 for this object suffers from the flattening problem in the 1988 July spectra.

### 7.53. *Q2223+2102* (*PKS 2223+21*, $z_{em} = 1.959$)

BTT obtained a spectrum of this object covering 3870–7750 Å, and they find a rich system at $z_{abs} = 1.9019$ showing C IV, Si II λ1526, and Fe II λ2344 absorption. Our spectrum 1 for this object potentially suffers from the flattening problem in the 1988 July spectra. However, it is apparent that this spectrum is not badly affected, since we are able to make reasonable identifications for the lines which appear. We confirm the lines in BTT and find additional lines at this redshift. We also find a new tentative C IV system:

$z_{abs} = 1.4407$.—This is a tentative C IV absorber in which the line C IV λ1550 is blended with Si II λ1304 from the $z_{abs} = 1.9019$ system. If this line is entirely Si II λ1304, then it is much too strong and the redshift match is poor.

$z_{abs} = 1.9019$.—In this definite system we find Fe II λ2344, C IV, Si II λ1526, Si IV λ1402, Si IV λ1393, C II λ1334, and possibly Si II λ1304. Fe II λ2374 and Fe II λ2382 may be present in our spectrum but unfortunately happen to lie in an $O_2$ band.

### 7.54. *Q2230+1128* (*CTA 102*, $z_{em} = 1.037$)

AWFC studied this object in the wavelength range 4040–5240 Å and found no absorption lines. We find Galactic Na I in our spectra, which was unresolved but fitted well with a Na I doublet. Spectrum 1 for this object suffers from the flattening problem in the 1988 July spectra.

### 7.55. *Q2249+1832* (*3C 454*, $z_{em} = 1.757$)

BTT studied this object in the range 3870–7800 Å. They tentatively identify an Mg II system at $z_{abs} = 0.782$, and either Mg II at $z_{abs} = 1.1045$ or Galactic Na I. However, the poor redshift matches in both these systems and confusion with Galactic Na I make the Mg II identifications unlikely. In our spectra, we rule out the $z_{abs} = 0.782$ system at the 2.5 σ level. We confirm the latter system of BTT, but it is significant in our spectrum only at 4 σ. We would attribute this line to an unresolved Galactic Na I doublet. We find no other confirmed absorption lines in our spectra. Spectrum 1 for this object suffers from the flattening problem in the 1988 July spectra.

### 7.56. *Q2251+2429* (*PKS 2251+24*, $z_{em} = 2.328$)

This object was previously studied by BTT in the range 3870–7730 Å. They found Mg II absorption at $z_{abs} = 1.0901$ and C IV absorption at $z_{abs} = 1.7495$, 2.1554, 2.352, and 2.3626. In our spectra we confirm the lines they see and find in addition Si II λ1393 at $z_{abs} = 2.1555$. No additional systems are present. The detection significance level of the Mg II system is below our threshold, and it is not included in our statistical analysis. Spectrum 1 for this object suffers from the flattening problem in the 1988 July spectra.

## 8. SAMPLE PROPERTIES

In Figure 2 we show the 5 σ rest equivalent width detection limits in each of the spectra as a function of Mg II redshift. The plots have been clipped above 2.5 Å, and regions in which Mg II is not observable at all are shown with the limit set to zero. Because there is uncertainty about the physical nature and environment of absorbers very near the quasar itself, we exclude from our statistical analysis any regions with a velocity relative to the quasar of less than 6000 km $s^{-1}$. We also apply the same criterion near the Lyα emission peak, since identification of heavy-element doublets is uncertain at wavelengths near or below the Lyα peak. These excluded regions, along with the $O_2$ bands and the dichroic gap of the double spectrograph at $z \approx 0.7$, are apparent in the plots of Figure 2.

The overall sensitivity and size of our sample are summarized in the plots of Figure 3. The left-hand plot shows the integrated redshift path length as a function of the 5 σ rest equivalent width detection limit. This is defined by

$$Z(W_0) = \sum_k \int g(W_0 - W_k(z))dz \,, \qquad (1)$$

where $W_k(z)$ is the detection limit in the $k$th quasar at redshift $z$, and $g(x)$ is the Heaviside step function [$g(x) = 0$ for $x < 0$ and $g(x) = 1$ for $x \geq 0$]. For comparison, the path length in the sample of SS (which we always take to include the data in SSB1) is 114.2 at $W_0 = 0.3$ Å and 131.1 at $W_0 = 1.0$ Å. In the right-hand plot of Figure 3 we show the number of quasar sight lines versus redshift at various equivalent width limits. This function is given by

$$S(z, W_0) = \sum_k g(W_0 - W_k(z)) .$$

The thickest line is $S(z, 0.3$ Å$)$, the medium line is $S(z, 0.6$ Å$)$, and the thinnest line is $S(z, 1.0$ Å$)$.

## 9. ABSORBER STATISTICS

A straightforward step in studying the intrinsic nature of absorption-line systems is to calculate their observed distribution in redshift and rest equivalent width. The redshift distribution can be easily compared with the prediction for a no-evolution model of absorbers and thus has a direct physical interpretation. The equivalent width distribution is more difficult to interpret because there are a number of contributing factors which are at present poorly understood. However, the observed distribution will certainly be a key ingredient in understanding these issues, so this calculation should be done where possible. In this section we first discuss the parametric forms commonly used in the literature to represent the distribution functions. We then derive two approximations which allow calculation of the normalization and the binned values of the equivalent width distribution for an inhomogeneous sample. Finally, we present and discuss the best-fit distribution parameters for 11 different subsamples of our data and the data of SS and SSB1.

### 9.1. *Distribution Functions and Computational Techniques*

The redshift distribution of absorbers is generally found to be well fitted with a single power law of the form

$$n(z) = n(1 + z)^{\gamma} , \tag{2}$$

where $n(z)$ is the number of absorbers per unit redshift above a specified equivalent width limit. Both the normalization $n$ and the power-law index $\gamma$ are functions of this limit. This power law is a special case of the redshift distribution for a nonevolving population in a Friedmann universe, $n(z) = n(1 + z)(1 + 2q_0z)^{-1/2}$, where $q_0$ is the deceleration parameter. For the limiting cases $q_0 = 0$ $(\Omega = 0)$ and $q_0 = 0.5$ $(\Omega = 1)$ we have $n(z) = n(1 + z)$ and $n(z) = n(1 + z)^{1/2}$, respectively. Thus any value of $\gamma$ between 0.5 and 1 is considered consistent with a nonevolving population of absorbers.

Two forms for the absorber equivalent width distribution function which are empirically found to fit the data are (SS; Tytler et al. 1987; Sargent et al. 1980):

$$n(W) = \frac{N^*}{W^*} \exp\left(-\frac{W}{W^*}\right) , \tag{3}$$

$$n(W) = CW^{-\delta} . \tag{4}$$

Here $n(W)$ is the number of absorbers per unit equivalent width, $z$ is the redshift, $W$ is the rest equivalent width, and the remaining variables are the fitted parameters. The distribution $n(W)$ is normalized so that

$$\int_{W=W_0}^{\infty} n(W) dW = \langle N(z) \rangle ,$$

where $\langle N(z) \rangle$ is number of absorbers per unit redshift in that sample and $W_0$ is the rest equivalent width limit. Note that SS find that increased rest equivalent width is weakly correlated with increasing redshift.

This means that the distribution parameters are in reality functions of redshift. However, the correlation is just barely detected by SS, and so for most purposes the redshift dependence can be ignored or accounted for by specifying the average redshift of absorbers in the sample.

The calculation of the parameters for equation (4), the power-law form of the equivalent width, generally also requires an upper cutoff $W_{\rm cut}$ in the equivalent width instead of integrating to infinity. This is because the integral of the power-law form converges rather slowly, and so the lack of very strong absorbers in the data has a large effect on the overall fit. The residuals of a fit with no upper cutoff are unacceptably large. A typical value used for the cutoff is the highest equivalent width observed in the sample, but since this is fairly arbitrary, it is important to verify that the fit parameters depend only weakly on the cutoff. However, using the published sample MG1 from SS, we have derived the best-fit values of $C_0$ and $\delta_0$ as a function of the upper cutoff $W_{\rm cut}$ and find a strong dependence, especially near their cutoff of about 3 Å. This is illustrated in Figure 4, which shows that the variation with small changes in $W_{\rm cut}$ is much greater than the formal uncertainties in the fitted values from SS, $C_0 = 0.38 \pm 0.03$ and $\delta_0 = 1.65 \pm 0.09$. Thus this power-law form of the distribution in essence requires the cutoff as an additional parameter. Since there is no good physical justification for either of the equivalent width forms, the one which gives a statistically acceptable fit with the fewest parameters should be used. For this reason we do not calculate best-fit parameters $C_0$ and $\delta_0$.

In our analysis the actual calculation of distribution parameters is done by the maximum-likelihood method, which allows robust fitting of inhomogeneous unbinned absorption-line data. We follow the method described by Murdoch et al. (1986), with a minor modification to allow different equivalent width limits in a single QSO.

The calculation of the best-fit parameters of equations (2)–(4) for a uniform sample with an equivalent width limit $W_0$ is straightforward. For a nonuniform sample, as outlined in Murdoch et al. (1986), the spectra are broken up into regions, each with its own detection limit. In this case the best-fit parameters $\gamma_0$ and $W_0^*$ are easily computed. However, the normalization $N_0^*$ is less straightforward because it depends on $\langle N(z) \rangle$, which is ill-defined for a nonuniform sample. For the purposes of plotting the computed distributions and comparing with results from uniform surveys, it is useful to have an approximate expression for this parameter. To do this, we first define the distribution

$$n(z, W) = \frac{A}{W^*} (1 + z)^{\gamma} \exp\left(-\frac{W}{W^*}\right) , \tag{5}$$

which is the number of absorbers per unit equivalent width per unit redshift. The normalization of $n(W)$ means we can approximate $n(W)$ by integrating the best-fit model of $n(z, W)$ over a unit redshift interval at the average absorber redshift of

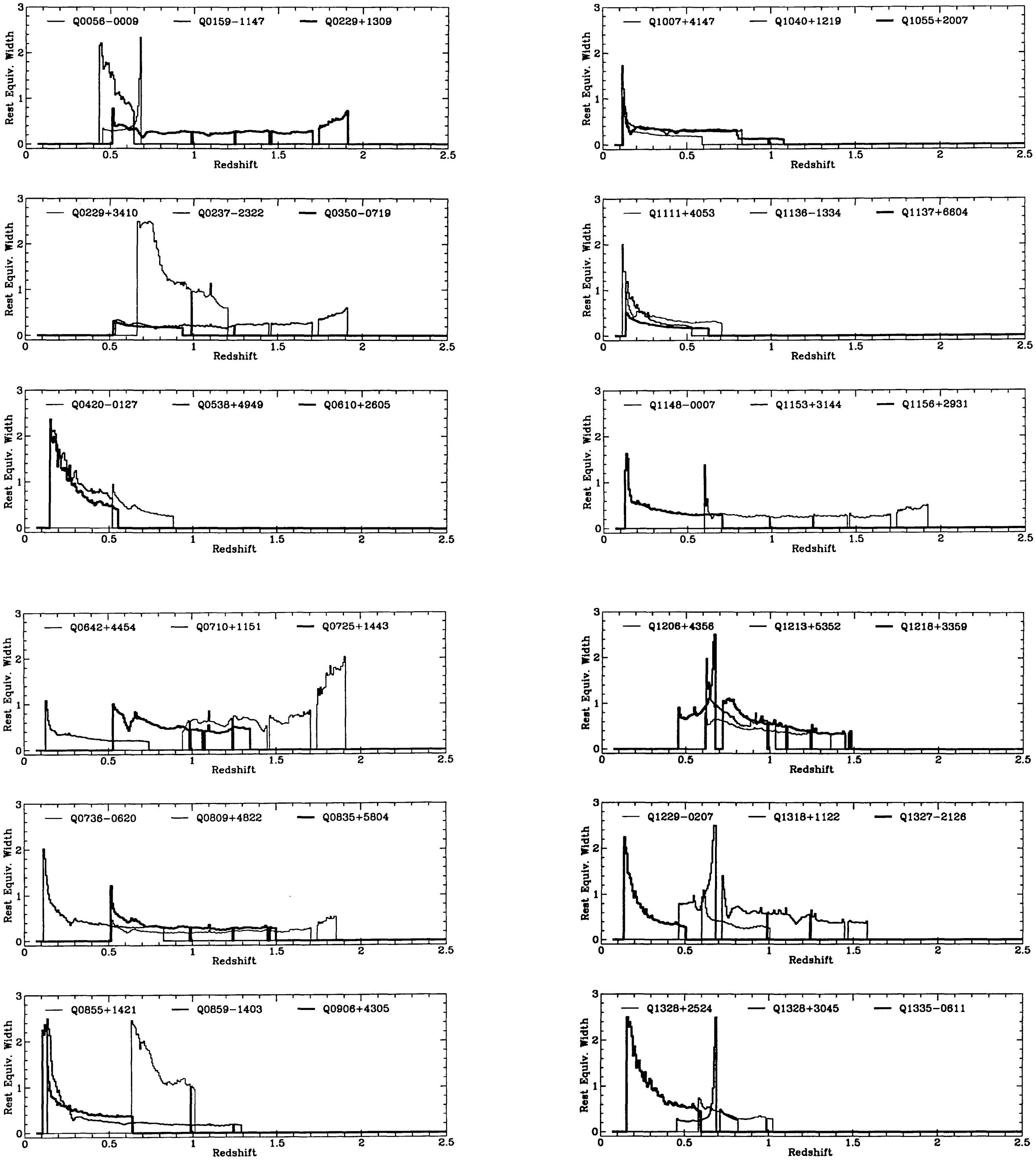


FIG. 2.—Rest equivalent width limits

the sample. This gives

$$n(W) \approx \int_{\langle z\rangle-1/2}^{\langle z\rangle+1/2} \frac{A_0}{W_0^*}(1+z)^{\gamma} \exp\left(-\frac{W}{W_0^*}\right) dz\,.$$

Comparing with the original form for $n(W)$ gives the value for the normalization.

The calculation of the binned values of $n(W)$ is also less straightforward in the case that the spectra have different equivalent width limits. The method we used is an approximation, but in the cases where we can check the results the agreement is good.

Define $N(W_A, W_B)$ to be the number of absorbers in $S(W_A)$ with $W_A \leq W_i < W_B$. Here $S(W_A)$ is the collection of spectral

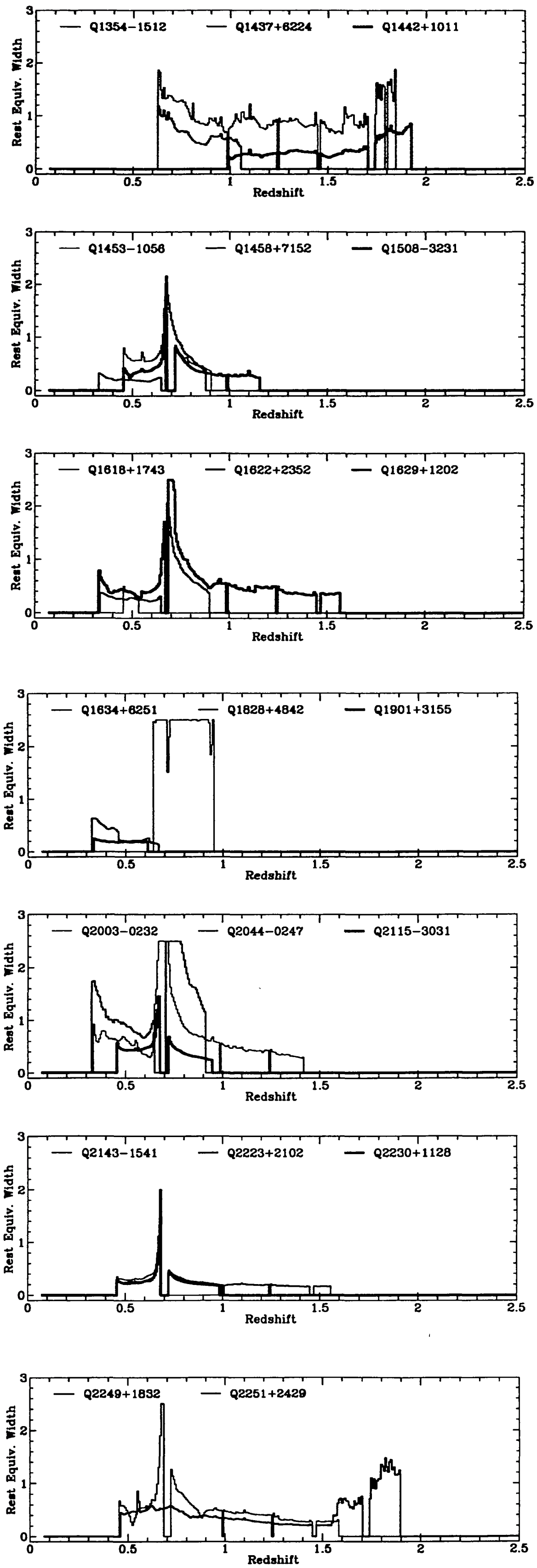


FIG. 2—*Continued*

regions in which a line of rest equivalent width $W_A$ could have been detected at 5 $\sigma$ confidence. Then the binned distribution $n(W_A, W_B)$ is just

$$n(W_A, W_B) = \frac{N(W_A, W_B)}{Z(W_A)(W_B - W_A)} .$$

Recall that $Z(W_A)$ is defined by equation (1). However, some absorbers near the detection limit with $W_A \leq W_i < W_B$ may not be in $S(W_A)$. We can make maximum use of available data by dividing $(W_A, W_B)$ into $N_W$ subregions defined by $w_j = j(W_B - W_A)/N_W + W_A$ and approximating

$$n(W_A, W_B) = \frac{1}{N_W} \sum_{j=1}^{N_W} n(w_{j-1}, w_j) .$$

If we make $N_W$ large enough, then $N(w_{j-1}, w_j)$ will be either 0 or 1, and we can replace the above equation by a sum over all the $N_{\rm obs}$ lines detected in the spectra, giving

$$n(W_A, W_B) = \sum_{i=1}^{N_{\rm obs}} \frac{g(W_i - W_A) g(W_B - W_i)}{Z(W_i)(W_B - W_A)} .$$

The uncertainty in this quantity is given by the standard counting statistics (Poisson deviations) on the number of lines with $W_A \leq W_i < W_B$.

### 9.2. *Distribution Function Results*

The results of our statistical analysis of our sample of 56 quasars are given in Table 5. Here $N_{\rm obs}$ is the number of observed lines, $Z$ is the redshift path length for the sample, $\langle z \rangle$ is the average redshift of absorbers in the sample, $\langle N(z) \rangle$ is the average number of absorbers per unit redshift, and $\gamma_0$, $W_0^*$, and $N_0^*$ are the best-fit values for the model parameters given in equations (2) and (3). We have calculated the distribution parameters for a number of different subsamples of our data, alone and in combination with the large data set of SS. The Kolmogorov-Smirnov (KS) probability for each of the samples was at least 0.46, indicating that the derived distributions are good fits to the data. The samples are defined as follows:

- A — Our entire sample, analyzed using a discrete set of $W_0$ limits to approximate the local equivalent width limit. Parameters which depend on a uniform equivalent width limit are not calculated.
- A2,3 — Lines in our sample which are in $S(0.6$ Å$)$ and $S(1.0$ Å$)$, respectively.
- MG1,2,3 — Lines from SS and SSB1 which are in $S(0.3$ Å$)$, $S(0.6$ Å$)$, and $S(1.0$ Å$)$, respectively.
- MG — MG2 + MG3.
- A*n*−MG*n* — Sample A*n*, with regions in MG*n* excluded. This sample is thus independent of the SS and SSB1 data. The value of *n* can be 2, 3, or blank (indicating the complete sample).
- A*n*+MG*n* — Sample A*n* combined with sample MG*n*. In the case of overlapping regions in the same QSO, the MG*n* data are used.

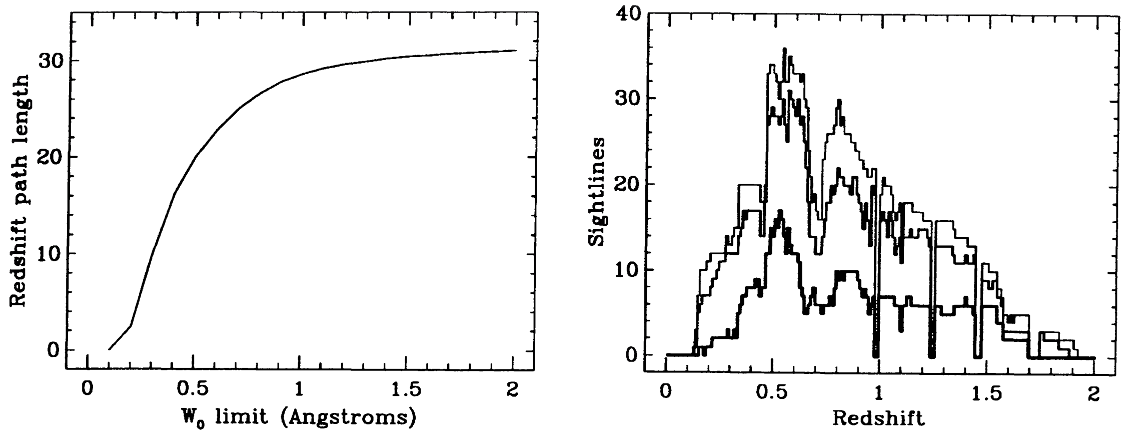


FIG. 3.—*Left:* redshift path length vs. rest equivalent width limit. *Right:* sight lines vs. redshift for various equivalent width limits. The thickest line is for $W_0 = 0.3$ Å, the medium line is for $W_0 = 0.6$ Å, and the thinnest line is for $W_0 = 1.0$ Å.

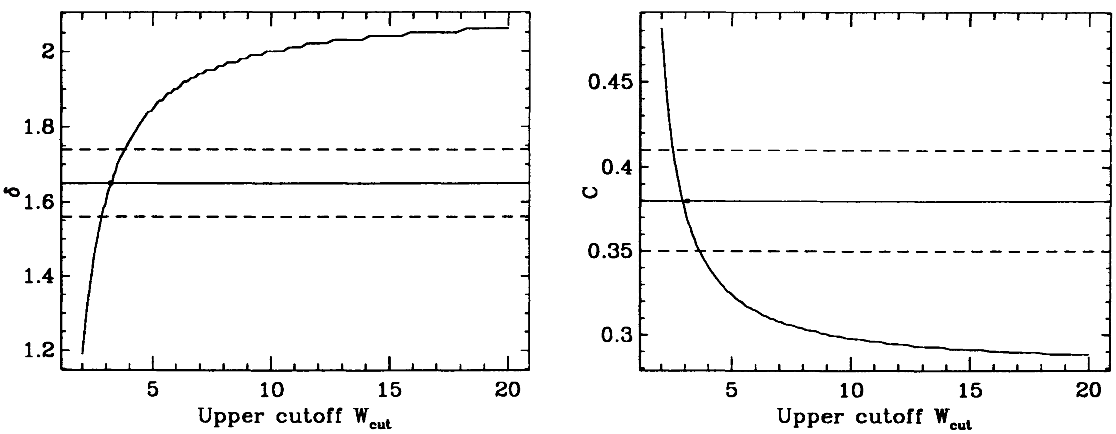


FIG. 4.—Power-law distribution function parameters $\delta$ and $C$ as a function of the upper cutoff $W_{cut}$ used in the maximum-likelihood fitting. The solid and dashed horizontal lines show the value and 1 $\sigma$ limits derived by SS for $\delta$ and $C$.

TABLE 5

RESULTS OF STATISTICAL ANALYSIS

| Sample | $N_{obs}$ | $Z$ | $\langle z \rangle$ | $\langle N(z) \rangle$ | $\gamma_0$ | $W_0^*$ | $N_0^*$ |
|---|---|---|---|---|---|---|---|
| A | 18 | ... | 1.00 | ... | $1.41 \pm 1.00$ | $0.62 \pm 0.13$ | $1.42 \pm 0.22$[a] |
| A+MG | 87 | ... | 1.13 | ... | $1.21 \pm 0.42$ | $0.65 \pm 0.07$ | $1.47 \pm 0.14$[a] |
| A–MG | 14 | ... | 0.93 | ... | $0.98 \pm 1.16$ | $0.56 \pm 0.13$ | $1.40 \pm 0.27$[a] |
| A2 | 14 | 26.6 | 1.03 | $0.60 \pm 0.15$ | $1.87 \pm 1.20$ | $0.58 \pm 0.14$ | $1.71 \pm 0.62$ |
| MG1 | 110 | 114.2[b] | 1.12 | $0.97 \pm 0.10$[b] | $0.78 \pm 0.42$[b] | $0.60 \pm 0.06$ | $1.55 \pm 0.20$[b] |
| A2+MG2 | 80 | 153.3 | 1.13 | $0.53 \pm 0.06$ | $1.11 \pm 0.46$ | $0.64 \pm 0.07$ | $1.36 \pm 0.21$ |
| A2–MG | 11 | 21.2 | 0.93 | $0.57 \pm 0.16$ | $2.07 \pm 1.42$ | $0.53 \pm 0.13$ | $1.77 \pm 0.77$ |
| MG2 | 69 | 132.0 | 1.14 | $0.53 \pm 0.06$ | $1.04 \pm 0.49$ | $0.66 \pm 0.08$ | $1.31 \pm 0.21$ |
| A3 | 7 | 31.9 | 0.98 | $0.25 \pm 0.09$ | $1.26 \pm 1.64$ | $0.62 \pm 0.22$ | $1.26 \pm 0.84$ |
| A3+MG3 | 44 | 161.0 | 1.26 | $0.28 \pm 0.04$ | $2.47 \pm 0.68$ | $0.68 \pm 0.10$ | $1.19 \pm 0.32$ |
| MG3 | 38 | 134.6 | 1.31 | $0.29 \pm 0.05$ | $2.58 \pm 0.73$ | $0.70 \pm 0.11$ | $1.22 \pm 0.34$ |

[a] Calculated using approximate formula described in text.

[b] Taken directly from SS and not calculated with our software.

Note that there were insufficient lines in sample A3−MG3 to do meaningful statistics. Samples MG2 and MG3 were assembled from the published tables and plots of equivalent width detection limits in SS and SSB1. These samples were then analyzed in exactly the same way as our own data. For sample MG1, determining the regions which comprise $S$(0.3 Å) from the published plots is difficult. Since our sample has a small redshift path length at this limit, there is little point in combining our data with MG1 for redshift evolution calculations. However, the equivalent width distribution calculations can be done using only the line lists.

The primary result shown by Table 5 is that our new sample is statistically consistent in all cases with the larger sample of SS and SSB1. In all cases our independent samples (such as A−MG) give redshift and equivalent width distribution parameter values which are consistent with SS and SSB1, but with larger uncertainties. The number of absorbers per unit redshift for various equivalent width limits is also consistent. By combining our new data with the published data, we have reduced the uncertainties in the distribution parameters, in most cases by 10%–20%.

In Figure 5 we graphically illustrate the values of $\gamma_0$ and $W_0^*$ for the samples in Table 5, grouped roughly by equivalent width limit. Note that we are plotting these two parameters together only as a convenient way of displaying the data, and not to imply any relationship between them. On the left are our complete sample and MG1, in the middle are the 0.6 Å data, and on the right are the 1.0 Å data. In these plots the triangle represents the values derived from our data, the square is for our data combined with SS, the circle is for our data in which the objects in common with SS have been excluded, and the cross is for the data from SS. Recall that we were unable to analyze the A3−MG3 sample. These plots show once again that our results are statistically consistent with the data in SS.

Referring back to Table 5, the value of $\gamma_0$ is clearly seen to be a function of the sample equivalent width limit. For the 0.3 Å (MG1) and 0.6 Å samples (MG2 and A2), the distribution of absorber redshifts is consistent with no evolution in galaxy number density and cross section, for $q_0$ = 0–0.5. However, the strong absorbers in the 1.0 Å samples (MG3 and A3) are inconsistent with no evolution at 2–3 $\sigma$, in the sense that the overall cross section was larger in the past. We also see that the value of the equivalent width distribution parameter $W_0^*$ is independent of the equivalent width limit for all of the samples. This implies that a single exponential is a good characterization of the absorber population over the entire range of observed equivalent widths.

The observed values of $n(z)$ for three different samples, MG1, A2+MG2, and A3+MG3, are shown in Figure 6. The data have been binned for display purposes, and the solid lines show the best-fit power-law distributions. The strong dependence of both the normalization and the power-law index on equivalent width limit is apparent.

In Figure 7 we plot the observed values of $n(W)$, binned for display purposes. The solid line in the figure is the plot of $n(W)$ using the form in equation (3) and the values for $N^*$ and $W^*$ given in the last row of Table 5. The dashed line is the same function using the values derived by SS of $N^* = 1.55 \pm 0.20$ and $W^* = 0.66 \pm 0.11$. Although our values are somewhat lower than those found by SS, they are consistent within the uncertainties.

### 9.3. *Associated Absorbers*

As was mentioned in the Introduction, the intrinsic properties of the quasars in our sample are very different from those of previous Mg II surveys. In particular, the quasars in our survey have an average absolute magnitude of −26.7, compared with −28.6 for SS, radio flux $S$(2.7 MHz) ≥ 1 Jy, and radio spectral index steeper than $\alpha = 0.4$. Within the paradigm which explains the broad properties of quasars by orientation effects (see, e.g., Antonucci 1993), the objects in our survey are relatively faint quasars with jets oriented toward the plane of the sky. Since both of these attributes could plausibly cause an increase in the number of low-ionization associated absorbers, an analysis of these systems is very useful.

In Figure 8 we show a histogram of the number of absorption systems in sample A versus the apparent ejection velocity $\beta c$ with respect to the quasar. The data are binned in 1000 km s$^{-1}$ intervals. In the calculation of $\beta$ we have used the emission-line redshifts which we determined in § 5. The plot suggests an excess of absorbers with apparent ejection velocity less than 6000 km s$^{-1}$. A total of six absorbers are found in the range −1000 to +6000 km s$^{-1}$. However, it is important to note that

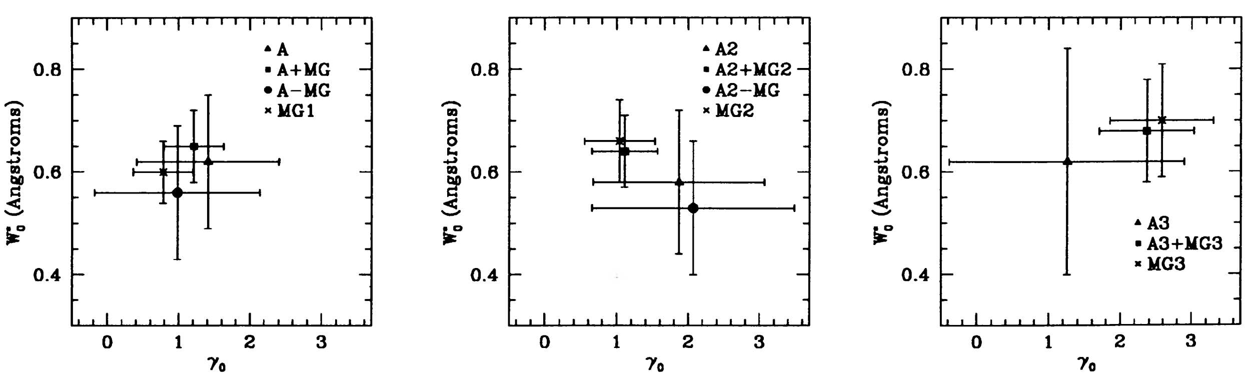


FIG. 5.—Equivalent width and redshift distribution parameters for all of our samples. On the left are our complete sample and MG1, in the middle are the 0.6 Å data, and on the right are the 1.0 Å data. The triangle represents the values derived from our data, the square is for our data combined with SS, the circle is for our data in which the objects in common with SS have been excluded, and the cross is for the data from SS.

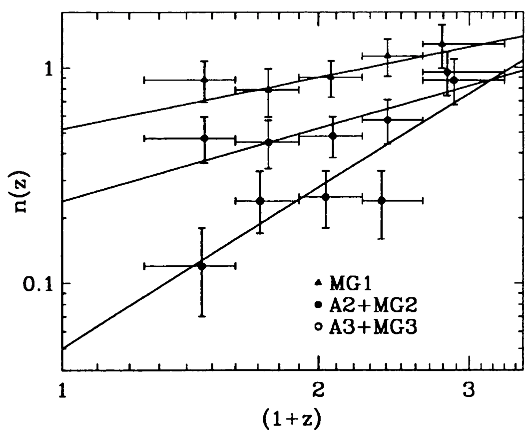


FIG. 6.—Number of absorbers per unit redshift for samples MG1, A2+MG2, and A3+MG3. The data have been binned for display purposes, and maximum-likelihood fits to the data are shown by the solid lines.

we have made no corrections to account for varying spectral coverage and signal-to-noise ratio within the spectra. The plot of Figure 8 is thus only a qualitative illustration of the distribution of velocities.

A quantitative measure of the excess of associated absorbers is easily obtained by integrating the derived distribution $n(z, W)$ over the regions within $\pm 6000$ km s$^{-1}$ of the Mg II emission peaks, using the local rest equivalent width limits. This gives an expected number of absorbers based on the "background" of intervening absorbers. For sample A, the expected number of absorbers within $\pm 6000$ km s$^{-1}$ of the emission peak is 2.17, with the formal uncertainty less than 0.1. Given this mean, the probability of observing six or more absorbers is 2.4%. If we limit the negative velocity to that which could plausibly occur in normal galaxies in front of the quasar, giving the interval from $-1500$ to 6000 km s$^{-1}$, the chance of seeing at least six absorbers is down to 0.3%.

This excess of Mg II absorbers over the background number is in contrast to the results of previous surveys which have addressed this question (SS; SSB1; Lanzetta et al. 1987). The best statistics are from SS, who observed 89 Mg II emission peaks and found six absorbers with $|\beta c| \leq 6000$ km s$^{-1}$. This is consistent with the number expected from distributed absorbers. As we have pointed out, the distinction lies in the intrinsic source properties, and a similar disagreement between surveys is found for the associated C IV lines. The spectra of 55 QSOs (both radio-loud and radio-quiet) obtained by SBS showed no excess, nor did the subsample of radio-loud quasars. However, in a survey of steep-spectrum 3C and 3CR quasars, a sample similar to ours, it was found that 10 out of 12 showed associated C IV absorption (AWFC). An excess of associated C IV absorbers was also found by Foltz et al. (1986) and Weymann et al. (1979). In all cases, the surveys which contain intrinsically faint, steep-spectrum radio sources show an excess, while the surveys containing QSOs selected by optical luminosity, with an assortment of radio properties, show no excess.

## 10. SUMMARY

We have presented moderate-resolution (100–360 km s$^{-1}$) optical spectra of 56 steep-spectrum quasars obtained at the Multiple Mirror Telescope and Palomar Observatory. These quasars were selected based on their radio and optical luminosity, radio spectral index, redshift, and declination, as described in Paper I. This selection gives us a sample with intrinsic source properties that are very different from those of previous Mg II surveys, and this has allowed our unexpected finding of an excess of associated Mg II absorbers.

The primary purpose of our survey was to find relatively strong Mg II absorption-line redshifts to allow a subsequent search for H I 21 cm absorption in these quasars (Paper I). This means that our sample is largely sensitive to rest equivalent widths above 0.6 Å. For limits of 0.3, 0.6, and 1.0 Å, the total redshift path lengths of our sample are 9.9, 22.8, and 28.6, respectively. The quasar emission redshifts fall in the range 0.5–3.5, with the majority being between 0.7 and 1.5.

In addition to the spectra and associated error arrays, we have presented plots of the Mg II rest equivalent width limit versus redshift in each of the quasars. We have given a statisti-

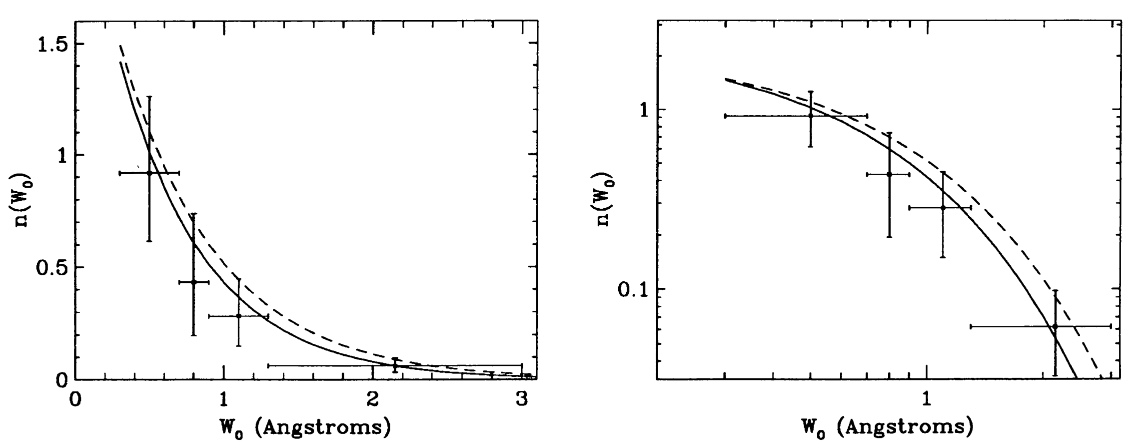


FIG. 7.—Number of absorbers per unit equivalent width. The solid line is the maximum-likelihood fit to our data for $n(W)$, and the dashed line is the best-fit curve given by SS. The same data are plotted in linear and logarithmic axes.

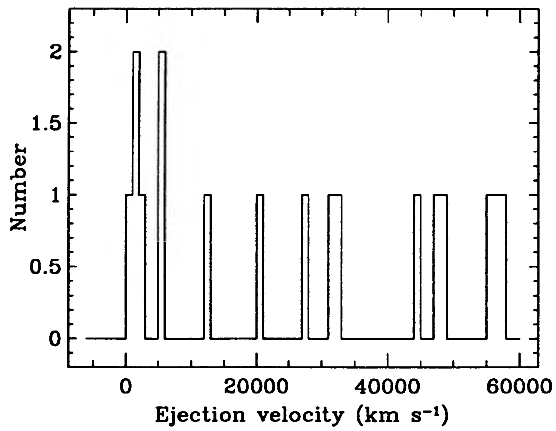


FIG. 8.—Histogram of the number of Mg II absorbers in sample A vs. apparent ejection velocity with respect to the quasar. The data have been binned in 1000 km $s^{-1}$ intervals. This plot of the raw data suggests an excess of associated absorbers; an unbiased, quantitative measure of this excess is given in the text.

cally complete list of all absorption lines found, both Galactic and extragalactic. In our spectra we find a total of 29 Mg II systems, 18 of which have not been previously reported.

We have derived the best-fit redshift and equivalent width distribution parameters for 11 different subsamples of our data and the data of SS and SSB1. We find that the values determined from our sample are statistically consistent with previously found values. The combination of our spectra with those presented in SS and SSB1 yield the following distribution parameters: for $W_{\rm min} = 0.6$ Å, $\gamma = 1.11 \pm 0.46$, $W^* = 0.64 \pm 0.07$ Å, and $N^* = 1.36 \pm 0.21$; for $W_{\rm min} = 1.0$ Å, $\gamma = 2.47 \pm 0.68$, $W^* = 0.68 \pm 0.10$ Å, and $N^* = 1.22 \pm 0.32$.

Of the 29 Mg II systems, six have an apparent ejection velocity from the quasar of less than 6000 km $s^{-1}$ and are termed "associated." The observed number of associated systems in our spectra is inconsistent with Poisson fluctuations of the nonassociated background systems at 97%–99% confidence. This is the first time such an excess of associated Mg II absorbers has been observed.

We thank the staff members at the VLA, the Multiple Mirror Telescope, and Palomar Observatory for their assistance. We also thank M. Birkinshaw for assistance in understanding the VLA calibrations and for comments on the manuscript. The work of T. L. A. was supported by NASA grant NGT-50938 awarded by the NASA Graduate Student Researchers Program. J. B. was supported by RII-8800660 and AST-9058510 from the National Science Foundation. M. E. was supported by NASA contracts NAS8-30751 (*HEAO 2*) and NAS8-39073 (ASC), and by NASA grant NASW-2201 (LTSA).

## REFERENCES

Aldcroft, T. L., Elvis, M., & Bechtold, J. 1993, AJ, 105, 2054 (Paper I)
———. 1994, in preparation
Anderson, S. F., Weymann, R. J., Foltz, C. B., & Chaffee, F. H. 1987, AJ, 94, 279 (AWFC)
Antonucci, R. 1993, ARA&A, 31, 473
Barthel, P. D., Tytler, D. R., & Thomson, B. 1990, A&AS, 82, 339 (BTT)
Bergeron, J., & Boissé, P. 1991, A&A, 243, 344
Bergeron, J., Cristiani, S., & Shaver, P. A. 1992, A&A, 257, 417
Boissé, P., & Bergeron, J. 1985, A&A, 145, 59
Boissé, P., Boulade, O., Kunth, D., Tytler, D., & Vigroux, L. 1992, A&A, 262, 401
Briggs, F. W. 1988, in QSO Absorption Lines, ed. J. C. Blades, D. A. Turnshek, & C. A. Norman (Cambridge: Cambridge Univ. Press), 275
Briggs, F. H., Turnshek, D. A., Schaeffer, J., & Wolfe, A. M. 1985, ApJ, 293, 387
Brown, R. L., Broderick, J. J., Johnston, K. J., Benson, J. M., Mitchell, K. J., & Waltman, W. B. 1988, ApJ, 329, 138
Brown, R. L., & Mitchell, K. J. 1983, ApJ, 264, 87
Burbidge, E. M., & Kinman, T. D. 1966, ApJ, 145, 654
Chaffee, F. H., Jr., & Latham, D. W. 1982, PASP, 94, 386
Cohen, R. D., Barlow, T. A., Beaver, E. A., Junkkarinen, V. T., Lyons, R. W., & Smith, H. E. 1992, ApJ, 421, 453
Elvis, M., Fiore, F., Mathur, S., & Wilkes, B. J. 1994, ApJ, 425, 103
Foltz, C. B., Chaffee, F. H., Jr., & Wolfe, A. M. 1988, ApJ, 335, 35
Foltz, C. B., Weymann, R. J., Peterson, B. M., Sun, L., Malkan, M. A., & Chaffee, F. H. 1986, ApJ, 307, 504
Junkkarinen, V., Hewitt, A., & Burbidge, G. 1991, ApJS, 77, 203
Khare, P., York, D. G., & Green, R. 1989, ApJ, 347, 627
Lanzetta, K. M., Turnshek, D. A., & Wolfe, A. M. 1987, ApJ, 322, 739
Latham, D. W. 1982, in IAU Colloq. 67, Instrumentation for Astronomy with Large Optical Telescopes, ed. C. M. Humphries (Dordrecht: Reidel), 245
Meyer, D. M., & York, D. G. 1992, ApJ, 399, L121
Morton, D. C., & Smith, W. H. 1973, ApJS, 26, 333
Murdoch, H. S., Hunstead, R. W., Pettini, M., & Blades, J. C. 1986, ApJ, 309, 19
Oke, J. B., & Gunn, J. E. 1982, PASP, 94, 586
Sargent, W. L. W., Boksenberg, A., & Steidel, C. C. 1988a, ApJS, 68, 639 (SBS)
Sargent, W. L. W., Steidel, C. C., & Boksenberg, A. 1988b, ApJ, 334, 22 (SSB1)
———. 1989, ApJS, 69, 703 (SSB2)
Sargent, W. L. W., Young, P., Boksenberg, A., & Tytler, D. 1980, ApJS, 42, 41
Schmidt, C. D., Weymann, R. J., & Foltz, C. B. 1989, PASP, 101, 713
Schneider, D. P., et al. 1992, preprint
Smith, H. E., & Spinrad, H. 1980, ApJ, 236, 419
Steidel, C. C. 1992, in The Evolution of Galaxies and Their Environment, ed. J. M. Shull & H. Thronson (Dordrecht: Kluwer), in press
Steidel, C. C., & Sargent, W. L. W. 1992, ApJS, 80, 1 (SS)
Tytler, D., Boksenberg, A., Sargent, W. L. W., Young, P., & Kunth, D. 1987, ApJS, 64, 667
Véron-Cetty, M.-P., & Véron, P. 1989, ESO Sci. Rep., No. 7
Weymann, R. J., Williams, R. E., Peterson, B. M., & Turnshek, D. A. 1979, ApJ, 234, 33
Wills, B. J., Netzer, H., Uomoto, A. K., & Wills, D. 1980, ApJ, 237, 319
Yanny, B. 1992, PASP, 104, 840
Yanny, B., & York, D. G. 1992, ApJ, 391, 569
York, D. G., Yanny, B., Crotts, A., Carilli, C., Garrison, E., & Matheson, L. 1991, MNRAS, 250, 24
Young, P., Sargent, W. L. W., & Boksenberg, A. 1982, ApJS, 48, 455 (YSB)